

# INTERACTION OF RETAINING STRUCTURES WITH SOIL

BY

BASHIR AHMED

A thesis submitted to the Department of Civil Engineering,  
Bangladesh University of Engineering and Technology, Dhaka  
in partial fulfilment of the requirements for the degree

of

MASTER OF SCIENCE IN CIVIL ENGINEERING



#86995#

November, 1993



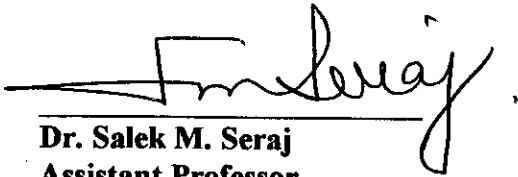
**INTERACTION OF RETAINING STRUCTURES  
WITH SOIL**

R  
624.151  
1993  
AHM

BY

**BASHIR AHMED**

A thesis approved as to the style and content by:



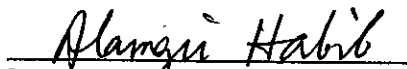
**Dr. Salek M. Seraj**  
Assistant Professor  
Dept. of Civil Engineering  
BUET, Dhaka.

: Chairman  
(Supervisor)

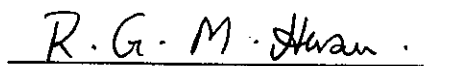


**Dr. A.M.M. Safiullah**  
Professor & Head  
Dept. of Civil Engineering  
BUET, Dhaka.

: Member

  
**Dr. Alamgir Habib**  
Professor  
Dept. of Civil Engineering  
BUET, Dhaka.

: Member

  
**Dr. R.G.M Hasan**  
Assistant Professor  
Dept. of Mechanical Engineering  
BUET, Dhaka.

: Member  
(External)

**This thesis is dedicated to my father Nazir Ahmed, to  
my mother Nurjahan Ahmed and to my wife Polash.  
Their constant love, support and encouragement made it possible.**

## DECLARATION

I hereby certify that the research work reported in this thesis has been performed by me and that this work has not been submitted elsewhere for any other purpose ( except for publication )

November, 1993



(Bashir Ahmed)

## ACKNOWLEDGEMENT

The author is greatly indebted to his supervisor Dr. Salek M. Seraj, Assistant Professor, Department of Civil Engineering, BUET for his constant guidance, continued encouragement, generous help and unfailing enthusiasm in the completion of this research work.

The author also expresses his gratitude to Dr. A.M.M. Safiullah, Professor and Head, Department of Civil Engineering, BUET for his suggestions and encouragement.

Among others, acknowledgements are made to Mr. M.A. Malek for typing the thesis and Mr. M. Shahiduddin for his assistance in drafting some of the figures presented in this thesis.

## SYNOPSIS

The thesis considers the interaction between rigid retaining walls and the soil retained by them and below them. Finite element method is employed for non-linear two dimensional retaining wall-soil interaction analysis. Data preparation for the computer program is largely automated.

A study of the stresses and strains in the soil revealed that the extent of soil to be included in the finite element mesh need not be very large. A horizontal extent of soil (retained) equal to six times the wall height and a vertical extent of soil below the footing equal to about three times the footing width have been found to be adequate for modelling a retaining wall-soil system.

A planned scheme of analyses of a number of rigid retaining walls with varying heights, thickness of the stem, thickness of the wall footing and different compressive strength of concrete were examined. The effect of soil properties such as effect of unit weight, Poisson's ratio, angle of internal friction and surface slope of backfill soil, on the lateral soil force and the bending moment at a given depth were investigated. In addition to this, effect of depth of embedment of the wall into the original soil was examined. After analysis for the self weight of the retaining wall-soil system, analyses were carried out for surcharge load, i.e., line load and distributed load. Magnitude and location of line load was varied to study the effect of these parameters. For uniformly distributed load, only the magnitude of the load was changed.

It was observed that the moment of inertia of stem of the wall and the wall footing do not affect the values of lateral soil force and moment. Concrete strength has shown little effect.

Results show that the slope of soil surface has considerable effect on the lateral soil force and the moment. It was observed that unit weight and Poisson's ratio produce linear variation to the lateral soil force and moment. Angle of internal friction was observed to have smaller effect than that predicted by the traditional analysis. Depth of embedment also affects the lateral soil force and the moment.

It has been found that magnitude of line load has linear variation with lateral soil force and moment. Distance of line load away from the wall face was

found to have exponentially decaying effect on lateral soil force and moment. Larger walls show a critical distance from the wall face at which the effect of line load is maximum. Uniformly distributed load also shows a linear variation like the previous case. It was observed that intermediate walls are subjected to greater lateral soil force and moment for this case.

Finally, results of finite element analyses were compared with a few commonly used methods. It was observed that for self weight of retaining wall-soil system, the lateral soil force is greater than that predicted by the selected methods. But for walls of larger height, moment was found to be smaller for horizontal backfill. Effect of slope of soil surface was found to have greater effect than that predicted by these methods. Location of the resultant of the lateral soil force was found to be a function of the wall height and the slope of the soil surface. Effect of line load was observed to be greater than that predicted by Boussinesq equation but smaller than Trial Wedge method. For uniformly distributed load, finite element method shows smaller effect than Rankine's or Coulomb's method. On the other hand, Ramon's method shows smaller effect than finite element method for small walls.

# CONTENTS

Page

<b>DECLARATION</b>	i
<b>ACKNOWLEDGEMENT</b>	ii
<b>SYNOPSIS</b>	iii
<b>CONTENTS</b>	v
<b>LIST OF FIGURES</b>	viii
<b>LIST OF TABLES</b>	xii
<b>NOTATION</b>	xiv
<b>CHAPTER 1      GENERAL INTRODUCTION</b>	
1.1 Introduction	1
1.2 Review of Interactive Analysis	1
1.3 Objective of the Present Research	4
1.4 Scope of the Work	5
<b>CHAPTER 2      ANALYSIS METHODS FOR RETAINING WALL</b>	
2.1 Introduction	7
2.2 Traditional Methods of Analysis	7
2.2.1 Coulomb Earth Pressure Theory	9
2.2.2 Rankine Earth Pressure Theory	12
2.2.3 Graphical and Computer Solution for Lateral Earth Pressure	14
2.2.4 Active Earth Pressure Using Theory of Plasticity	15
2.3 Analysis for Surcharge Load	15
2.3.1 Boussinesq Equation	16
2.3.2 Trial Wedge Solution	16
2.3.3 Ramon's Solution for Strip Loading	16
2.3.4 Analysis for Surcharge Load by Coulomb's and Rankine's Method	19
2.4 Methods Selected for Comparing Results of Finite Element Analysis	19
<b>CHAPTER 3      ANALYTICAL REPRESENTATION OF THE INTERACTION PROBLEM</b>	
3.1 Introduction	21
3.2 Beam Element	24
3.3 Truss Element	25



3.4	Four Noded Isoparametric Element	25
3.5	Characterisation of Soil Response	29
3.5.1	Linear Elastic models	29
3.5.2	Non-linear Elastic Models	30
3.5.3	Higher Order Elasticity Models	31
3.5.4	Plasticity Models	32
3.5.5	Selection of Soil Model for Analysis	32
3.6	The Incremental Method	33

#### **CHAPTER 4 THE FINITE ELEMENT COMPUTER PROGRAM**

4.1	Introduction	34
4.2	General Features of the Computer program	34
4.2.1	Storage of the Stiffness Matrix	35
4.2.2	Construction of the Stiffness Matrix	35
4.2.3	The Solution Routine	36
4.2.4	The Use of Spline Functions	36
4.2.5	Automatic Data Generation	38
4.3	Structure of the Computer Program	38

#### **CHAPTER 5 INTERACTION ANALYSIS OF RIGID RETAINING WALL**

5.1	Introduction	44
5.2	Loads on Structures	44
5.3	Material Properties	45
5.4	Finite Element Discretization and Boundary Conditions	47
5.5	Summary of Analysis Scheme	47
5.5.1	Effect of Moment of Inertia of Area of Wall	47
5.5.2	Effect of Moment of Inertia of Area of Wall Footing	50
5.5.3	Effect of Concrete Strength	50
5.5.4	Effect of Slope of Soil Surface	50
5.5.5	Effect of Unit Weight of Backfill	51
5.5.6	Effect of Poisson's Ratio	51
5.5.7	Effect of Angle of Internal Friction of Soil	51
5.5.8	Effect of Embedded Depth of Wall into the Original Soil	51
5.5.9	Effect of Line Load	52
5.5.10	Effect of Distributed Load	52
5.6	Selection of Horizontal and Vertical Extent of Soil in the Finite Element Mesh.	52

**CHAPTER 6      DISCUSSION ON FINITE ELEMENT ANALYSIS  
RESULTS**

6.1	Introduction	56
6.2	Effect of Various Parameters on Lateral Soil Force and Moment	56
6.2.1	Effect of Moment of Inertia of Retaining Wall	56
6.2.2	Effect of Moment of Inertia of Wall Footing	59
6.2.3	Effect of Compressive Strength of Concrete	61
6.2.4	Effect of Slope of Soil Surface	61
6.2.5	Effect of Unit Weight of Backfill Material	65
6.2.6	Effect of Poisson's Ratio of Backfill Material	65
6.2.7	Effect of Angle of Internal Friction of Backfill Material	68
6.2.8	Effect of Embedded Depth of Wall into the Original Soil	70
6.3	Effect of Line Load	72
6.4	Effect of Distributed Load	82
6.5	Deflected shape and stress-strain in soil	82
6.6	Limitations of Equations Derived From Interaction Analyses	83

**CHAPTER 7      COMPARISON OF FINITE ELEMENT ANALYSES  
RESULTS WITH RESULTS OF CONVENTIONAL  
METHODS**

7.1	Introduction	86
7.2	Comparison of Results for Self Weight only	86
7.3	Comparison of Results for Line Load	92
7.4	Comparison of Results for Uniformly Distributed Load	97

**CHAPTER 8      CONCLUSIONS AND RECOMMENDATIONS FOR  
FUTURE RESEARCH**

8.1	Conclusions	102
8.2	Recommendations for Future Research	104

**REFERENCES** 105

**APPENDIX A** 109

## LIST OF FIGURES

2.1	Mohr's Failure Stress Circle for a Triaxial Compression Test	8
2.2	Illustration of the Concept of Plastic Equilibrium	8
2.3	Failure Wedge used in Deriving the Coulomb Equation for Active Pressure	10
2.4	Forces Acting on the Failure Wedge used in Coulomb's Theory	10
2.5	Soil-structure System for the Rankine Solution for $\alpha = 90^\circ$	13
2.6	General Conditions and Mohr's Circle to Derive the Rankine Earth Pressure Equation	13
2.7	Identification of Terms Used in the Boussinesq Equation for Lateral Pressure	17
2.8	Notations Used in Ramon's Solution for Uniformly Distributed Load	17
2.9	Determination of Lateral Force and its Location for Uniformly Distributed Load by Coulomb's or Rankine's method	20
3.1	Beam Element	22
3.2	Truss Element	22
3.3	Four Node Isoparametric Element	23
4.1	Layout of a Typical Stiffness Matrix	37
4.2	Simplified Flow Chart of the Computer Program	40
5.1(a)	Octahedral Shear Stress & Strain Curves for Different Continuing Pressure of Original Soil.	46
5.1(b)	Octahedral Shear Stress & Strain Curves for Different Confining Pressure of Filled Soil.	46
5.2(a)	Finite Element Mesh of Retaining Wall-Soil System (Horizontal Backfill)	48
5.2(b)	Finite Element Mesh of Retaining Wall-Soil System (Slopping Backfill)	49
5.3	Variation of Moment with Horizontal Extent of Soil	53
5.4	Variation of Nodal Strain in Soil With Depth for a Wall of 9 ft Height	55
6.1	Effect of Inertia of Wall at its Base on Lateral Soil Force	58
6.2	Effect of Inertia of Wall at its Base on Moment to be Resisted by the wall	58
6.3	Effect of Inertia of Wall Footing on Lateral Soil Force	60
6.4	Effect of Inertia of Wall Footing on Moment to be Resisted by the Wall	60
6.5	Effect of Concrete Strength on Lateral Soil Force	62

6.6	Effect of Concrete Strength on Moment to be Resisted by the Wall.	62
6.7	Effect of Slope of Soil Surface on Lateral Soil Force	63
6.8	Effect of Slope of Soil Surface on Moment to be Resisted by the Wall.	63
6.9	Effect of Unit Weight of Backfill on Lateral Soil Force	66
6.10	Effect of Unit Weight of Backfill on Moment to be Resisted by the wall.	66
6.11	Effect of Poisson's Ratio on Lateral Soil Force	67
6.12	Effect of Poisson's Ratio on Moment to be Resisted by the Wall	67
6.13	Effect of Angle of Internal Friction on Lateral Soil Force.	69
6.14	Effect of Angle of Internal Friction on Moment to be Resisted by the Wall.	69
6.15	Effect of Embedded Depth on Lateral Soil Force.	71
6.16	Effect of Embedded Depth on Moment to be Resisted by the Wall.	71
6.17	Effect of Line Load on Lateral Soil Force For a Wall of 9 ft Height.	73
6.18	Effect of Line Load on Moment to be Resisted by a Wall of 9 ft Height.	73
6.19	Effect of Line Load on Lateral Soil Force For a Wall of 12 ft Height.	74
6.20	Effect of Line Load on Moment to be Resisted by a Wall of 12 ft Height.	74
6.21	Effect of Line Load on Lateral Soil Force For a Wall of 15 ft Height.	75
6.22	Effect of Line load on Moment to be Resisted by a Wall of 15 ft Height.	75
6.23	Effect of Line Load on Lateral Soil Force For a Wall of 18 ft Height	76
6.24	Effect of Line Load on Moment to be Resisted by a Wall of 18 ft Height.	76
6.25	Effect of Distance of Load on Lateral Soil Force for a Wall of 9 ft Height.	78
6.26	Effect of Distance of Load from Wall Face on Moment to be Resisted by a Wall of 9 ft Height	78
6.27	Effect of Distance of Load on Lateral Soil Force for a Wall of 12 ft Height.	79
6.28	Effect of Distance of Load from Wall Face on Moment to be Resisted by a Wall of 12 ft Height.	79
6.29	Effect of Distance of Load on Lateral Soil Force	

	For a Wall of 15 ft Height.	80
6.30	Effect of Distance of Load from Wall Face on Moment to be Resisted by a Wall of 15 ft Height.	80
6.31	Effect of Distance of Load on Lateral Soil Force For a Wall of 18 ft Height.	81
6.32	Effect of Distance of Load From Wall Face on Moment to be Resisted by a Wall of 18 ft Height.	81
6.33	Effect of Distributed Load on Lateral Soil Force	84
6.34	Effect of Distributed Load on Moment to be Resisted by the Wall.	84
6.35	Deflected Shape for the 9 ft High Retaining wall (wall height = 9ft)	85
6.36	Stress-strain diagram at two different locations in soil below the wall footing	85
7.1	Comparison of Lateral Soil Force Varying Slope of Soil Surface.(For Wall of 9 ft Height)	87
7.2	Comparison of Lateral Soil Force Varying Slope of Soil Surface.(For Wall of 12 ft Height)	87
7.3	Comparison of Lateral Soil Force Varying Slope of Soil Surface.(For Wall of 15 ft Height)	88
7.4	Comparison of Lateral Soil Force Varying Slope of Soil Surface.(For Wall of 18 ft Height)	88
7.5	Comparison of Moment with Varying Slope of Soil Surface ( forWall of 9 ft Height)	89
7.6	Comparison of Moment with Varying Slope of Soil Surface ( for Wall of 12 ft Height)	89
7.7	Comparison of Moment with Varying Slope of Soil Surface ( for Wall of 15 ft Height)	90
7.8	Comparison of Moment with Varying Slope of Soil Surface ( for Wall of 18 ft Height)	90
7.9	Comparison of Lateral Soil Force by Varying Position of Line Load ( for Wall of 9 ft Height)	93
7.10	Comparison of Lateral Soil Force by Varying Position of Line Load ( for Wall of 12 ft Height)	93
7.11	Comparison of Lateral Soil Force by Varying Position of Line Load ( for Wall of 15 ft Height)	94
7.12	Comparison of Lateral Soil Force by Varying Position of Line Load ( for Wall of 18 ft Height)	94
7.13	Comparison of Moment to be Resisted by Wall for Varying Position of Line Load (for Wall of 9 ft Height)	95

7.14	Comparison of Moment to be Resisted by Wall for Varying Position of Line Load (for Wall of 12 ft Height)	95
7.15	Comparison of Moment to be Resisted by Wall for Varying Position of Line Load (for Wall of 15 ft Height)	96
7.16	Comparison of Moment to be Resisted by Wall for Varying Position of Line Load (for Wall of 18 ft Height)	96
7.17	Comparison of Lateral Soil Force for Uniformity Distributed Load ( for Wall of 9 ft Height)	98
7.18	Comparison of Lateral Soil Force for Uniformity Distributed Load ( for Wall of 12 ft Height)	98
7.19	Comparison of Lateral Soil Force for Uniformity Distributed Load ( for Wall of 15 ft Height)	99
7.20	Comparison of Lateral Soil Force for Uniformity Distributed Load ( for Wall of 18 ft Height)	99
7.21	Comparison of Moment to be Resisted by Wall for Uniformly Distributed Load ( for Wall of 9 ft Height)	100
7.22	Comparison of Moment to be Resisted by Wall for Uniformly Distributed Load ( for Wall of 12 ft Height)	100
7.23	Comparison of Moment to be Resisted by Wall for Uniformly Distributed Load ( for Wall of 15 ft Height)	101
7.24	Comparison of Moment to be Resisted by Wall for Uniformly Distributed Load ( for Wall of 18 ft Height)	101

## LIST OF TABLES

5.1	Unit Weight of Materials Used	45
6.1	Values of K for Equation $M_1 = K.P$	72
6.2	Values of a' and b' for the Equation $M_1 = a'e^{-b'x} P$	77
A.1	Effect of Moment of Inertia of Area of Wall at its Base on Lateral Soil Force ( $P_a$ ) and Moment (M)	110
A.2	Effect of Moment of Inertia of Area of Wall Footing on Lateral Soil Force ( $P_a$ ) and Moment (M)	110
A.3	Effect of Concrete Strength on Lateral Soil Force ( $P_a$ ) and Moment (M)	110
A.4	Effect of Slope of Soil Surface on Lateral Soil Force ( $P_a$ ) and Moment (M)	111
A.5	Percentage of Increase in Moments with Respect to Horizontal Backfill, for Increase of Slope of Soil Surface by Finite Element Method and by Proposed Formulae.	111
A.6	Effect of Unit Weight of Backfill Material on Lateral Soil Force ( $P_a$ ) and Moment to be Resisted by the Wall (M)	111
A.7	Percentage of Change in Lateral Soil Force ( $P_a$ ) and Moment (M) for Changing Unit Weight.	112
A.8	Effect of Poisson's ratio on Lateral Soil Force ( $P_a$ ) and the moment (M)	112
A.9	Effect of Angle of Internal friction on Lateral Soil Force ( $P_a$ ) and Moment (M).	113
A.10	Effect of Embedded Depth on Lateral Soil Force ( $P_a$ ) and Moment (M).	113
6.11	Effect of Magnitude and Location of Line Load on Lateral Soil Force ( $P_a$ ) and Moment (M) for 9 ft Height Wall.	114
A.12	Effect of Magnitude and Location of Line load on Lateral Soil Force ( $P_a$ ) and Moment (M) for 12 ft Height Wall.	114
A.13	Effect of Magnitude and Location of Line Load on Lateral Soil Force ( $P_a$ ) and Moment (M) for 15 ft Height Wall.	115
A.14	Effect of Magnitude and Location of Line Load on Lateral Soil Force ( $P_a$ ) and Moment (M) for 18 ft Height Wall.	115
A.15	Effect of Uniformly distributed Load on Lateral Soil Force ( $P_a$ ) and Moment (M)	116
A.16	Lateral Soil Force and the Moment for Dead Load only From Coulomb, Rankine and Finite Element analysis ( $\phi=28^\circ$ )	117

A.17	Ratio of Wall Height and Distance of Resultant Horizontal Lateral Soil Force from the Base of Wall Obtained from Finite Element Analyses.	117
A.18	Percentage of Difference in Lateral Soil Force ( $P_a$ ) and Moment ( $M$ ) in Rankine's and Coulomb's Method with respect to Finite Element Method.	118
A.19	Lateral Soil Force and Moment for Line Load by Boussinesq, Trial Wedge and Finite Element Method (Excluding self Weight).	119
A.20	Lateral Soil Force and Moment for Uniformly Distributed Load by Rankine, Coulomb, Ramon, Finite Element Method.	120



## NOTATION

A	Cross sectional area
a	Length of strip loading
B	Strain-displacement matrix
b	Distance of strip load from the wall face
D	Elasticity matrix
E	Young's modulus of elasticity
E'	Modulus of elasticity in plane strain condition
E <sub>c</sub>	Modulus of elasticity of concrete
f' <sub>c</sub>	Compressive strength of concrete at 28 th day
G	Shear modulus
H,h	Height of wall
K	Bulk modulus, stiffness matrix
K <sub>a</sub>	Coefficient of active earth pressure
L	Length of beam element
M	Constrained modulus, Moment at depth H
M <sub>O</sub>	Moment at depth H for horizontal backfill
M <sub>β</sub>	Moment at depth H for slope of soil surface β degree
N <sub>1</sub> ,N <sub>2</sub> ,N <sub>3</sub> ,N <sub>4</sub>	Shape functions
P	Line load
P <sub>a</sub>	Wall force due to lateral soil pressure
q	Intensity of strip load
R	Resultant force between failure wedge and remaining soil mass, in Coulomb and Rankine theories. radial distance of the point from the point of application of load Boussinesq equation.
r	Horizontal distance of the point considered from the point of application of load in Boussinesq equation, radius of Mohr's circle (Rankine's method )
T	Transformation matrix
u,v	Global deflection
$\bar{y}$	Distance of resultant Lateral Soil Force for uniformly distributed load from soil surface
W	Weight of failure wedge
X,Y,Z	Local Cartesian co-ordinate
Z	Vertical distance of the point where stress is calculated from the point of application of load.

$\alpha$	Angle of wall with horizontal
$\beta$	Slope of soil surface with horizontal
$\gamma$	Unit weight of soil
$\gamma_{xy}$	Shear strain
$\rho$	Rupture angle of soil wedge retained by a wall
$\delta$	Angle of wall friction
$\phi$	Angle of internal friction of soil
$\nu$	Poisson's ratio
$\sigma_x, \sigma_y$	Normal stress
$\sigma_1$	Major principal stress
$\sigma_3$	Minor principal stress
$\sigma_{a,hor}$	Horizontal component of stress (active)
$\sigma_r$	Radial stress (Boussinesq)
$\sigma_h$	Horizontal stress (Ramon)
$\theta$	Angle between a line connecting the point of interest with the point of applied load, and the vertical line passing through the loaded point
$\theta_a$	Angle between the vertical axis and the line connecting the starting point of strip load with the point where stress is calculated
$\theta_b$	Angle between the vertical axis and the line connecting the end point of strip load with the point where stress is calculated.
$\theta_1$	Angle between the vertical axis and the line connecting the starting point of strip load with the base of the wall.
$\theta_2$	Angle between the vertical axis and the line connecting the end point of strip load with the base of the wall.
$\{\delta\}$	Vector of nodal deflections
$\{\epsilon\}$	Strain vector
$\epsilon_{xx}, \epsilon_{yy}$	Normal strain
$\tau_{xy}$	Shear stress.

## CHAPTER 1

# GENERAL INTRODUCTION

### 1.1 INTRODUCTION

Moderate to large height retaining walls are frequently used to retain soil which may support highway, railway or ordinary building systems. Structural performance of these walls are influenced by the soil under them and by the soils retained by them.

Retaining wall, being a structure supported on earth and supporting the soil on one of its side, interacts with the soil. Soil, which is retained by the wall, contributes to the performance of the wall; it helps to distribute the surcharge load ( surface loads ) more evenly and reduces their intensity. At present state, loads on the wall are calculated simply by the soil property. The structural properties of the wall and its base are not taken into account. Due to the deformation and rigid body movement of the retaining wall, stress redistribution in the structure takes place. Thus the behaviour of a retaining wall and the soil mass poses a complex problem and must be addressed by applying the principles of structure-soil interaction. This interaction can only be studied by a realistic and comprehensive finite element model.

In this study attempts have been made to construct an analytical model that closely resembles the real field behaviour. Detailed investigations have been performed to study the fundamental behaviour of rigid retaining walls under various conditions.

### 1.2 REVIEW OF INTERACTIVE ANALYSIS

For an interactive analysis few exhaustive methods are available. Most of these methods simplify the behaviour of the structure or the soil or both and give results which are insufficient. The traditional concept attacks the problem as a two phase system. The structure is one and the soil is the other. Attempts are then made to account for the interaction between these two phases by some simplified approach. Either the structure is supported by a fictitious soil or the soil is analysed, with the structure being represented by an artificial model.

Since the original development of the concept of interaction of building frames with their supporting soil and the need for inclusion of structural rigidity in calculating settlements of their supports by Meyerhof (1947), much progress has been made and the phenomenon of structure-soil interaction has received extensive attention of research workers. An extensive review is obtained in the works performed by Rahman (1978). In the recent past a number of texts dealing specially with structure-soil interaction problems and their solutions have appeared, most significant among them is that by Desai and Christian (1977), which covers a wide range of problems and gives a useful introduction to analysis techniques. Other important texts are by Gudehus (1977), Zienkiewicz (1978) and Selvadurai (1979). Selvadurai presents an exhaustive treatment of analytical methods for the solution of problems involving beams and plates on a soil mass represented by either a winkler material or an elastic continuum. Of particular value is the summary of solutions for a plate on a elastic half-space, which is of direct utility in the design of raft foundations. Three comprehensive general reviews have also been published. Hooper (1978) summarises methods and solutions for the linear elastic analysis of foundation under static loading, including raft, pile groups, pile-raft foundations and problems in which superstructure stiffness is accounted for. Meyerhof (1979) considers a similar range of problems but also summarises some available data on allowable deformation of structures. A feature of Meyerhof's paper is the compact and clear representation of a number of theoretical and experimental results in a readily usable form. Poulos (1981) gives a general report reviewing the development in the area of structure-soil interaction since 1977. Karim (1985) performed a series of plane strain finite element analyses of large diameter flexible pipe culverts. In the interaction analysis Karim (1985) represented the culvert by straight Beam-Column elements and the soil by four node Iso-P elements. He studied the effects of soil and structural parameters such as stiffness of culvert, depth of cover above the crown, size and shape of the culvert and Poisson's ratio of soil on the performance of flexible metal culverts. Nazneen (1986) studied the interaction between framed structures with orthotropic wall infills and their supporting soil by employing the finite element methods, which considered the non-linear three dimensional structure-soil interaction. Parameters such as deflections, bending moments, soil stresses, wall stresses and crack propagation were examined in detail by her. Seraj (1986) developed a two-dimensional non-linear finite element program to cater for the interaction analysis of various rigid culverts buried in soil. In his study

Seraj (1986) examined the effects of installation conditions, depth of cover above the crown and thickness of culvert on axial force, bending moment, shear force and deflection at various points of the rigid pipe culvert. He represented the rigid culvert by circular beam elements, soil by eight node isoparametric element and used interface elements at the interface of soil and culvert. He took care of tensile separation of the soil mass. Further development in this field was carried out by Seraj and Rahman (1987). Later Bhattacharjee (1989) extended the numerical model of Seraj (1986) and Seraj and Rahman (1987) for dynamic analysis. He studied the dynamic response of soil without buried structure and the interactive response of a buried structure subjected to impulsive loading on the surface. Base conditions of rigid and semi-infinite cases were investigated to study their influence on the response of the system. He performed a parallel series of non-linear static analyses for the maximum magnitude of shock loading. Ziegler (1987) studied the displacement dependent earth pressure on retaining walls interacting with sand. He confirmed that both magnitude and the distribution of the earth pressure depends considerably on the type of wall motions. Small displacements of the wall can cause significant change in the earth pressure. His interaction analyses studied in the magnitude of resulting active earth pressure force smaller than the classical value obtained with Coulomb's theory and he recommended to consider displacement dependent earth pressure in the design, instead of the classical theory with a linear earth pressure distribution. Tien et al, (1988) studied the soil reinforcement using roots by considering the contribution of the tensile force in a root segment that intersects a potential slip surface in a soil-root system. They evaluate the tensile force when the system is subjected to a shear displacement by considering the root segment as a beam on elastic plastic support and as a cable for small and large deflection. Equilibrium and displacement compatibility at a branch point was used to analyse the distribution of forces between two root branches of a root system, by them. Mauricio and Michel (1989) performed the interaction analysis of pile groups for displacement and distribution of loads among the pile heads by means of a stiffness matrix equation that incorporates individual pile stiffness and the influence of piles on their neighbours using pile head interaction factors. Harry (1988) found that if the soil between the piles in a group is considered to be stiffer than the soil directly adjacent to the pile, the settlement interaction between piles in a group is reduced. The extent of this reduction depends on the ratio of Young's modulus of soil mass to the Young's modulus of pile, the geometry and relative stiffness of the piles. He found that

conventional analysis techniques provide conservative answers. Chow and Teh (1991) presented a numerical model to study the behaviour of vertically loaded pile groups embedded in a non-homogeneous soil with the pile caps in contact with the ground. The considered soil profiles consist of soil with Young's moduli increasing linearly with depth. They did not consider the non-linear behaviour. They presented parametric solution to show the influence of the distribution of the soil Young's moduli on the behaviour of the groups. John (1993) proposed an improved model for soil-structure interaction analysis which he termed as Reissner simplified continuum (RSC) and claimed it to be the most accurate subgrade model developed to date for use in routine practice. Software modifications to accommodate this model in structural analysis software are relatively simple. Although the significantly improved accuracy of this model compared to Winkler's hypothesis has been demonstrated both theoretically and using case histories of mat foundations, acceptance and implementation of the RSC in practice has been slow to date. Seraj (1993) proposed physical models, in compliance with the concept of Compressive-Force Path (CFP), to encompass reinforced concrete footings and retaining structures. He opined that, a reappraisal of the current design concepts, rather than changes in the design equations, should be prerequisite for any future code revision. The author claimed that by introducing new design models the CFP method, which departs radically from established design philosophy, may be extended to a more realistic ultimate limit state design of reinforced concrete geotechnical structures.

### **1.3 OBJECTIVE OF THE PRESENT RESEARCH**

The general objective of the research are:

- (a) To use a plane strain finite element computer program for the non-linear incremental analysis of rigid retaining wall and soil as an integral system, and write routines to incorporate such features as automatic data generation, footing shape, slope of soil surface, soil reinforcement etc.
- b) To use the program to analyse a series of different retaining wall-soil systems to gain an insight into their behaviour.
- c) To study the effect of several parameters such as wall thickness, footing

shape, wall height, surcharge load, slope of soil surface, unit weight of soil, Poisson's ratio, strength of concrete, on the performance of the retaining wall.

d) To compare the values obtained from the analysis with the values obtained from available methods.

#### 1.4 SCOPE OF THE WORK

By using a finite element computer program the interaction in a retaining wall-soil system can be dealt with. It was decided to use plane strain finite element method for interactive analysis. The retaining wall was represented by a series of beam elements having linear elastic properties. The soil was represented by plane strain four noded isoparametric quadrilateral elements. The non-linear properties of the soil were represented by a set of curves relating octahedral shear stress and octahedral shear strain. The curves were followed in the analysis by using cubic spline function and adopting an incremental solution technique.

Chapter 2 of this thesis describes the currently available methods for the analysis of retaining walls. In Chapter 3 the analytical representation of the interaction problem is discussed. Computer programs were developed to analyse the system represented by the model described in Chapter 4. The program considers the retaining wall-soil as an integral system. The problem is huge and would ordinarily be beyond the storage capacity and calculating speed of most ordinary computers. Novel techniques, for the efficient storage of various matrices and solution of simultaneous equations, use of different soil and materials properties to accommodate different shape and size of base, soil reinforcement, surface slope, surcharge load are all included in the program. These result in an efficient utilisation of storage and time and make the program viable for even microcomputers like 386 and 486.

As soon as the new subroutines ( programs ) are developed, and associated with the available plane-strain computer program for soil-structure interaction, it can be used as an analytical tool to gain an insight into the behaviour of different retaining wall-soil systems. A planned scheme of analysis of retaining wall with different height, wall and base thickness, soil and its surface slope, shape of footing was undertaken. The analyses are described in Chapter 5. Results are

discussed in Chapter 6. Comparison of finite element analysis results with results obtained from available methods for various cases are presented in Chapter 7. Conclusions and recommendations for future research are presented in Chapter 8.



## CHAPTER 2

# ANALYSIS METHODS FOR RETAINING WALL

### 2.1 INTRODUCTION

When a retaining wall is being designed, the designer must check the stability of the wall. The wall must be stable against:

1. Stem shear and bending due to lateral earth pressure on the stem. This is computed from soil parameter and height of the stem.
2. Base shear and bending moment at the stem caused by wall loading producing earth pressure on the base.
3. Overall wall stability, i.e.,
  - a) Sliding-produced by earth pressure on the vertical plane.
  - b) Overturning about the toe
  - c) Rotational stability
4. Stability against bearing capacity failure.

An attempt is made to estimate the shear and bending moment developed at the base of stem by the lateral pressure due to soil and surcharge load by finite element method for different types of soil, wall height etc. These values will be compared with the values obtained from the traditional methods. A brief discussion on the lateral earth pressure and its estimation by traditional methods is made first.

### 2.2 TRADITIONAL METHODS OF ANALYSIS

For estimating the lateral pressure from earth, the most generally used method is the method of plastic equilibrium as defined by Mohr's rupture envelope of Figs 2.1 and 2.2. Active earth pressure refers to the plastic equilibrium state defined by rupture circle AC of Fig.2a. The minimum principal stress,  $OC = \sigma_3$  is termed the active earth pressure which is given by

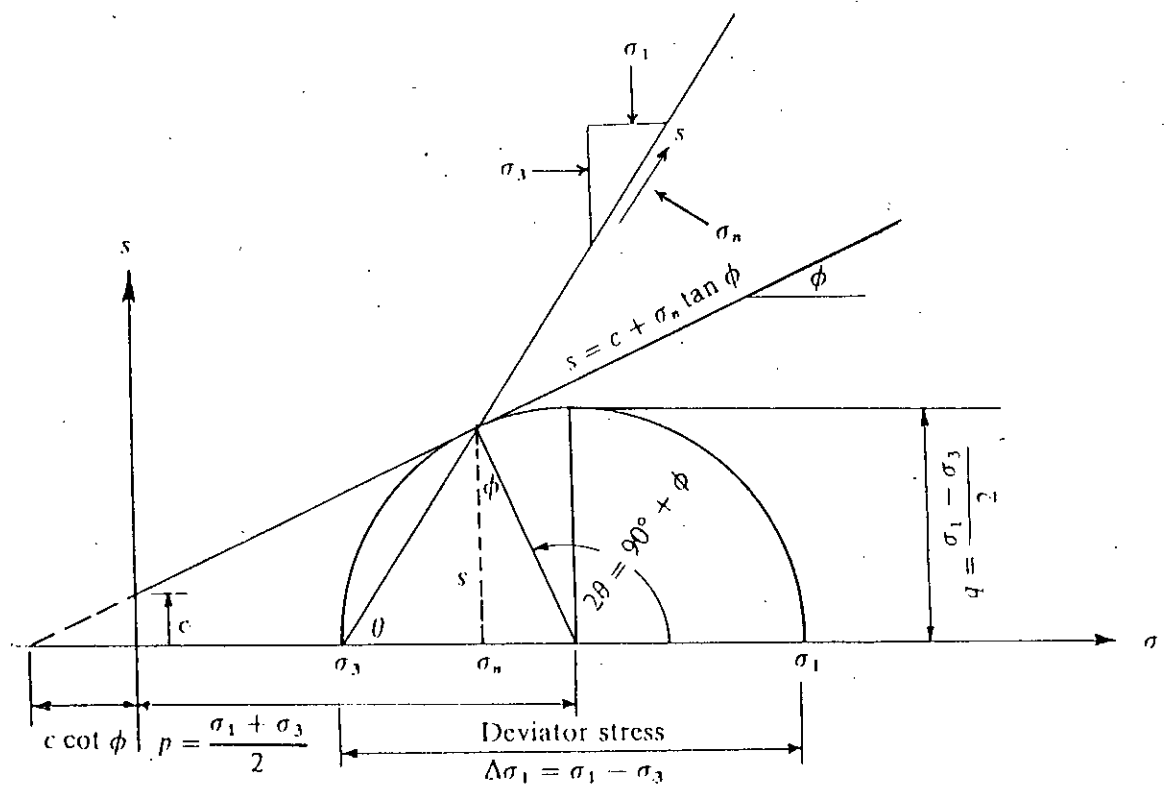


**Figure 2.1 Mohr's failure stress circle for a triaxial compression test (Bowles, 1988)**

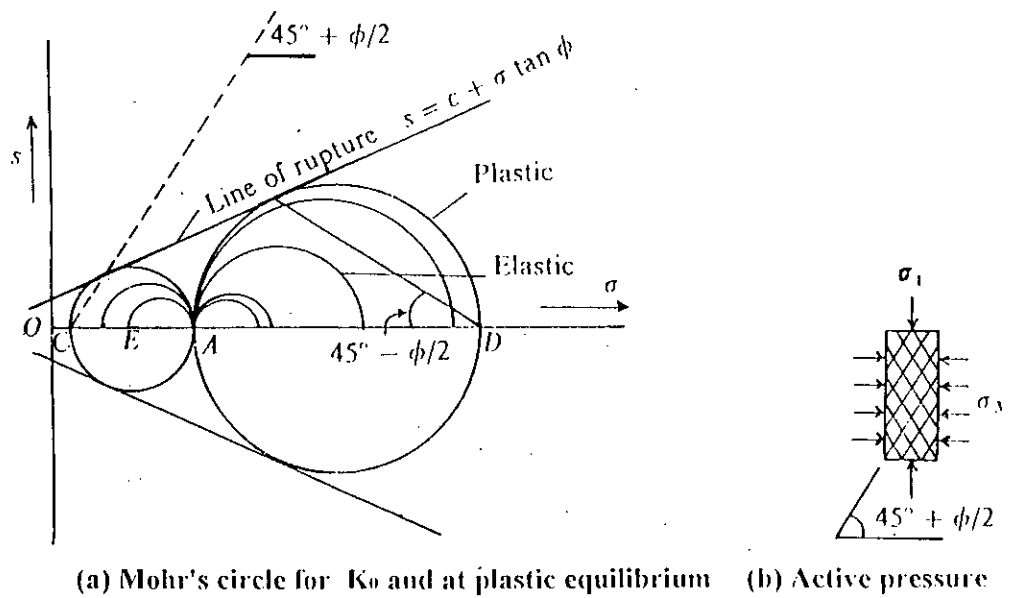


**Figure 2.2 Illustration of the concept of plastic equilibrium (Bowles, 1988)**

$$\sigma_3 = \sigma_1 \tan^2 (45^\circ - \phi/2) - 2C \tan (45^\circ - \phi/2)$$

for cohesionless soil putting  $C = 0$ ,

$$\sigma_3 = \sigma_1 \tan^2 (45^\circ - \phi/2).$$

Here,  $\tan^2 (45^\circ - \phi/2)$  is termed as the active earth pressure coefficient, the usual range of it for cohesionless soil is between 0.22 to 0.33.

To determine the loads on a retaining wall, following theoretical methods are available:

- a) Coulomb earth pressure theory
- b) Rankine earth pressure theory
- c) Active earth pressure using theory of plasticity
- d) Graphical solution for lateral earth pressure.  
(Culmann's solution, trial-wedge method)

### 2.2.1 Coulomb Earth Pressure Theory

This is one of the earliest method for estimating earth pressure against wall by Coulomb (1776). He made the following assumptions:

- i) Soil is isotropic, homogeneous and has both internal friction and cohesion.
- ii) The rupture surface is a plane surface (like AE in Fig. 2.3) and the backfill surface is planer (it may have slope but is not irregularly shaped).
- iii) The friction resistance is distributed uniformly along the rupture surface and the soil-to-soil friction coefficient is given by,  $f = \tan \phi$ .
- iv) The failure wedge is a rigid body undergoing translation.
- v) There is wall friction i.e., as the failure wedge moves with respect to the backface of the wall, a friction force is developed between soil and wall. This friction angle is usually denoted as  $\delta$ .
- vi) Failure is a plane strain problem; consider a unit slice from an infinitely long wall.

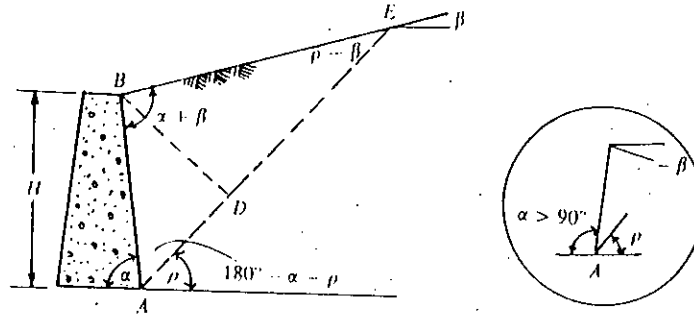
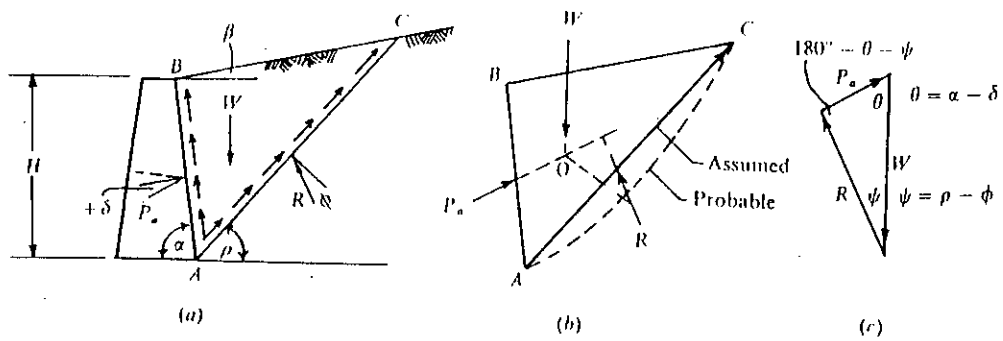


**Figure 2.3** Failure wedge used in deriving the Coulomb equation for active pressure (Bowles, 1988)



(a) Assumed conditions for failure (b) Indicates all force vectors may not pass through point O  
 (c) Force triangle to establish  $P_a$

**Figure 2.4** Forces acting on the failure wedge used in Coulomb's theory (Bowles, 1988)

The principal deficiencies in the Coulomb theory are in the assumption of an ideal soil and that the rupture zone is a plane. But for clean sand in the active pressure case photographs of model wall indicates ( Bowles, 1988 ) that the rupture zone is very nearly a plane.

In Fig 2.3 from triangle ABD

$$BD/AB = \sin ( 180 - \alpha - \rho )$$

$$BD = AB \sin ( \alpha - \rho )$$

also from Triangle ABE

$$\frac{AE}{\sin(\alpha + \beta)} = \frac{AB}{\sin(\rho - \beta)}$$

From Fig 2.3

$$\frac{H}{AB} = \sin \alpha$$

$$AB = H \sin \alpha$$

Hence area of the failure wedge ABE

$$= \frac{1}{2} BD \cdot AE$$

$$= \frac{1}{2} \cdot AB \cdot \sin(\alpha + \rho) \cdot AB \cdot \frac{\sin(\alpha + \beta)}{\sin(\rho - \beta)}$$

$$\text{Area} = \frac{H^2}{2 \sin^2 \alpha} \cdot \frac{\sin(\alpha + \rho) \cdot \sin(\alpha + \beta)}{\sin(\rho - \beta)}$$

so, weight of the wedge per unit width

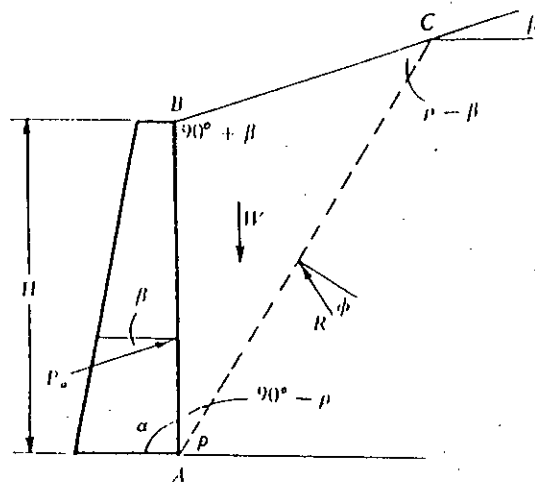
$$W = \frac{\gamma \cdot H^2}{2 \sin^2 \alpha} \left[ \sin(\alpha + \rho) \cdot \frac{\sin(\alpha + \beta)}{\sin(\rho - \beta)} \right]$$

The active force  $P_a$  is a component of the weight vector as shown Fig 2.4c.

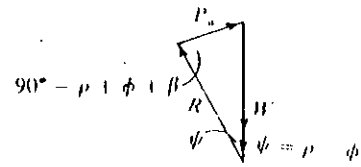
Applying law of sines,

$$\frac{P_a}{\sin(\rho - \phi)} = \frac{W}{\sin(180 - \alpha - \rho + \phi + \delta)}$$

or,

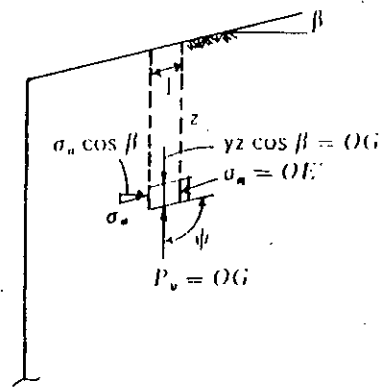


(a) Soil-structure system

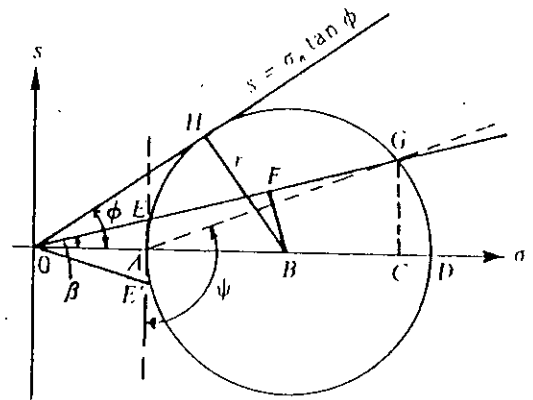


(b) force triangle

**Figure 2.5 Soil-structure system for the Rankine solution for  $\alpha = 90^\circ$  (Bowles, 1988)**



(a) General case.



(b) Mohr's circle.

**Figure 2.6 General conditions and Mohr's circle to derive the Rankine earth pressure equation (Bowles, 1988)**

$$OF = OB \cos \beta$$

$$OG = \gamma z \cos \beta$$

$$K_a = \frac{OE}{OG} = \frac{OF - EF}{OF + FG} = \frac{OE'}{OG}$$

after simplification and noting that,  $\sigma_{a, \text{hor}} = \sigma_a \cos \beta$

Equation becomes,

$$P_a = \frac{1}{2} K_a \gamma H^2 \quad (2.3)$$

where,

$$K_a = \cos \beta \cdot \frac{\cos \beta - \sqrt{\cos^2 \beta - \cos^2 \phi}}{\cos \beta + \sqrt{\cos^2 \beta - \cos^2 \phi}}$$

### 2.2.3 Graphical and Computer Solution for Lateral Earth Pressure

To estimate lateral forces when the backfill is irregular-shaped or there are line loads, there are several graphical solutions. These two conditions do not fit the Coulomb or Rankine theory. Available methods are: Culmann's (1986) method, the Trial-Wedge method (1877), and logarithmic spiral method.

The Culmann and Trial-wedge methods are very similar except for the general orientation on the force polygons. Both methods rely on computing the known forces on a trial wedge which includes any external load on the backfill, the weight of the trial wedge, the shear force on the trial rupture surface and from known slopes of the wall force  $P_a$  and the resultant force  $R$  on the rupture surface, plot a force polygon and graphically obtain  $P_a$ . The log spiral is similar but uses a part of a log spiral to define the rupture surface where the Culmann and trial wedge method use a plane surface.

The point of application of the active earth pressure is suggested by Terzaghi (1943) for different load cases i.e., (i) No concentrated load, but may have other surcharge (ii) concentrated load as line load within the failure wedge (iii) concentrated load or line load outside the failure wedge. Bowels suggests that the best solution for total wall force and point of application when there are

concentrated load of any type is to:

1. Obtain the coulomb or Rankine solution.
2. Obtain theory of Elasticity solution
3. Combine solutions 1 and 2 to find total force and point of application using

$$P = \sum P_i$$
$$\bar{y} = \frac{\sum P_i y_i}{P}$$

Then use the value of  $\bar{y}$  with trial wedge  $P_a$

#### 2.2.4 Active earth Pressure Using Theory of Plasticity

Caquot and Kerisel (1948) produced tables of earth pressure based on non plane-failure surfaces, later Janbu (1957) and more recently Shields and Tolunay (1973) proposed an approach to the earth pressure problem similar to the method of slices used in slope-stability analysis. Sokolovski (1960) presented a finite difference solution using a highly mathematical method. All these methods give smaller values for passive-earth pressure coefficient. None of the methods improves on the Coulomb or Rankine active-earth pressure coefficients.

Rosenfarb and Chen (1972) developed a closed form solution using plasticity theory which also solves earth pressure problem for active and passive pressure. They considered several failure surfaces, and the combination of a long sandwich mechanism which compared most favourably with the Sokolovski solution.

#### 2.3 ANALYSIS FOR SURCHARGE LOAD

Surcharge loads may be (i) Line load (ii) Uniformly distributed load. Traditional methods such as Coulomb's method or Rankine's method can not deal with line load but can deal with uniformly distributed load. To estimate the effect of surcharge load in addition to the above stated methods, following methods are available.



- i) Boussinesq equation
- ii) Trial wedge solution
- iii) Ramon's solution for strip loading

### 2.3.1 Boussinesq Equation

To compute the lateral earth pressure against the wall from surface surcharge one of the methods which appears in the text books is the use of Boussinesq equation. The equation is based on theory of elasticity. The Boussinesq equation is

$$\sigma_r = \frac{P}{2\pi z^2} \left[ 3 \sin^2 \theta \cdot \cos^3 \theta - \frac{(1-2\nu) \cos^2 \theta}{1 + \cos \theta} \right] \quad (2.4)$$

Equation 2.4 can also be written as

$$\sigma_r = \frac{P}{2\pi} \left[ \frac{3r^2 z}{R^5} - \frac{(1-2\nu)}{R(R+z)} \right] \quad (2.5)$$

Where terms as  $\theta$ ,  $z$ ,  $r$ ,  $R$  is shown in Fig. 2.7,  $\nu$  is the Poisson's ratio and  $P$  is the line load. The method can be used both for concentrated and line loading.

### 2.3.2 Trial Wedge Solution

The Trial-wedge method seems to be overly conservative in estimating the lateral force against a wall when there are surcharge on the backfill. For this reason this method is not very popular now a days.

### 2.3.3 Ramon's Solution for Strip Loading

Ramon Jarquio(1981) provides an analytical approach for direct solution for the surcharge pressure due to strip load as shown in Fig. 2.8.

Ramon doubled the horizontal pressure against unyielding walls from surcharge load to fit experiment data and proposed

$$\sigma_h = \frac{2 \cdot q}{\pi} (\beta - \sin \beta \cdot \cos 2\alpha) \quad (2.6)$$

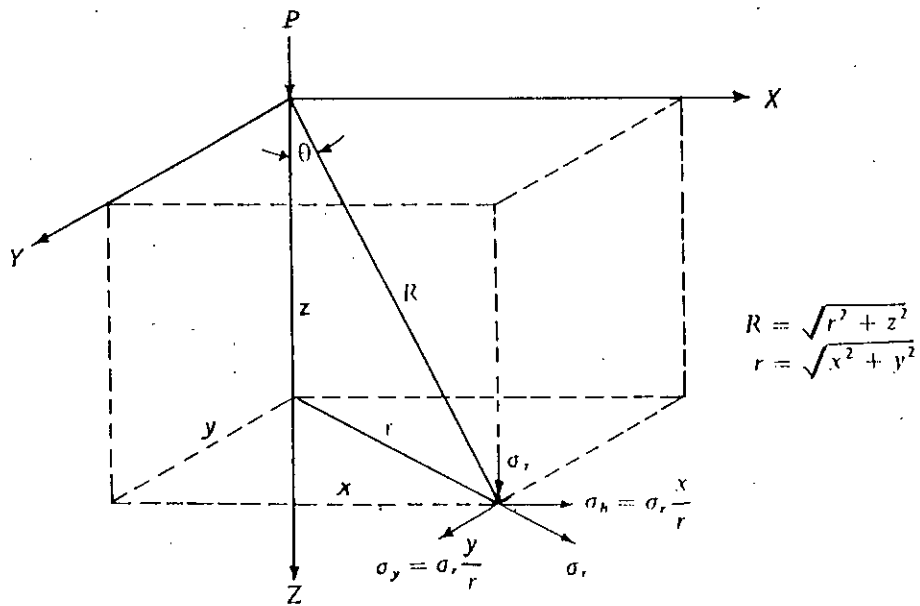


**Figure 2.7** Identification of terms used in the Boussinesq equation for lateral pressure (Bowles, 1988)

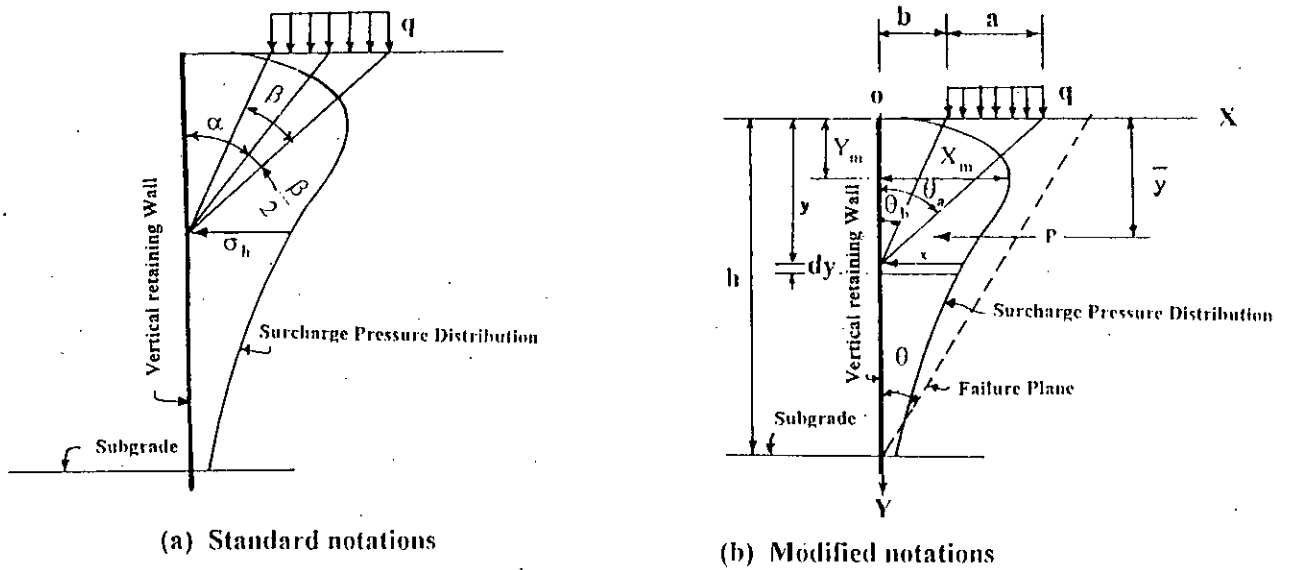


**Figure 2.8** Notations used in Ramon's solution for uniformly distributed load (Ramon, 1981)

Transforming above equation and substituting.

$$\beta = (\theta_a - \theta_b)$$

$$\alpha = \frac{(\theta_a + \theta_b)}{2}$$

$$\sigma_h = X,$$

equation 2.6 yields

$$X = \frac{2q}{\pi} [(\theta_a - \theta_b) - (\sin \theta_a \cos \theta_a - \sin \theta_b \cos \theta_b)]$$

or,

$$X = \frac{2q}{\pi} \left[ \left[ \cot^{-1} \frac{y}{a+b} - \cot^{-1} \frac{y}{b} \right] - \left[ \frac{y}{(a+b) + \frac{y^2}{a+b}} - \frac{y}{b + \frac{y^2}{b}} \right] \right]$$

Now

$$dP = X dy$$

$$P = \int X dy$$

Integrating and evaluating limits

$$P = \frac{2qh}{\pi} (\theta_2 - \theta_1) \quad (2.7)$$

when  $\theta_2$  and  $\theta_1$  are expressed in degrees

$$P = \frac{qh}{90} (\theta_2 - \theta_1) \quad (2.8)$$

and distance of resultant from the top is given by

$$\bar{y} = \frac{h^2 (\theta_2 - \theta_1) + (R - Q) - 57.03.ah}{2h(\theta_2 - \theta_1)} \quad (2.9)$$

where ,

$$R = (a+b)^2 (90 - \theta_2)$$

$$Q = b^2 (90 - \theta_1)$$

so bending moment  $M$  is given by

$$M = P(h - \bar{y}) \quad (2.10)$$

For active earth pressure condition  $(a+b) < h \tan (45^\circ - \phi/2)$   
i.e., load should be applied within the failure plane.

### **2.3.4 Analysis for Surcharge Load by Coulomb's and Rankine's Method**

The surcharge load, which is essentially an uniformly distributed load, is converted into an equivalent depth of soil and then analysis is made for the given height of the wall. These methods are explained in Fig. 2.9.

### **2.4 Methods selected for comparing results of finite element analyses:**

For comparing results of finite element analyses, the following methods are selected and listed with the particular cases:

Case 1: For self weight only

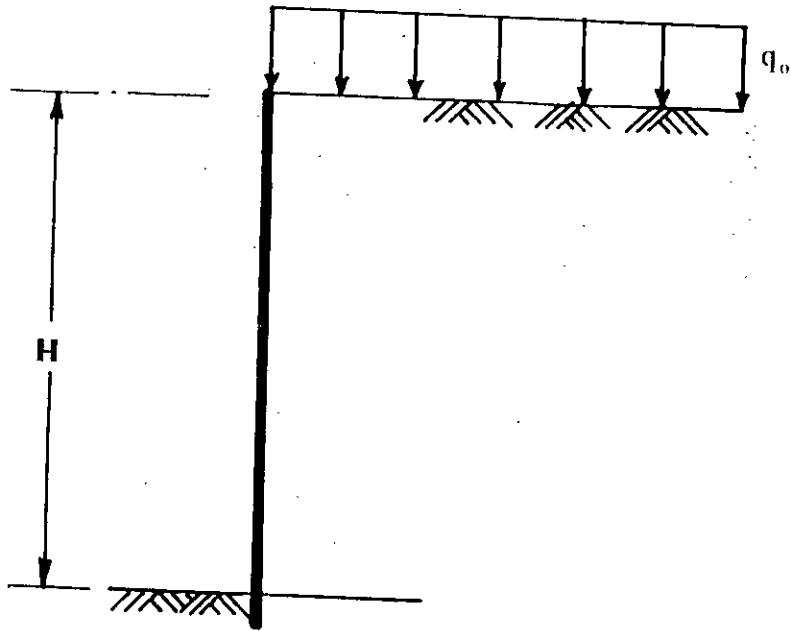
- a) Rankine's method.
- b) Coulomb's method.

Case 2: For line loading (excluding self weight)

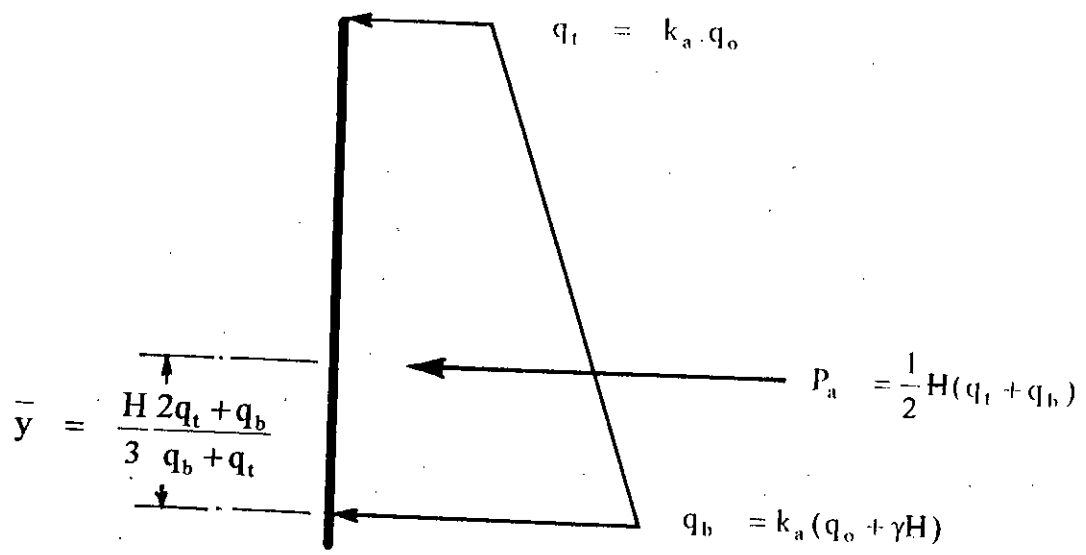
- a) Boussinesq equation.
- b) Trial wedge solution.

Case 3: For uniformly distributed load

- a) Rankine's method
- b) Coulomb's method
- c) Ramon's method



(a) Wall with surcharge load



(b) Equivalent pressure diagram with magnitude and location of resultant force

Figure 2.9 Determination of lateral force and its location for uniformly distributed load by Coulomb's or Rankine's method

## CHAPTER 3

# ANALYTICAL REPRESENTATION OF THE INTERACTION PROBLEM

### 3.1 INTRODUCTION

To determine the actual behaviour of the retaining wall-soil system it is essential to apply the finite element method. The main difficulties encountered during the programming phase was the construction of analytical models that closely resemble actual field behaviour and at the same time, striking a balance between rigorous mechanics and engineering simplicity. In case of retaining wall-soil system, construction of the analytical model considers the aspect of structure-soil system, i.e., structural constitutive model, soil constitutive model, simulation of footing shape, wall size, non-linearity of soil, boundary conditions etc. Considering all the above mentioned aspects of the retaining wall-soil system, a finite element computer program has been suitably adapted so that these aspects representing the actual field behaviour are included.

Three types of elements have been used in the computer program to study the behaviour of the retaining wall-soil system.

- a) To represent the retaining wall, beam element (Fig.3.1) having three degrees of freedom at each node, was used. The degrees of freedom are horizontal and vertical displacement and a rotation in its plane.
- b) To represent the tie/soil reinforcement (whenever used) truss element (Fig.3.2) with two degrees of freedom at each node, was used. The degrees of freedom are horizontal and vertical movement.
- c) Four noded isoparametric/quadrilateral elements (Fig.3.3) with two degrees of freedom at each node was used to represent the soil. The degrees of freedoms are horizontal and vertical displacement.

To simulate the non-linear stress-strain characteristics of soil, spline function has been used.

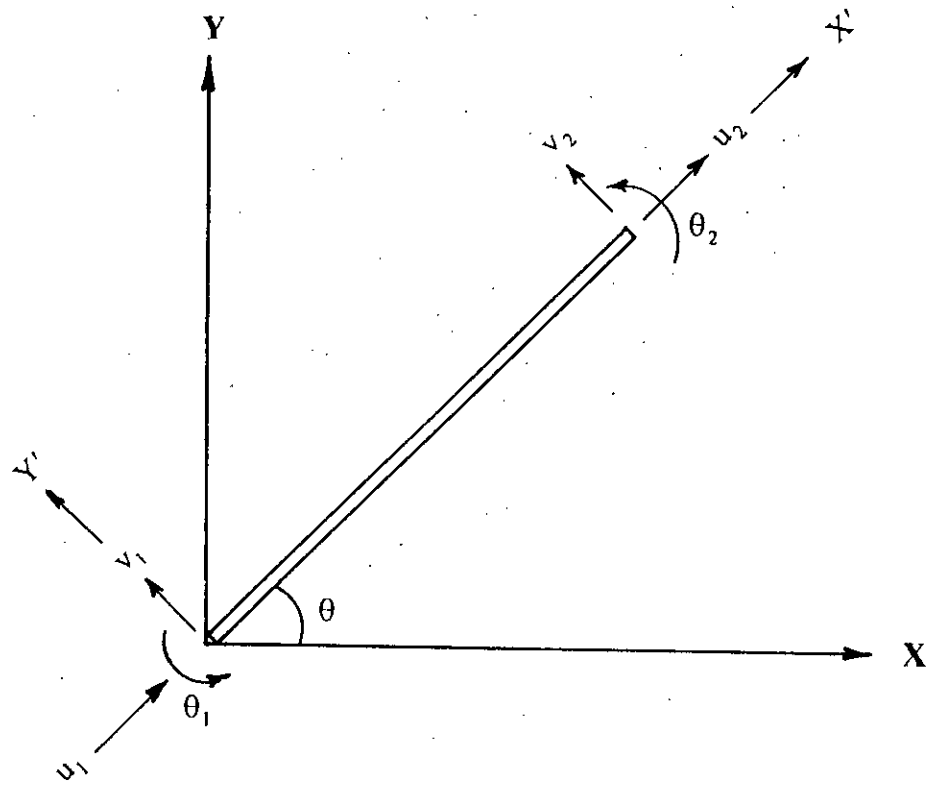


Figure 3.1 Beam element

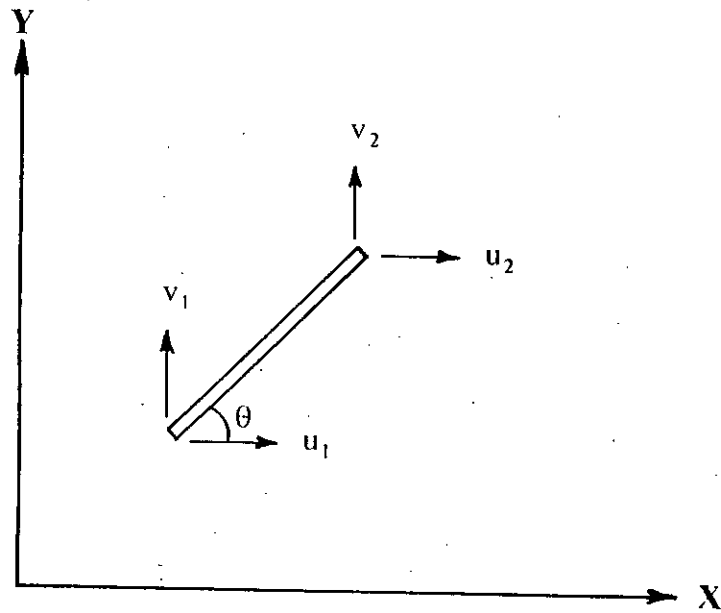


Figure 3.2 Truss element

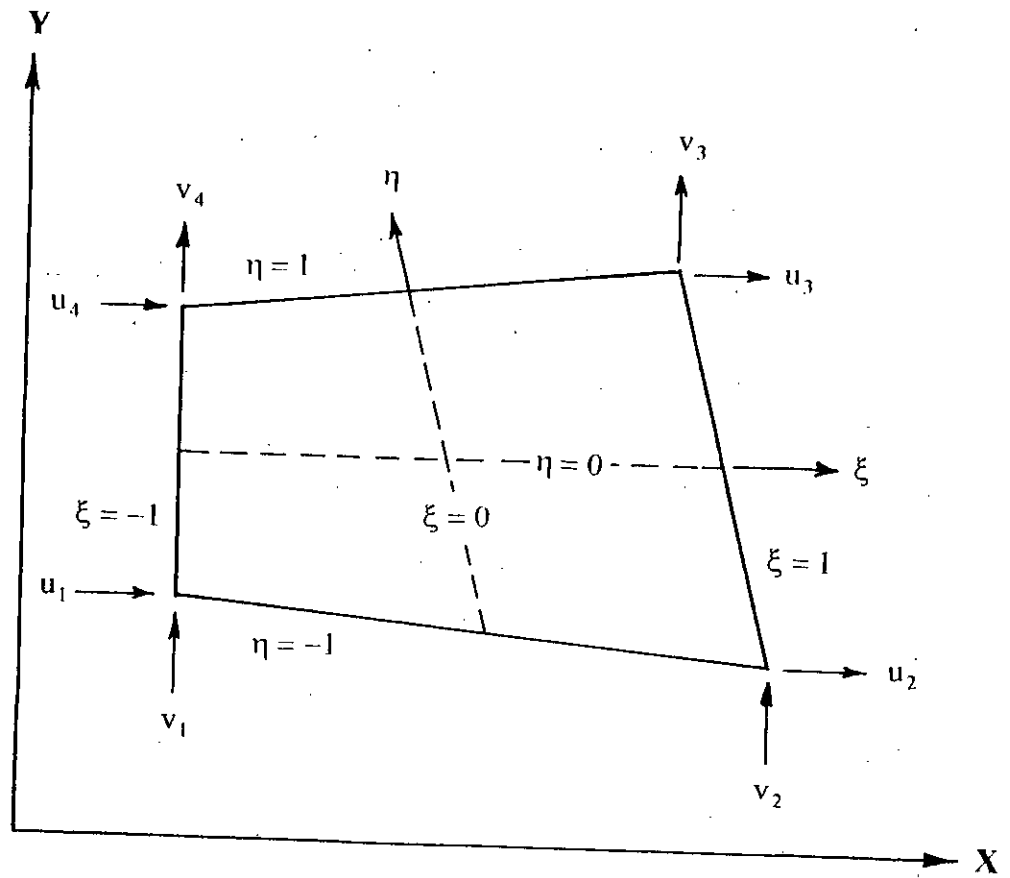


Figure 3.3 Four Node Isoparametric element



### 3.2 BEAM ELEMENT

Stiffness matrix of a two noded beam element with three degrees of freedom at each node (axial and transverse displacement and rotation) in local co-ordinates is given by

$$K = \begin{bmatrix} \frac{EA}{L} & 0 & 0 & -\frac{EA}{L} & 0 & 0 \\ 0 & \frac{12EI}{L^3} & \frac{6EI}{L^2} & 0 & -\frac{12EI}{L^3} & \frac{6EI}{L^2} \\ 0 & \frac{6EI}{L^2} & \frac{4EI}{L} & 0 & -\frac{6EI}{L^2} & \frac{2EI}{L} \\ \frac{EA}{L} & 0 & 0 & \frac{EA}{L} & 0 & 0 \\ 0 & -\frac{12EI}{L^3} & -\frac{6EI}{L^2} & 0 & \frac{12EI}{L^3} & -\frac{6EI}{L^2} \\ 0 & \frac{6EI}{L^2} & \frac{2EI}{L} & 0 & -\frac{6EI}{L^2} & \frac{4EI}{L} \end{bmatrix} \quad (3.1)$$

For the local axes system  $x'y'$  making an angle  $\theta$  with the global axes system  $xy$ , the transformation matrix can be written as

$$T = \begin{bmatrix} \cos\theta & \sin\theta & 0 & 0 & 0 & 0 \\ -\sin\theta & \cos\theta & 0 & 0 & 0 & 0 \\ 0 & 0 & 1 & 0 & 0 & 0 \\ 0 & 0 & 0 & \cos\theta & \sin\theta & 0 \\ 0 & 0 & 0 & -\sin\theta & \cos\theta & 0 \\ 0 & 0 & 0 & 0 & 0 & 1 \end{bmatrix} \quad (3.2)$$

When stiffness matrix for an element in local axes and transformation matrix with respect to global Cartesian axes is known, stiffness matrix in global co-ordinate can be obtained from following equation.

$$K = T^T K T \quad (3.3)$$

It should be noted that values of modulus of elasticity for simple tension and plane strain analysis are not the same. The expression of modulus of elasticity for plane strain can be written as

$$E' = \frac{E}{1 - \nu^2} \quad (3.4)$$

Where  $E'$  is the apparent Young's modulus for the plane-strain case and used in place of  $E$  in equation (3.1).

### 3.3 TRUSS ELEMENT

Stiffness matrix of a truss element with two degrees of freedom at each node (horizontal and vertical displacement) in global co-ordinate can be directly written as

$$K = \frac{EA}{L} \begin{bmatrix} C_x^2 & C_x C_y & -C_x^2 & -C_x C_y \\ C_x C_y & C_y^2 & -C_x C_y & -C_y^2 \\ -C_x^2 & -C_x C_y & C_x^2 & C_x C_y \\ -C_x C_y & -C_y^2 & C_x C_y & C_y^2 \end{bmatrix} \quad (3.5)$$

Where

$$C_x = \cos\theta \quad (3.6)$$

$$C_y = \sin\theta \quad (3.7)$$

### 3.4 FOUR NODED ISOPARAMETRIC ELEMENT

Stiffness matrix in plane strain case is given by

$$K = t \int [B]^T [D] [B] d(\text{Area}) \quad (3.8)$$

where

$B$  = strain-displacement matrix

$D$  = elasticity matrix

For plane-strain case, the  $D$  matrix is given by

$$D = G \begin{bmatrix} \frac{2(1-\nu)}{(1-2\nu)} & \frac{2\nu}{(1-2\nu)} & 0 \\ \frac{2\nu}{(1-2\nu)} & \frac{2(1-\nu)}{(1-2\nu)} & 0 \\ 0 & 0 & 1 \end{bmatrix} \quad (3.9)$$

Strain-displacement relation for small displacement is given by

$$\varepsilon = \begin{bmatrix} \varepsilon_{xx} \\ \varepsilon_{yy} \\ \gamma_{xy} \end{bmatrix}$$

$$= \begin{bmatrix} \frac{\partial u}{\partial x} \\ \frac{\partial v}{\partial y} \\ \frac{\partial u}{\partial y} + \frac{\partial v}{\partial x} \end{bmatrix}$$

$$= \begin{bmatrix} \frac{\partial}{\partial x} & 0 \\ 0 & \frac{\partial}{\partial y} \\ \frac{\partial}{\partial y} & \frac{\partial}{\partial x} \end{bmatrix} \begin{bmatrix} u \\ v \end{bmatrix} \quad (3.10)$$

For a four noded Isoparametric element

$$\begin{bmatrix} u \\ v \end{bmatrix} = \begin{bmatrix} N_1 & 0 & N_2 & 0 & N_3 & 0 & N_4 & 0 \\ 0 & N_1 & 0 & N_2 & 0 & N_3 & 0 & N_4 \end{bmatrix} \begin{bmatrix} u_1 \\ v_1 \\ u_2 \\ v_2 \\ u_3 \\ v_3 \\ u_4 \\ v_4 \end{bmatrix}$$

$$= [N] [\delta] \quad (3.11)$$

where,

$N_1, N_2, N_3, N_4$  are the shape functions for node 1,2,3,4 respectively.

$u_1, u_2, u_3, u_4$  are the displacements along x-direction of nodes 1,2,3,4 respectively.

$v_1, v_2, v_3, v_4$  are the displacements along y-direction of nodes 1,2,3,4 respectively.

Shape function  $N$  in local co-ordinate  $\xi, \eta$  (Fig. 3.4) are given as

$$\begin{aligned} N_1 &= \frac{1}{4}(1-\xi)(1-\eta) \\ N_2 &= \frac{1}{4}(1+\xi)(1-\eta) \\ N_3 &= \frac{1}{4}(1+\xi)(1+\eta) \\ N_4 &= \frac{1}{4}(1-\xi)(1+\eta) \end{aligned} \quad (3.13)$$

From equation 3.10 and 3.11

$$\varepsilon = \begin{bmatrix} \frac{\partial}{\partial x} & 0 \\ 0 & \frac{\partial}{\partial y} \\ \frac{\partial}{\partial y} & \frac{\partial}{\partial x} \end{bmatrix} [N][\delta]$$

$$\varepsilon = [B][\delta] \quad (3.13)$$

Where,

$$[B] = \begin{bmatrix} \frac{\partial N_1}{\partial x} & 0 & \frac{\partial N_2}{\partial x} & 0 & \frac{\partial N_3}{\partial x} & 0 & \frac{\partial N_4}{\partial x} & 0 \\ 0 & \frac{\partial N_1}{\partial y} & 0 & \frac{\partial N_2}{\partial y} & 0 & \frac{\partial N_3}{\partial y} & 0 & \frac{\partial N_4}{\partial y} \\ \frac{\partial N_1}{\partial y} & \frac{\partial N_1}{\partial x} & \frac{\partial N_2}{\partial y} & \frac{\partial N_2}{\partial x} & \frac{\partial N_3}{\partial y} & \frac{\partial N_3}{\partial x} & \frac{\partial N_4}{\partial y} & \frac{\partial N_4}{\partial x} \end{bmatrix} \quad (3.14)$$

Since shape functions are in terms of local co-ordinates( $\xi, \eta$ ) and equation 3.14 contain derivatives in global Cartesian xy co-ordinates, transformation of the derivatives is necessary.

Considering any function  $\phi(\xi, \eta)$ , the chain rule of differentiation in matrix form can be written as

$$\begin{bmatrix} \frac{\partial \phi}{\partial \xi} \\ \frac{\partial \phi}{\partial \eta} \end{bmatrix} = \begin{bmatrix} \frac{\partial x}{\partial \xi} & \frac{\partial y}{\partial \xi} \\ \frac{\partial x}{\partial \eta} & \frac{\partial y}{\partial \eta} \end{bmatrix} \begin{bmatrix} \frac{\partial \phi}{\partial x} \\ \frac{\partial \phi}{\partial y} \end{bmatrix}$$

$$= [J] \begin{bmatrix} \frac{\partial \phi}{\partial x} \\ \frac{\partial \phi}{\partial y} \end{bmatrix}$$

The Jacobian matrix J is given by

$$J = \begin{bmatrix} \frac{\partial N_1}{\partial \xi} & \frac{\partial N_2}{\partial \xi} & \frac{\partial N_3}{\partial \xi} & \frac{\partial N_4}{\partial \xi} \\ \frac{\partial N_1}{\partial \eta} & \frac{\partial N_2}{\partial \eta} & \frac{\partial N_3}{\partial \eta} & \frac{\partial N_4}{\partial \eta} \end{bmatrix} \begin{bmatrix} x_1 & y_1 \\ x_2 & y_2 \\ x_3 & y_3 \\ x_4 & y_4 \end{bmatrix} \quad (3.15)$$

Obtained J is inversed numerically, giving

$$\begin{bmatrix} \frac{\partial \phi}{\partial x} \\ \frac{\partial \phi}{\partial y} \end{bmatrix} = J^{-1} \begin{bmatrix} \frac{\partial \phi}{\partial \xi} \\ \frac{\partial \phi}{\partial \eta} \end{bmatrix}$$

and in particular the following array can be evaluated

$$\begin{bmatrix} \frac{\partial N_1}{\partial x} & \frac{\partial N_2}{\partial x} & \frac{\partial N_3}{\partial x} & \frac{\partial N_4}{\partial x} \\ \frac{\partial N_1}{\partial y} & \frac{\partial N_2}{\partial y} & \frac{\partial N_3}{\partial y} & \frac{\partial N_4}{\partial y} \end{bmatrix} = J^{-1} \begin{bmatrix} \frac{\partial N_1}{\partial \xi} & \frac{\partial N_2}{\partial \xi} & \frac{\partial N_3}{\partial \xi} & \frac{\partial N_4}{\partial \xi} \\ \frac{\partial N_1}{\partial \eta} & \frac{\partial N_2}{\partial \eta} & \frac{\partial N_3}{\partial \eta} & \frac{\partial N_4}{\partial \eta} \end{bmatrix} \quad (3.16)$$

with the Cartesian derivatives known, B matrix can be obtained with equation 3.14 and K matrix can be obtained from equation 3.8 by numerical integration.

### 3.5 CHARACTERISATION OF SOIL RESPONSE

The mechanical behaviour of soil is dependent upon a number of factors such as dry density, void ratio, stress level, stress path, stress history, temperature, time and degree of saturation. If the results of an analysis is to be realistic, it is important that the stress-strain characteristics of the soil be represented in a proper way. It is difficult to evolve a general constitutive (stress-strain) law which is valid for all soils under all placement and loading conditions. Simplified constitutive models based on phenomenological consideration have been employed to represent soil behaviour in analysing stress and displacement of soil mass.

Various simplified models for defining time independent behaviour of soil can be classified as: (1) Linear elastic models (2) Non-linear elastic models (3) Higher order elastic models (4) Plasticity models.

#### 3.5.1 Linear Elastic Models

This is the simplest approach to model the stress-strain behaviour of soil. The stress-strain relationship, which is governed by the generalised Hook's law of elastic deformations, may be expressed as follows for plane strain condition

$$\begin{bmatrix} \sigma_x \\ \sigma_y \\ \tau_{xy} \end{bmatrix} = \begin{bmatrix} C_{11} & C_{12} & 0 \\ C_{12} & C_{22} & 0 \\ 0 & 0 & C_{33} \end{bmatrix} \begin{bmatrix} \epsilon_x \\ \epsilon_y \\ \gamma_{xy} \end{bmatrix} \quad (3.17)$$

in which  $\{\sigma_x, \sigma_y, \tau_{xy}\}^T$  and  $\{\epsilon_x, \epsilon_y, \gamma_{xy}\}^T$  are the stress and strain vectors respectively.

To define coefficients  $C_{11}, C_{12}, C_{22}, C_{33}$ , only two independent elastic moduli are needed, assuming material isotropy. Any pair of the following elastic moduli may be selected : Young's modulus (E) and Poisson's ratio ( $\nu$ ), shear modulus (G) and bulk modulus (k), shear modulus (G) and constrained modulus (M), Lamé's parameter ( $\lambda$ ) and principal stress ratio in uniaxial strain ( $K_0$ ). A summary of the relationships between the various elastic moduli was given by Baladi (1979).

### 3.5.2 Non-linear Elastic Models

Non-linear elastic models have been used successfully by many authors including Cunnell (1974), Girija, Vallabhan and Jain (1972), Lee and Shen (1969), Nobari and Duncan (1972), Desai (1974) and Ruser and Dawkins (1972). The state of stress is assumed to be a function of state of strain only.

In non-linear elastic models, a given set of stress-strain curves are represented by using mathematical functions such as a hyperbolic function, power function, parabolic function, Lagrangian formula, spline function or others. The most widely used functional relationship was developed by Duncan and Chang (1970). The model is based on Kondner's finding (1963) that stress-strain curves for a number of soils could be approximated by hyperbolas. Wong and Duncan (1974) listed the values of the hyperbolic parameters determined for more than one hundred different soils tested under drained and undrained conditions. This wide data base can be used to estimate reasonable values of the parameter in cases where the available information on the soil is restricted to descriptive classification.

The Hardin model (1970) provides a relationship for the recent shear modulus of soils as a function of accumulated shear strain and hydrostatic pressure. The major advantage of the model lies in the extensive correlation's between Hardin parameters and soil index properties (Void ratio, percent saturation and

plasticity index) that have been established for a wide variety of soils. Katona (1978) developed a hyperbolic Poisson's ratio function which provided the second elastic soil modulus for the Hardin model.

Duncan et al. (1978) proposed a modified hyperbolic model which employed bulk modulus in place of Poisson's ratio in Duncan-Chang model. The model assumed that bulk modulus is independent of deviatoric stress and that varies with confining pressure. Duncan et al. (1978) provided values of the bulk modulus parameters for a wide variety of soils and revised and summarised in 1979.

Desai (1971) proposed the use of cubic spline functions for simulating a set of stress-strain data. The cubic spline function approximates a given set of stress-strain data by a piece wise cubic polynomial such that the polynomial along with its first and second derivatives is continuous over the entire range of the data.

Leonards and Roy (1976), Rahman (1978), employed the cubic spline function to represent soil behaviour and compared the results with those obtained by other functional representation (e.g. Duncan-Chang model, Hardin models, modified Duncan model etc.). They also compared the results obtained by the analyses with their experimental results. The cubic spline function representation was found to provide better simulation of stress-strain criteria than those obtained by other functional representations.

### **3.5.3 Higher Order Elasticity Models**

There are two types of models (a) hyper elastic models (b) hypo elastic models.

The hyper elastic models rely on finding constitutive relations by differentiation of a strain energy function, with respect to invariants of strain.

In hypo elastic models rely on finding constitutive relations by differentiation of a strain energy.

In hypo elastic formulation the stress increment is a function of strain increment and the function is dependent upon the state of stress. However, a



number of difficulties are encountered in the use of the models:

- 1) The response parameters are not unique, their values being dependent on the types of test that are selected to be performed.
- 2) No relation has been found between the response parameter and the resulting change in stress-strain-volume change behaviour of soils.

#### **3.5.4 Plasticity Models**

In recent years, many plasticity soil models have been proposed and some were incorporated in finite element analysis of stresses and deformation of soil masses.

It has been shown experimentally that yield function and plastic potential function are not identical for most soils. Plasticity soil models encounter two serious difficulties:

- 1) The elastic plastic stress-strain matrix is not usually symmetrical, which results in a huge increase of computer storage and computation effort over the use of soil model with associated plasticity, and
- 2) Unlike associated plasticity soil models, the uniqueness and stability of the solutions is no longer guaranteed.

#### **3.5.5 Selection of Soil Model for Analysis**

Poor representation of the stress-strain characteristics of soil can lead to calculated modes of behaviour which are completely different from actual ones. In spite of considerable work, as mentioned previously, a general and versatile way of representing the stress-strain characteristics of soils has not yet been established. A compromise between simplicity and accuracy is necessary.

Assumption of linear elastic behaviour of soil is unrealistic, because soils never behave as a linear elastic material (Rahman, 1978). Non-linear elastic soil models have been found to provide an expedient, and often satisfactory means for solving many geotechnical engineering problems. The cubic spline function

representation was found to provide better simulation of stress-strain curves compared with other functional relationships for non-linear elastic model (Desai, 1971, 1974; Leonard and Roy, 1976; Rahman, 1978). Plasticity models of soil usually produce unsymmetric stress-strain matrix. In addition plasticity model does not assure uniqueness and stability of solution. So the non-linear elastic model is selected.

### **3.6 The Incremental Method**

To account for the non-linear behaviour of soil, incremental method of analysis is adopted in the program. Octahedral shear stress and octahedral shear strain curves are used to represent the non-linear soil properties. Four node isoparametric elements representing the soil have different values of octahedral initial normal stress which is a function of the depth of the soil element. This influence their stress-strain behaviour under subsequent loading. In this method of analysis, the total load on the structure is divided into a number of small increment. The system of load displacement equation is solved repeatedly with each of these incremental loads. The stiffness matrix is obtained each time by substituting the values of shear modulus,  $G$ , that correspond to current level of octahedral shear strain in each element.

## CHAPTER 4

# THE FINITE ELEMENT COMPUTER PROGRAM

### 4.1 INTRODUCTION

Important aspects of the retaining wall-soil interaction problem along with the methods of considering non-linearity have been presented in the preceding chapters. The purpose of this chapter is to utilise these methods and to develop programs for the analysis of rigid retaining wall and their surrounding soil as an integral system. The nature of the programs is general and they can be used to analyse a variety of retaining wall soil systems. They provide facilities for the incorporation of various backfill, and loading conditions. Special care has been taken to reduce the use of computer core storage and execution time. The programs described here are written in FORTRAN 77 and were tested and run on the 486 microcomputer at the Computer Centre of Civil Engineering Department, Bangladesh University of Engineering and Technology. The programs were originally developed around a suite of routines by Rahman (1978) for CDC 7600 computer ; Karim (1985) for IBM 370 computer and Seraj (1986) for IBM 4331-K02 computer. Seraj and Rahman (1987) developed a two-dimensional non-linear finite element computer program for the interaction analysis of rigid culverts. The numerical model incorporated various routines developed by Rahman (1978) and Karim (1985). In the present study, special routines for generating data, automated finite element mesh adjustment for different height of wall and soil surface slope in the finite element analysis etc. were written, tested and subsequently adopted by the author.

### 4.2 GENERAL FEATURES OF THE COMPUTER PROGRAM

The general features of the program are as follows:

- (a) Reduction of the use of core storage by utilising an efficient storage scheme of the stiffness matrix.
- (b) To utilise the backing storage facilities so that only a part of the stiffness matrix is held in the core at a time.

- (c) Development of routines for computation of stiffness of Truss element, Beam element and four node isoparametric element.
- (d) Utilisation of a construction scheme of the stiffness matrix in two phases in order to isolate the part of it which remains unaltered in successive analyses from that which is changed by contributions of non-linear elements.
- (e) Utilisation of a technique of assembling stiffness matrix joint by joint to simplify the storage techniques and minimise I/O operations with disc.
- (f) Use of an efficient solution routine ensuring an efficient transfer between the core and the backing store of the stiffness matrix solution blocks.
- (g) Use of spline functions to implement a smooth representation of non-linear soil properties.
- (h) Computer implementation of data generation and mesh adjustment.

#### **4.2.1 Storage of the Stiffness Matrix**

The analysis of a retaining wall, its shape and the soil gives rise to a large, sparse, symmetric and positive definite stiffness matrix. The number of equations to be solved is also very high. The problem becomes more complex with the adoption of a non-linear incremental technique. Therefore, the scheme of storage of the stiffness matrix has been carefully selected to reduce the use of core space without an undue increase in the execution time. A variable band width storage scheme suggested by Jennigs (1966, 1977) was adopted. Only the elements between the first non-zero and the leading diagonal in each row of the lower triangle of the matrix were stored (Fig. 4.1). This was achieved by storing the elements in a continuous one dimensional array in a row-by-row sequence.

#### **4.2.2 Construction of the Stiffness Matrix**

Program modules take advantage of the backing storage facilities so that only a part of the stiffness is held in the core at a time. This was attained by opening five working files in the disc backing store. When a part of the stiffness matrix

is fully constructed it is written into the backing store. The same area of the core space is then used to construct the next part of the stiffness matrix. To reduce the number of transfers, stiffness matrix K was subdivided in such a way as to make its parts independent of each other during the assembly process.

The overall stiffness matrix is constructed in two phases. In the first phase, the matrix is constructed with the contributions from the linear elastic beam elements only. This incomplete stiffness matrix remains unaltered in the successive analyses. In the second phase of construction, the contribution from the non-linear elements are superimposed on this matrix. In each increment of the load only the second phase of construction is repeated by incorporating appropriate value of instantaneous shear modulus of each soil element.

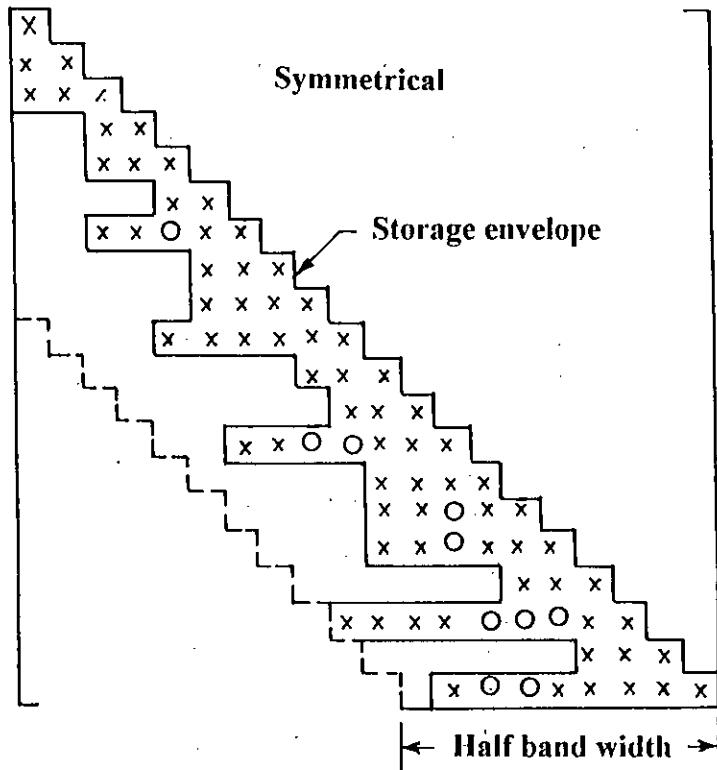
#### **4.2.3 The Solution Routine**

A program for solution of simultaneous linear equations by Gaussian elimination technique modified to suite the compact storage scheme developed by Rahman (1978) is used in this thesis. The stiffness matrix is divided into a number of segments in such a way that each segment contains a number of complete rows. The direct access backing store file is also divided into fixed length blocks such that each complete segment wholly or partly fills the block.

#### **4.2.4 The Use of Spline Functions**

A program was written by Rahman (1978) to formulate the spline functions for a set of  $\tau_{oct} - \gamma_{oct}$  curves. For any particular set of curves obtained for a given soil, this program is run only once and the output is used repeatedly for all the analyses with this soil. This output consists of the nodal values of  $\tau_{oct}$ ,  $\gamma_{oct}$  and the second derivatives  $\phi$  at each node for each curve.

Two subroutines GVALUE and GVALU1 are included in the main program to calculate the values of  $\tau_{oct}$  and G for any value of  $\gamma_{oct}$  of original soil and filled soil respectively ( Seraj and Rahman, 1987; Seraj 1986 ). the routines are entered before each increment of the load to obtain the instantaneous shear modulus of each isoparametric element representing soil.



Note: Each X indicates a non-zero element

Figure 4.1 Layout of a typical Stiffness Matrix

#### **4.2.5 Automatic Data Generation**

To reduce the manual data preparation, a facility is included in the programs to generate automatically significant portion of the input data. Data such as nodal co-ordinates of line elements, isoparametric soil elements and the nodal degrees of freedom are generated by appropriate subroutines. Appropriate material properties of the elements representing retaining wall-soil are also specified within the routines. The subroutine MESH is capable of adjusting the co-ordinates of a tentative finite element mesh.

### **4.3 THE STRUCTURE OF THE COMPUTER PROGRAM**

The general retaining wall-soil interaction finite element program was developed by a logical combination of some thirty six subroutines and a main program spreading over about 2500 FORTRAN 77 source statements. The subroutines can be grouped into four categories depending on the functions they perform. These are (i) control routines, (ii) ancillary routines, (iii) element routines, and (iv) speciality routines.

The control routines perform such functions as the overall management of the data and control of incremental analysis process. The main segment of the program connects different routines together and regulates the overall interactive analysis. A few routines in this group reads and generates the nodal co-ordinates and element connectivity. The non-linear analysis is initiated by generating initial values of non-linear elastic parameters. The assembly of the global stiffness matrix in each increment of load is performed by another routine belonging to this group. A separate routine alters the non-linear elastic properties of soil as the analysis progresses.

Ancillary routines are used for performing various computational chores. These routines include the generation of the least joint number of each joint, reconstruction of the load vector after each increment of load, formulation of joint displacement matrix from the solution vector, calculation of instantaneous values of  $G$  and so on.

The element subroutines formulate each type of finite element used in the program. They evaluate the element stiffness matrices and calculate the

stresses, the strains, the forces and the moments at various locations of the retaining wall and soil.

Three speciality subroutine perform the solution of simultaneous equations, Gaussian elimination method coupled with the compact storage scheme is used in the solution routine.

An executable module is formed by combining the subroutines during linkage editing. A simplified flow chart of the complete program is shown in Fig. 4.2.



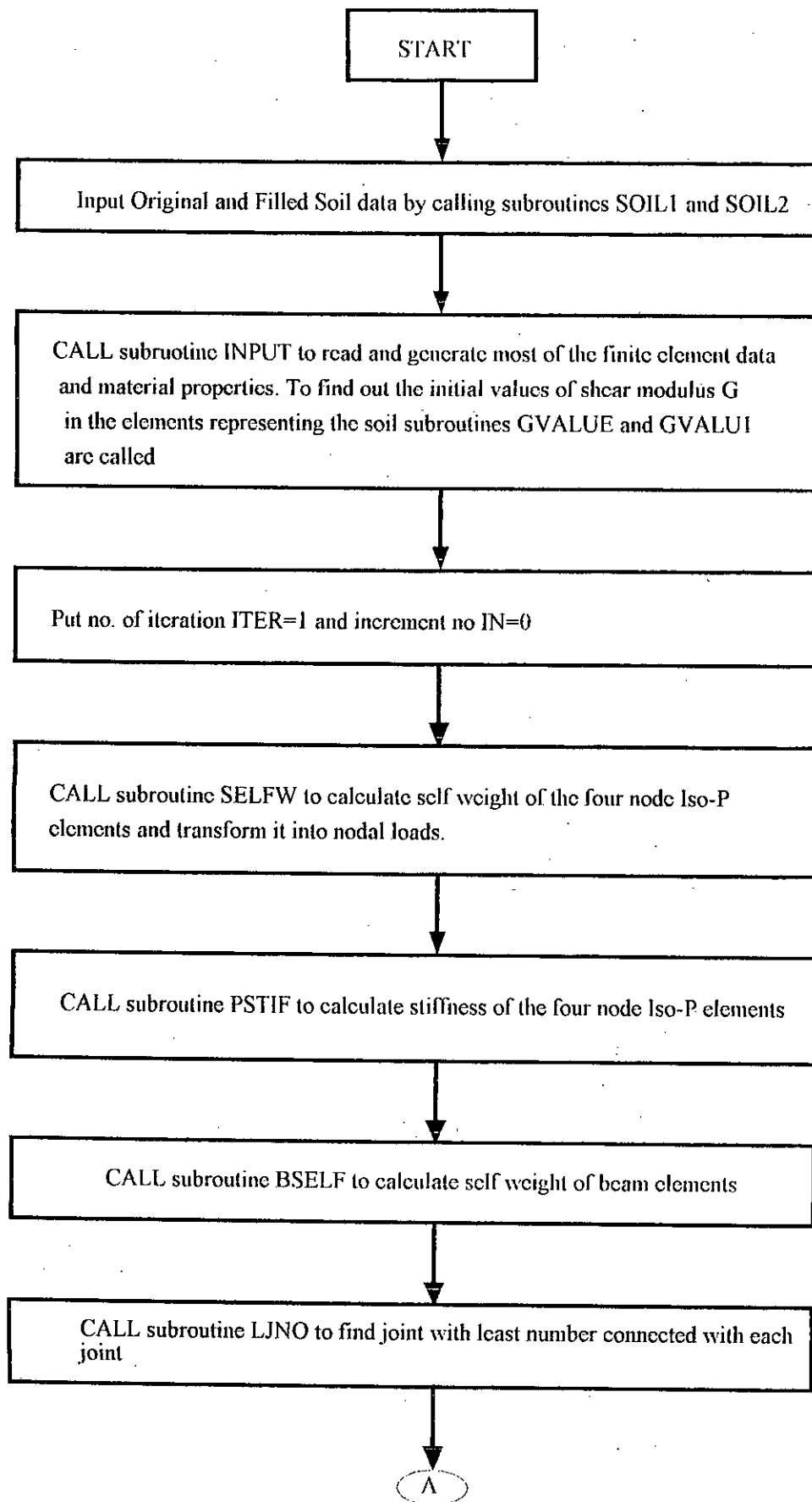


**Figure 4.2 Simplified flow chart of the computer program**

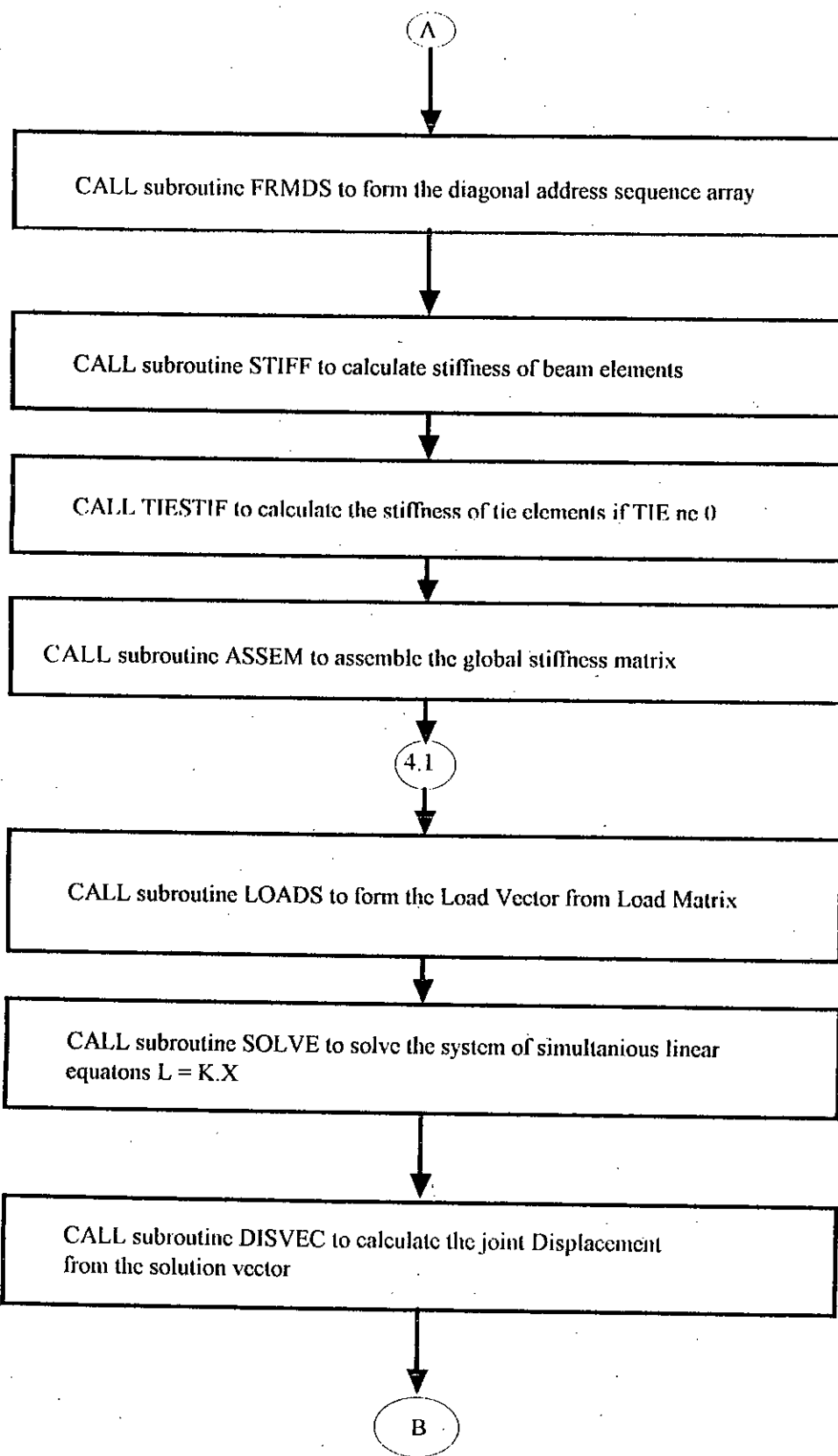


**Figure 4.2 Simplified flow chart (continued) of the computer program**

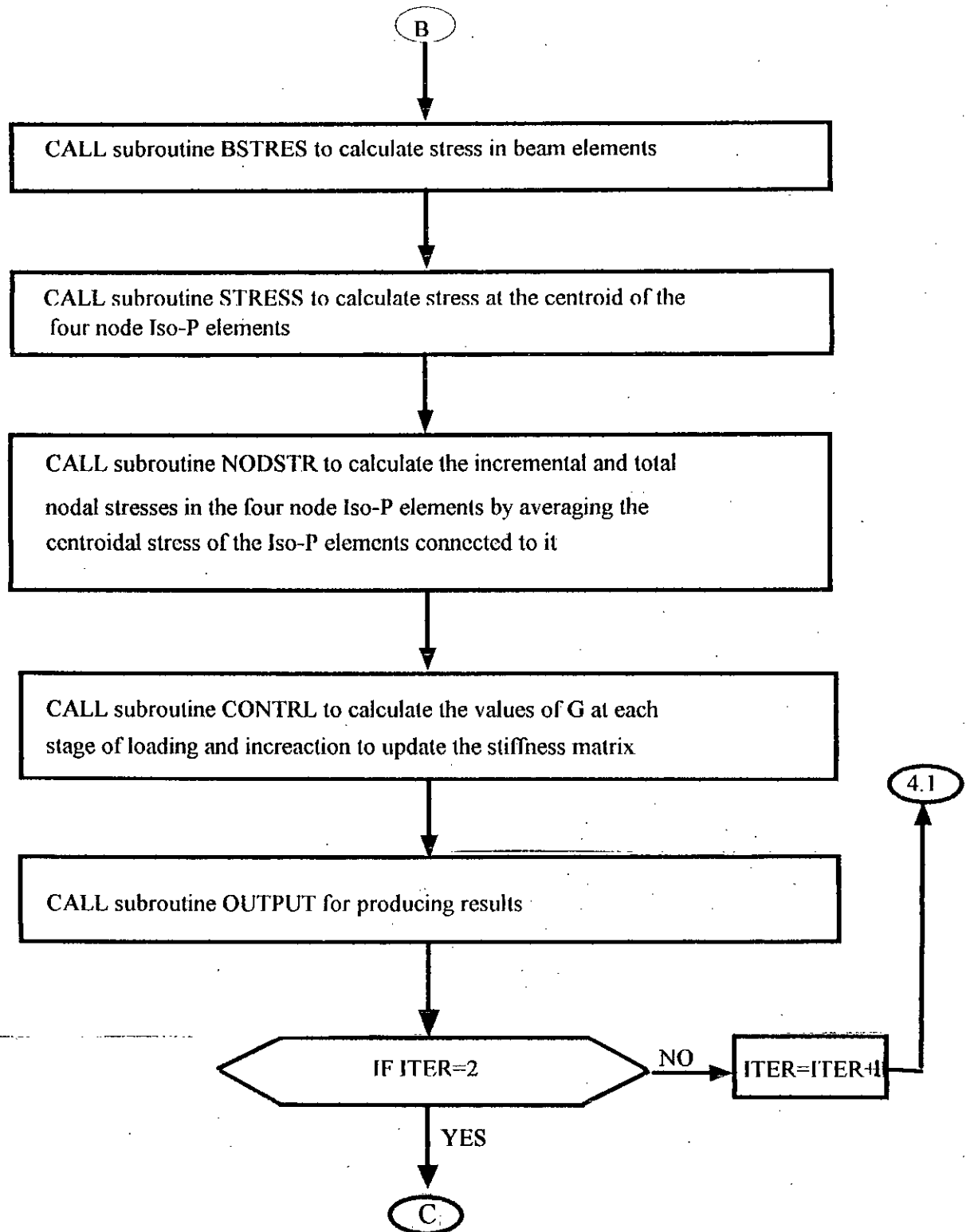


Figure 4.2 Simplified flow chart (continued) of the computer program

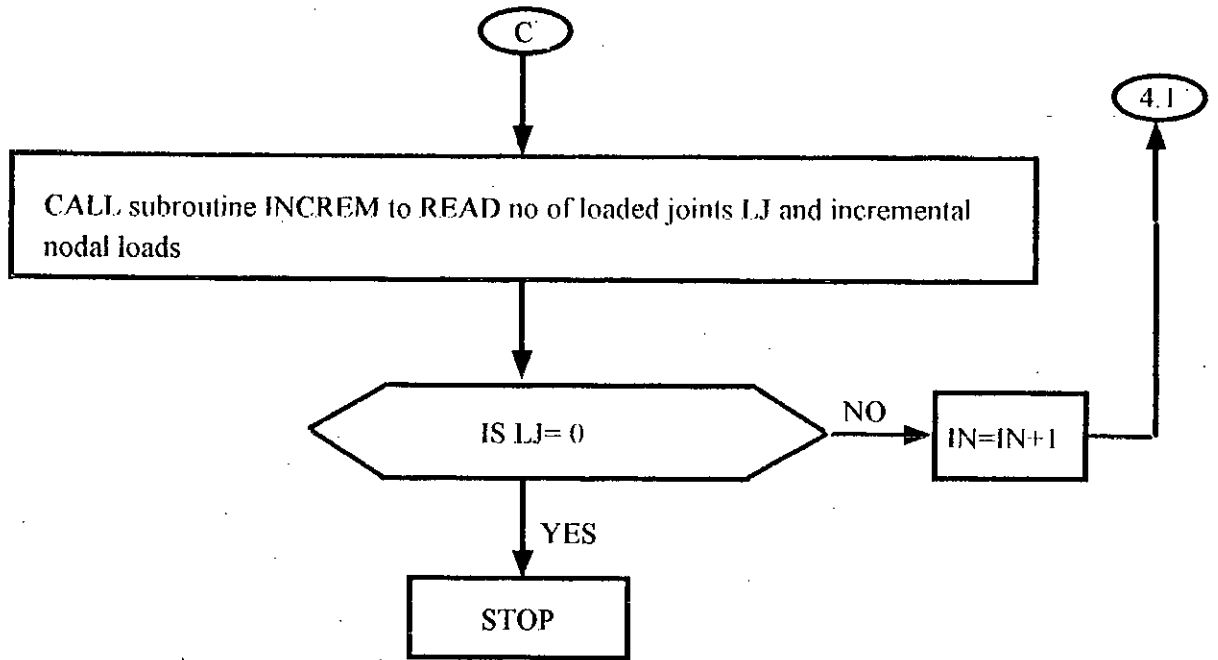


Figure 4.2 Simplified flow chart (continued) of the computer program

## CHAPTER 5

# INTERACTION ANALYSIS OF RIGID RETAINING WALLS

### 5.1 INTRODUCTION

The method of analysing an integrated retaining wall-soil system has been described in the preceding chapters. The finite element computer program used in this study can now be employed for analysing a variety of retaining wall-soil interaction problems.

A series of analyses on rigid retaining walls were carried out in order to study the interaction behaviour and to investigate the influence of various parameters. The height of wall, thickness of wall stem, thickness of wall footing, concrete strength, embedded depth, slope of retained soil surface, soil properties (such as Poisson's ratio, unit weight of backfill, angle of internal friction), effect of magnitude and location of line load, effect of uniformly distributed load were the variable parameters. This chapter describes the analyses scheme, properties of different elements of the structure-soil system, and the loading conditions. The finite element discretization and boundary conditions and the selected soil model have also been presented in detail.

### 5.2 LOADS ON STRUCTURES

Since the analysis of a retaining wall is a plane strain problem, thus a slice of unit thickness through the retaining wall-soil system is considered in the numerical modelling. The vertical load comprises the dead weight of the retaining wall, the soil and any surcharge load placed on the soil surface. Unit weight of different materials used in the studies are listed in Table 5.1. These values are utilised in calculating the self weight of the various components of the system.

Both line load and uniformly distributed loads were considered in the course of analysing different retaining walls. Line loads of magnitude of 1 kip, to 10 kips were applied at steps of 1 kip at varying distance from the wall face. Similarly Distributed load of 1 kip/ft to 10 kip/ft in steps of 1 kip/ft was applied for the

analyses purpose.

**Table 5.1 Unit weight of materials used**

Member	Unit weight kip/ft <sup>3</sup>
Concrete wall and base	0.150
Highly compacted soil	0.120
Medium compacted soil	0.110
Loose backfill	0.100

### 5.3 MATERIAL PROPERTIES

For the analysis purpose, the retaining wall and its base material is assumed to behave elastically. For all but the analyses concerning the effect of concrete strength,  $E_c$  was calculated for a concrete cylinder strength,  $f'_c$ , of 2700 psi.

In the analyses exploring the effect of modulus of elasticity of concrete on the interaction of retaining wall with soil  $f'_c$  value of 2500, 2700, 3000, 3500 psi were used. Modulus of Elasticity  $E_c$  was calculated using the relationship  $E_c = 57500 \sqrt{f'_c}$  psi.

Poisson's ratio of concrete was kept constant at 0.2 in all the runs.

The soil properties were obtained from two sets of octahedral shear stress and octahedral shear strain curves shown in Fig. 5.1 ( Seraj, 1986 and Seraj and Rahman 1987 ). The curves of Fig. 5.1(a) were used to represent original soil or highly compacted fill. The curves of Fig. 5.1(b) were used for representing moderately and loosely compacted backfill. For properties of soil element with  $\sigma_{octi}$  values not coinciding with the values indicated in the curves, suitable interpolation or extrapolation schemes were used. Although the curves shown in Fig. 5.1 are tentative, they represent a set of practical values of soil properties. These were used in the absence of test results for a particular type of original and filled soil. For all the analysis Poisson's ratio of the original soil and backfill were chosen to be 0.45.

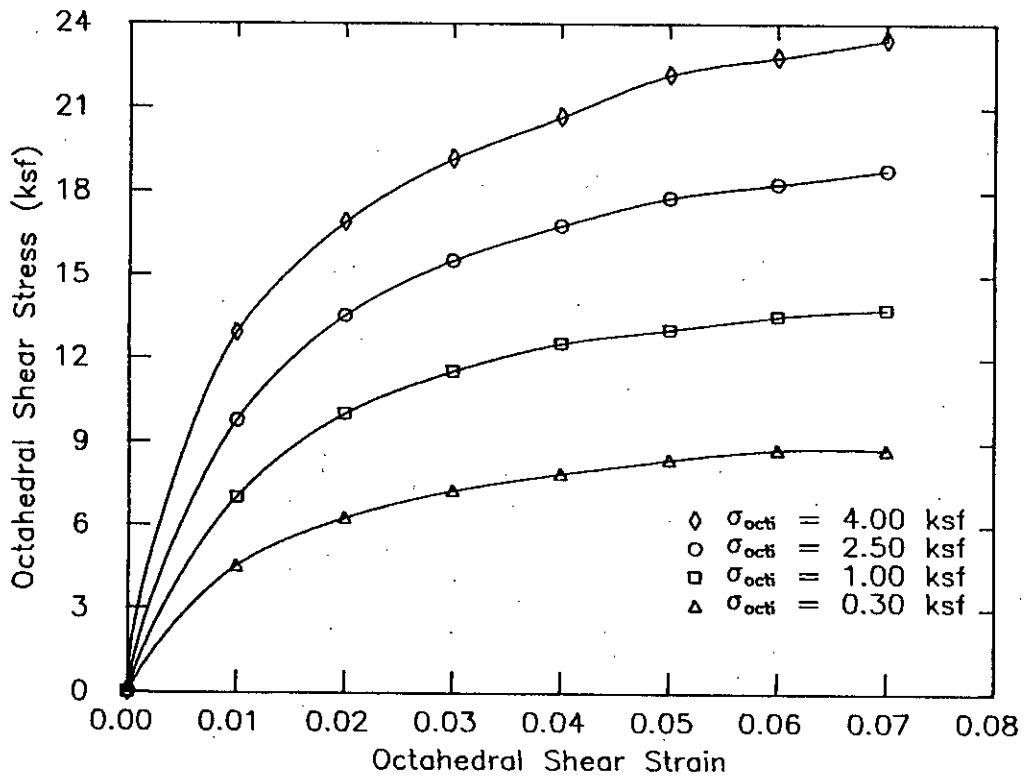


Fig.5.1(a) Octahedral Shear Stress & Strain Curves For Different Confining Pressure of Original Soil

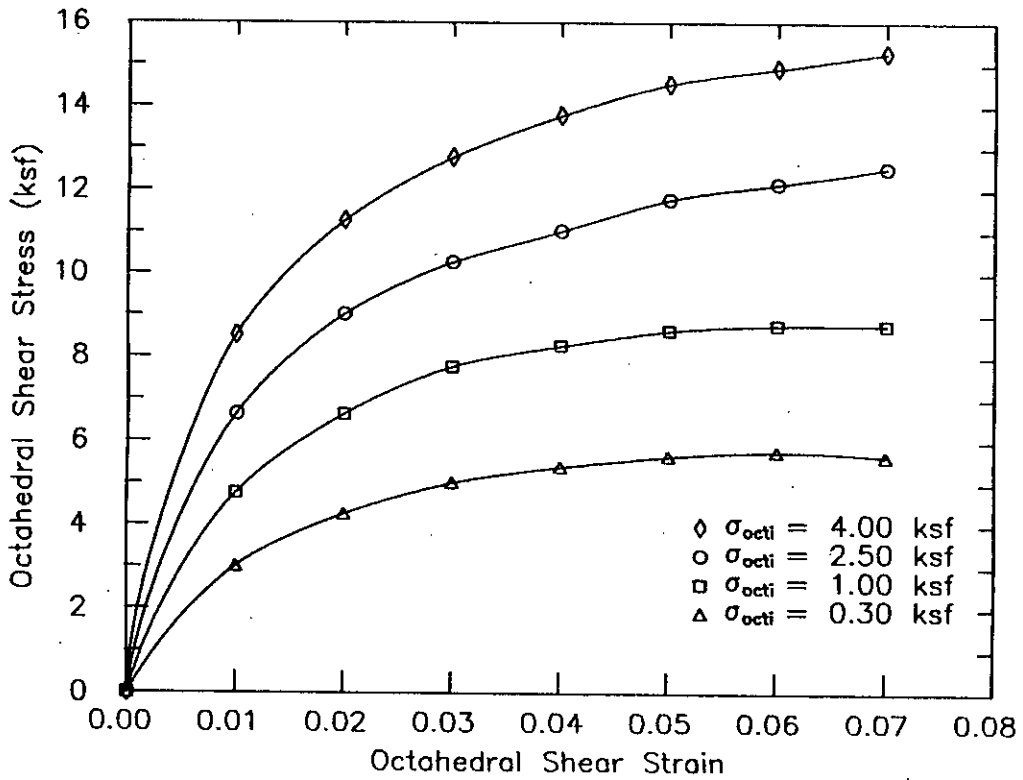


Fig.5.1(b) Octahedral Shear Stress & Strain Curves For Different Confining Pressure of Filled Soil

To study the effect of Poisson's ratio on the interaction of retaining wall with soil, Poisson's ratio of 0.45, 0.46 and 0.47 were used. The values of angle of internal friction of original and backfill soil were taken as  $40^\circ$ ,  $28^\circ$  respectively. The value of cohesion for all types of soil were considered to be zero.

#### **5.4 FINITE ELEMENT DISCRETIZATION AND BOUNDARY CONDITIONS**

In the retaining wall-soil interaction, the effect of loading or disturbance in soil decreases with increasing distance from the wall. There should be an optimum distance from the wall after which the soil and load will have no effect on the wall. Similarly, the extent of soil below the wall footing should be large enough to simulate infinite depth of homogeneous soil mass. Figure 5.2 shows configuration of the finite element mesh of retaining wall-soil systems considered in this thesis.

In the analysis, the bottom boundary was restrained from vertical displacement but could move horizontally. The lateral boundaries were restrained against horizontal movement but they were free to displace vertically. Nodes at the surface of soil were allowed to move vertically as well as horizontally. Nodes representing the wall were allowed to move vertically, horizontally and rotate in its own plane.

#### **5.5 SUMMARY OF ANALYSIS SCHEME**

To analyse the interaction of retaining wall with soil and to evaluate the effect of different parameters, following analyses were conducted. ("Moment" and "Lateral soil force" throughout the text refers to the moment and lateral soil force at depth H from the top of soil surface, as shown in Figures of Chapter 6 and Chapter 7)

##### **5.5.1 Effect of Moment of Inertia of Area of Wall :**

To study the effect of moment of inertia of area of the wall on the lateral soil force, walls with thickness of 12 inch at the top and of bottom thickness 12 inch to 20 inch at steps of 2 inch were used. Accordingly, moment of inertia at the base of the wall was found to be equal to  $0.0833 \text{ ft}^4$ ,  $0.1323 \text{ ft}^4$ ,  $0.1975 \text{ ft}^4$ ,



FE mesh: 186 Nodal points  
 157 Isoparametric elements  
 12 Beam elements

Isoparametric elements representing soil

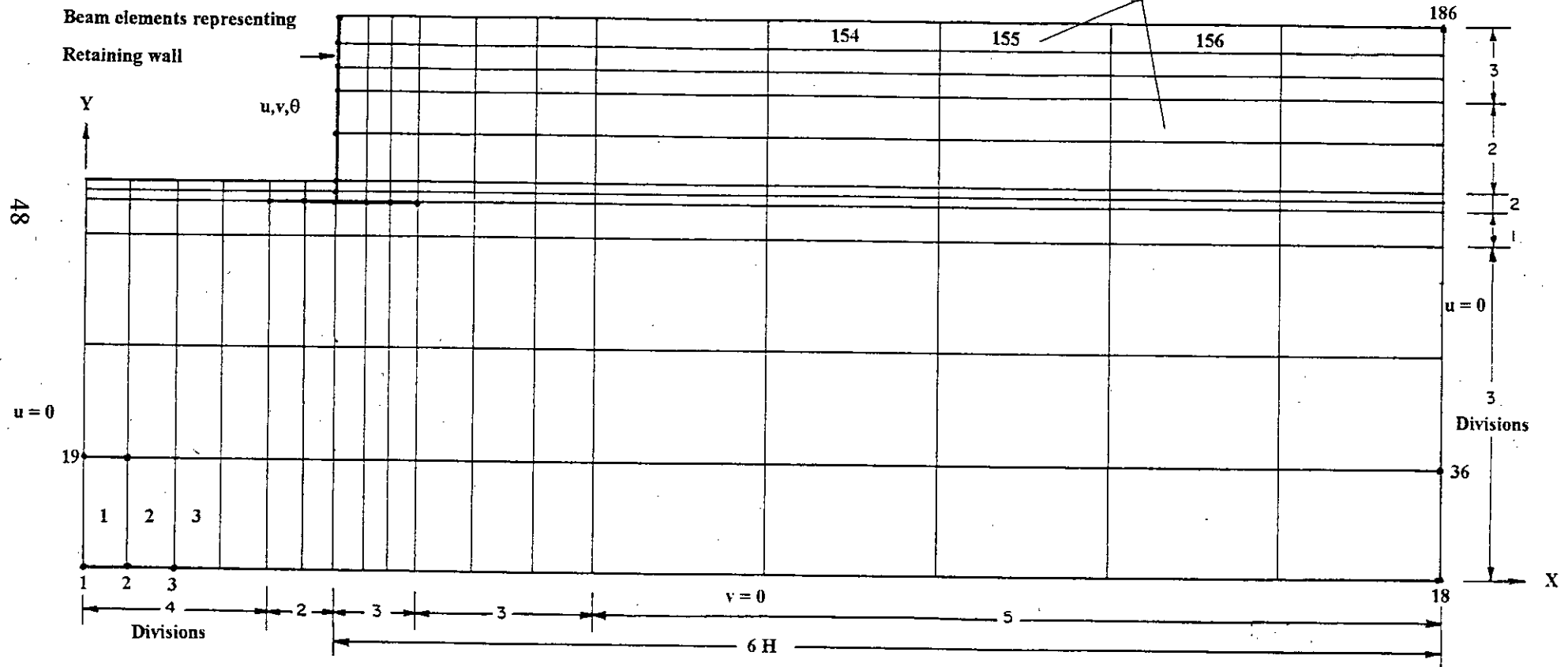


Figure 5.2a. Finite element mesh of Retaining Wall-Soil system (Horizontal Backfill)

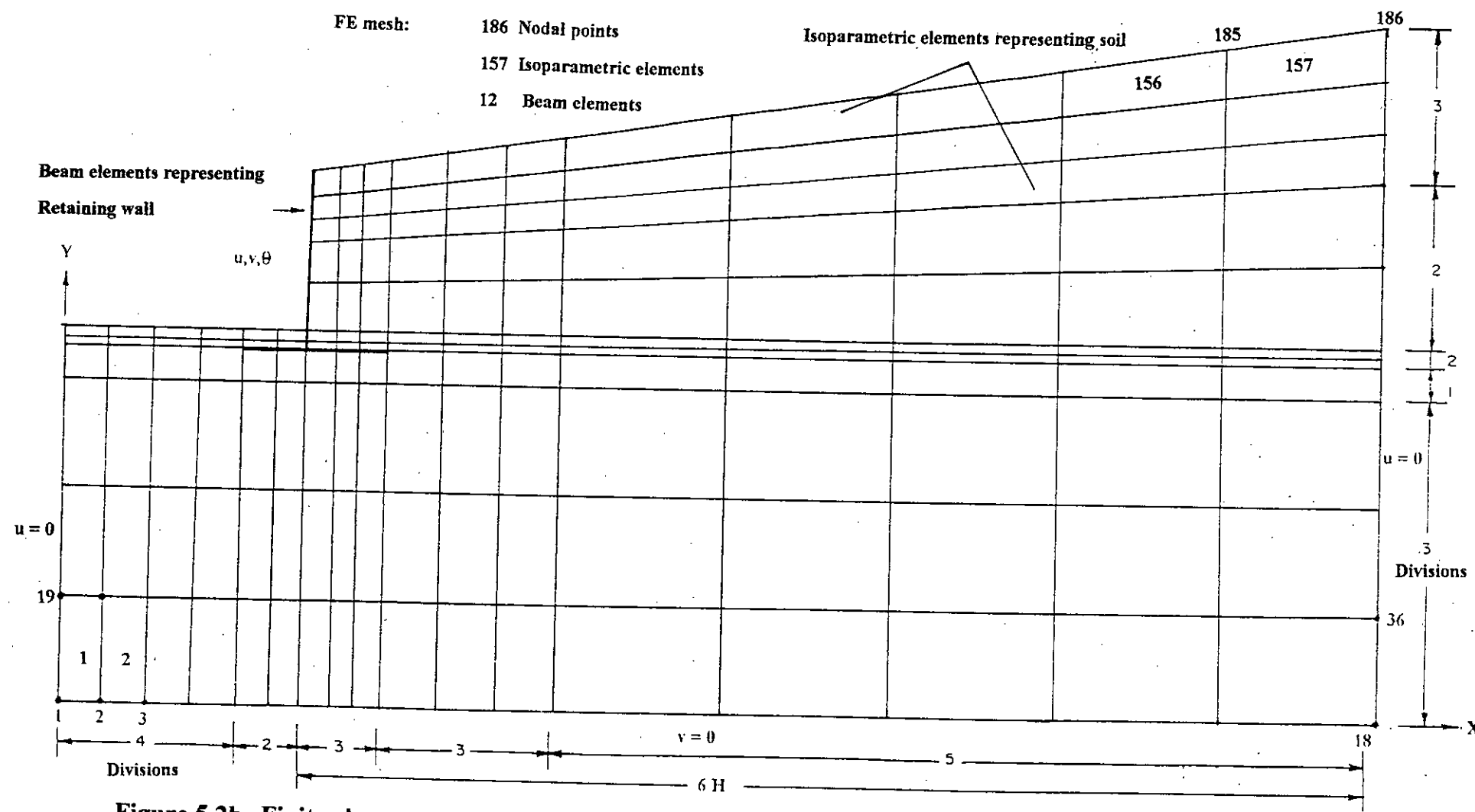


Figure 5.2b Finite element mesh of Retaining Wall-Soil system (Sloping Backfill)

0.2813 ft<sup>4</sup>, 0.3858 ft<sup>4</sup>. Inertia between the top and bottom of wall had a fourth degree parabolic variation with respect to wall depth, since the thickness from top to bottom varied linearly. To study the effect of this parameter thoroughly, walls with heights 9 ft, 12 ft, 15 ft and 18 ft were studied. Thickness of wall footing was kept constant at 24 inch. Soil below the wall was taken as original soil with angle of internal friction,  $\phi = 40^\circ$ , unit weight  $\gamma = 120$  pcf and Poisson's ratio  $\nu = 0.45$ . The backfill material used had properties,  $\phi = 28^\circ$ ,  $\gamma = 120$  pcf and  $\nu = 0.45$ . The soil surface was taken as horizontal surface. Embedded depth of wall within the soil was kept constant at 1 feet. Strength of concrete was considered as 2700 psi and Poisson's ratio of concrete was taken to be 0.2.

### **5.5.2 Effect of Moment of Inertia of Area of Wall Footing:**

To study the effect of moment of inertia of area of wall footing on lateral soil force and the moment on wall, the thickness of wall footing was taken as 24 inch, 28 inch, 30 inch and 36 inch i.e., inertia of wall footing were taken as 0.6667 ft<sup>4</sup>, 1.0587 ft<sup>4</sup>, 1.5803 ft<sup>4</sup> and 2.2500 ft<sup>4</sup>. Similar to the case study (5.5.1), in an effort to gain an insight into the interaction behaviour studies were made for walls having height equal to 9 ft, 12 ft, 15 ft and 18 ft. Other properties were same as described in section 5.5.1.

### **5.5.3 Effect of Concrete Strength :**

To study the effect of concrete strength on the retaining wall-soil interaction, concrete having  $f'_c$  equal to 2500 psi, 2700 psi, 3000 psi and 3500 psi were used. From these values the modulus of elasticity were calculated as  $4.140 \times 10^5$  ksf,  $4.302 \times 10^5$  ksf,  $4.540 \times 10^5$  ksf and  $4.900 \times 10^5$  ksf. Like the previous analyses, height of wall was taken as 9 ft, 12 ft, 15 ft and 18 ft. Thickness of wall at top and bottom were taken as 12 inch and 16 inch, respectively. Thickness of wall footing was taken as 24 inch. Other concrete and soil properties were same as those described in section 5.5.1.

### **5.5.4 Effect Slope of Soil Surface :**

To study the effect of slope of soil surface with horizontal, angle of the soil surface with horizontal was taken as  $0^\circ$ ,  $5^\circ$ ,  $10^\circ$ ,  $15^\circ$  and  $20^\circ$ . Height of wall,

thickness of wall, thickness of wall foundation were same as those described in section 5.5.3. Other material properties were same as described in section 5.5.1.

#### **5.5.5 Effect of Unit Weight of Backfill:**

Traditional methods shows a linear variation of lateral soil force and moment values with unit weight of backfill. An attempt was made to check this assumption. For this purpose the unit weight of backfill were varied from 100 pcf to 120 pcf in steps of 10 pcf, while the unit weight and Poisson's ratio of the original soil below the wall were kept constant at 120 pcf and 0.45 respectively. Properties of wall and soil were as described in section 5.5.3 and section 5.5.1, respectively.

#### **5.5.6 Effect of Poisson's Ratio of Soil:**

Conventional analysis methods do not include the effect of Poisson's ratio of soil on the lateral soil force or moment. From the knowledge of elasticity, it is clear that Poisson's ratio must influence these values because it establishes the relation between vertical and horizontal forces. According to Bowles(1988), the conventional methods probably uses a value of 0.5 for Poisson's ratio which may or may not be realistic for a given problem. In this study, Poisson's ratio of 0.45, 0.46 and 0.47 were used to study the effect of this parameter on lateral soil force and moment. Once again, wall height, properties of soil and structure are available in section 5.5.1 and section 5.5.3.

#### **5.5.7 Effect of Angle of Internal Friction of Soil:**

Traditional methods show a specified variation of earth pressure with the angle of internal friction of soil. To study this effect and to compare the values with the available methods, angle of internal friction were selected as  $28^{\circ}$  and  $40^{\circ}$ . Unit weight of backfill was taken as 120 pcf. Other structural properties are described in section 5.5.3 and soil properties in section 5.5.1.

#### **5.5.8 Effect of Embedded Depth of the Wall Into the Original Soil:**

To study the effect of depth of embedment of the wall into the ground, embedded depth of 1.0 ft, 1.5 ft, 1.75 ft and 2.0 ft were used in the analysis.

Like the previous investigations, studies were carried out for walls of height 9 ft, 12 ft, 15 ft, 18 ft with properties described in section 5.5.3. Soil properties are described in section 5.5.1.

#### **5.5.9 Effect of Line load:**

Methods that appear in the available literature show a linear variation of lateral earth force and bending moment with the magnitude of the applied load. An attempt was made to study the effect of magnitude and distance of load on the lateral soil force and the bending moment. Wall height used in the analysis were 9 ft, 12 ft, 15 ft, 18 ft. Magnitude of applied load was varied from 1 kip to 10 kip with an increment of 1 kip. Distances of applied load from the face of the wall were 4 ft, 7.25 ft, 10.50 ft and 13.75 ft for wall of 9 ft height and 4 ft, 8.92 ft, 12.83 ft, 18.75 ft for 12 ft, 15 ft and 18 ft high wall. Properties of the wall are described in section 5.5.4 and soil properties are described in section 5.5.1.

#### **5.5.10 Effect of Distributed Load:**

To study the effect of distributed load, studies were carried out for walls with height 9 ft, 12 ft, 15 ft and 18 ft. Distributed load of 1 kip/ft was applied first and then increased by 1 kip/ft up to 10 kip./ft. The loads were applied 4 ft away from the wall face. For 9 ft high wall loaded length was 9.75 ft and for other cases loaded length was 14.75 ft.

### **5.6 SELECTION OF HORIZONTAL AND VERTICAL EXTENT OF SOIL IN THE FINITE ELEMENT MESH.**

Traditional methods take an inclined failure plane, to determine the lateral soil force on the retaining wall. Instead of taking such a plane, for finite element analyses the horizontal extent of soil was varied by a factor multiplying the wall height to obtain an optimum extent of soil for which the lateral soil forces becomes almost constant. Inclusion of soil elements, in the finite element discretization, beyond this extent is not warranted. Results of the analyses are shown in Fig.5.3. It was observed that this distance becomes optimum at about six times the wall height. To determine the suitable depth of

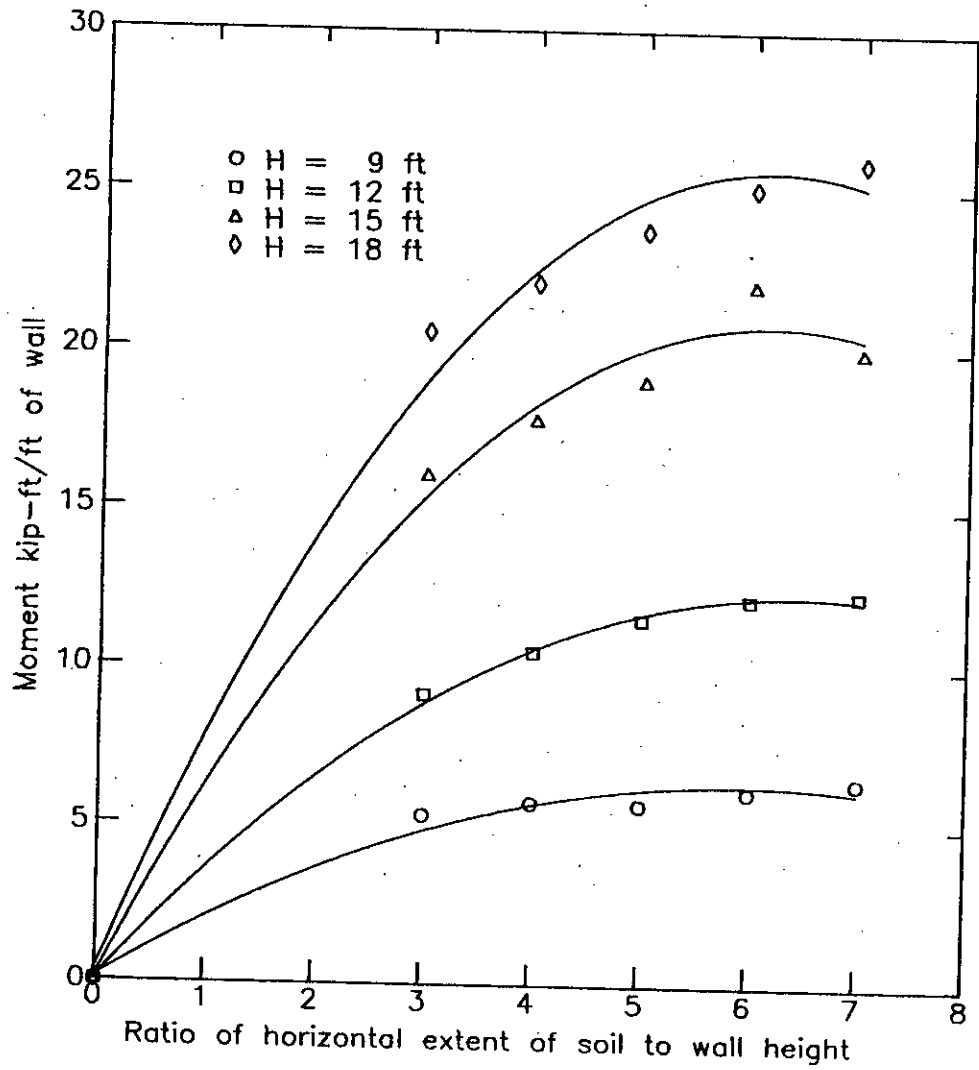


Fig.5.3. Variation of moment with horizontal extent of soil

soil below the wall footing in the finite element mesh nodal strain  $\epsilon_y$ , in the soil was considered. Variation of nodal strain  $\epsilon_y$  for a wall of 9 ft height along the vertical line coinciding with the wall is plotted in Fig.5.4. The steep gradient of the strain distribution along the depth demonstrates that contribution of soil at greater depths to deformation of structure diminish rapidly. This is because the soil elements become stiffer with the increase in depth by having a higher value of confining stress,  $\sigma_{octi}$ . This leads to the conclusion that a large extent of soil need not to be included below the footing in the finite element analysis of rigid retaining walls. The finding confirms that of Seraj (1986), who investigated the interaction of buried rigid culverts with soil and of Nazneen (1986), who investigated the interaction of building structures with soil. It was observed that at a depth of 20 ft, which is about three times the width of wall footing, below the wall footing the strain becomes very small so for all analyses purpose this depth was kept constant at 20 ft. Since the interaction problem requires a large number of matrices for the solution of simultaneous linear equations, the execution of the computer program requires a huge computer memory and long time. For this reason, first of all, mesh dependency of the program was checked. For this at first it was checked whether there should be any difference in the number of beam elements between walls of 9 ft and 18 ft height. The 9 ft height wall was analysed with seven vertical beam elements, The 18 ft wall was analysed with both seven and fourteen vertical beam elements. It was observed that due to this increase i.e., the number of vertical beam elements were increased by 100%, soil elements by 57%, and the resulting moment was increased by 5.04% only. The next step was to check the width of soil elements at the right most side of the mesh, since the aspect ratio of these elements was large. In Figs.5.2(a) and 5.2(b) in the horizontal direction five divisions are shown. To check the above mentioned effect, eight divisions were used instead. It caused an increase in the number of soil elements by 21%, while the moment was reduced by 1.04% only. So when both the number of beam elements and the soil elements are increased by increasing the number of divisions, the change in moment would be less than 5%, while the increase in execution time of the program and memory required by it will be formidable. To make a rational compromise between accuracy and time of execution and computer memory, the same mesh as shown in Figs.5.2(a) and 5.2(b) was selected for all wall height, only the dimension of the beam elements and soil elements was varied using automated mesh adjustment routines.

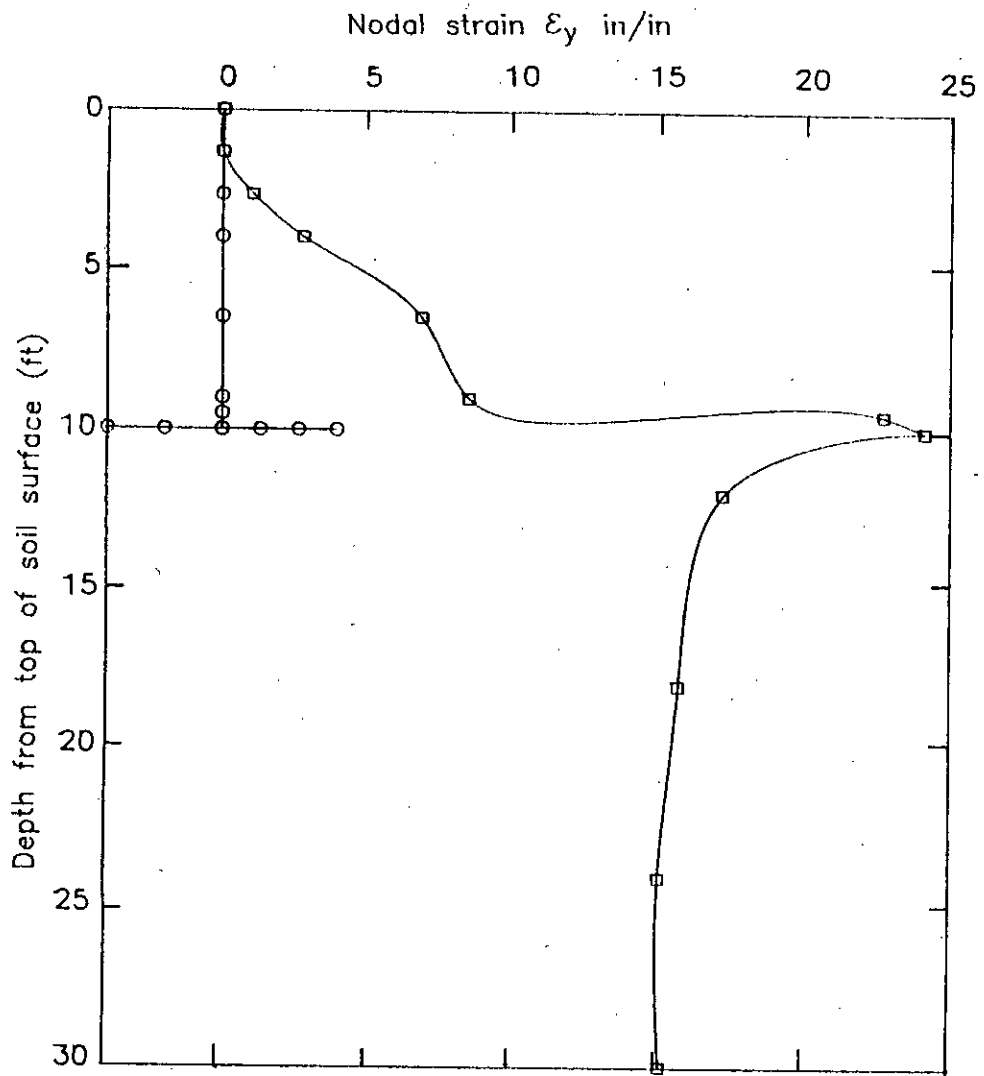


Fig.5.4 Variation of nodal strain in soil with depth for a wall of 9 ft height.



## CHAPTER 6

# DISCUSSION ON FINITE ELEMENT ANALYSES RESULTS

### 6.1 INTRODUCTION

In the previous chapters 3, 4 and 5, the finite element representation of retaining wall, selection of soil model, the computer program and the analyses scheme have been described. This chapter describes the results obtained from the finite element analyses. The influence of various parameters are reported in this chapter. From results of analyses a few equations are derived in this chapter, these equations are subjected to some limitations and described in sec.6.6.

### 6.2 EFFECT OF VARIOUS PARAMETERS ON LATERAL SOIL FORCE AND MOMENT

As described earlier, the various parameters considered for the interaction behaviour of retaining wall-soil system, can be classified as i) structural parameters and ii) soil parameters.

Structural parameters considered were:

- a) Moment of Inertia of wall
- b) Moment of Inertia of wall footing
- c) Compressive Strength of concrete.

The following Soil parameters were considered :

- i) Slope of soil surface
- ii) Unit weight of backfill material
- iii) Poisson's ratio of backfill
- iv) Angle of internal friction of soil.

In addition to the above stated parameters, studies were carried out for embedment ratio also.

#### 6.2.1 Effect of Moment of Inertia of Retaining Wall

To study the effect of moment of inertia of the retaining wall on the interaction behaviour, moment of inertia of sectional area of wall was varied. This study

was carried out since the traditional methods do not include any effect of the wall stiffness on the magnitude of lateral soil force and moment to be resisted by the wall.

To investigate the effect of this parameter, instead of increasing the thickness of wall from top to bottom by same amount, thickness of wall was changed linearly from top to bottom. In all the investigations, thickness of wall at the top was kept constant at 12 inch and the thicknesses at the bottom were 12 inch, 14 inch, 16 inch, 18 inch and 20 inch. This resulted in an increase in the moment of inertia of the wall at the base by 59%, 137%, 238% and 363% with respect to the wall having 12 inch bottom thickness. For separating the effect of this parameter from the effect of other parameters, all other variables were kept constant. Results of finite element analyses are graphically presented in Figs. 6.1 and 6.2. These results are also tabulated in Table A.1 in appendix A.

It has been observed that for walls of 9 ft height, increasing the moment of inertia of wall at the base by 59%, 137%, 238% and 363%, the lateral soil force were changed by 2.65%, 8.30%, 1.07%, 2.40% and the change in moment was 0.4%, 2.4%, 1.9% and 4.6% respectively.

For wall of 12 ft height, changing the moment of inertia of wall at base by the amounts adopted in the preceding study, the percentage of change in lateral soil force of 3.4%, 4.9%, 6.5% and 3.6% was observed. For the same runs, the change in moment was 2.2%, 4.8%, 4.5% and 8.0%, respectively. And for walls of 15 ft height the same changes in the moment of inertia of wall at its base causes a change of 3.2%, 2.7%, 1.3%, and 2.0% in lateral soil force and 3.3%, 17.5%, 5.0% and 6.4% change in the magnitude of moment. For the walls of 18 ft height changing the moment of inertia of wall by same amount the lateral soil force was changed by 0.2%, 6.0%, 7.0% and 0.3% where as the moments were changed by 5%, 6.5%, 5.7%, 9.5%, respectively.

Comparing the large percentage of change in moment of inertia of wall at its base with the small percentage of change in lateral soil forces and observing Fig. 6.1 and Fig 6.2 it can be concluded that neglecting the effect of moment of inertia of wall traditional methods do not introduce any significant error and no

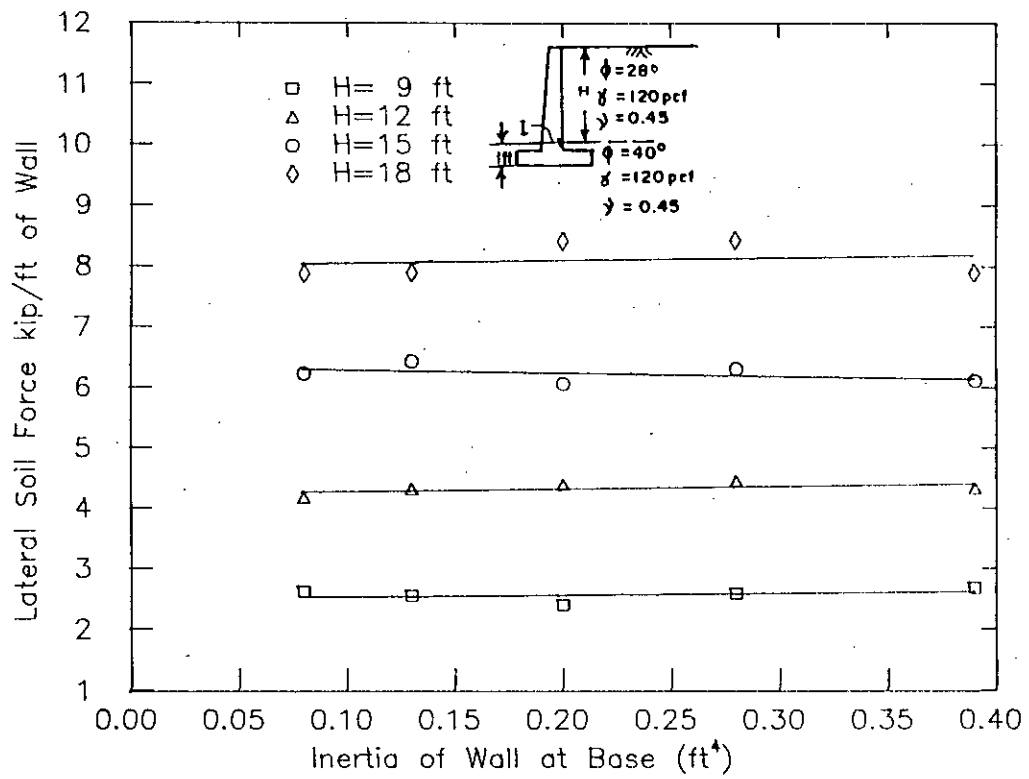


Fig.6.1 Effect of Inertia of Wall at its Base on Lateral Soil Force

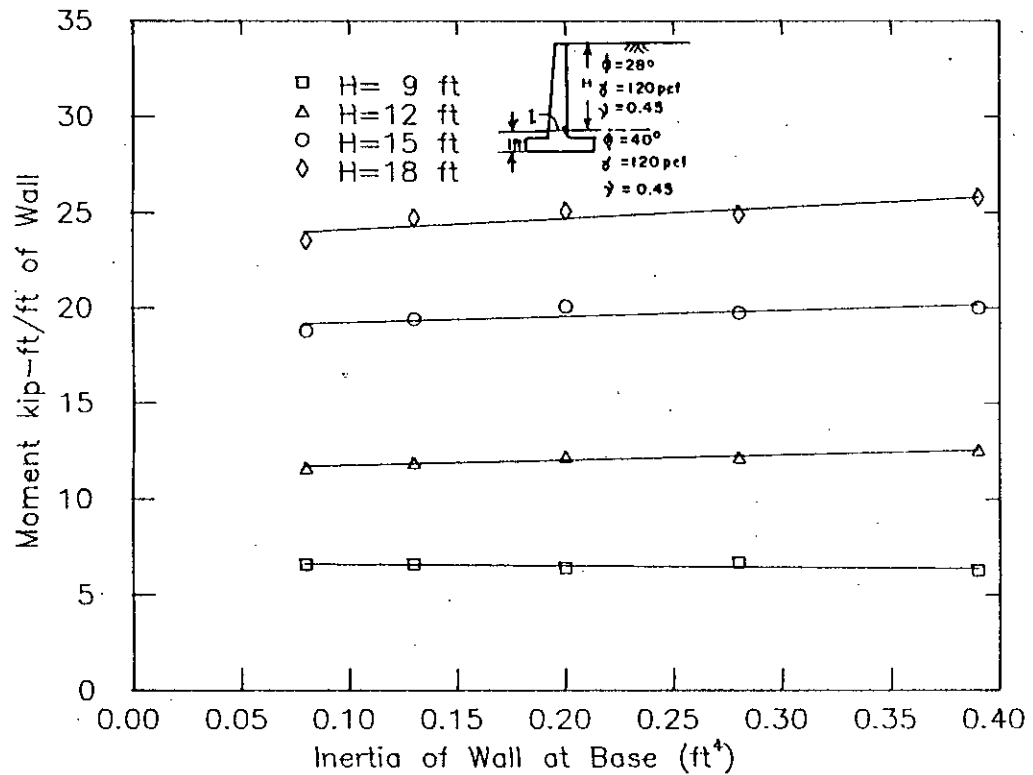


Fig.6.2 Effect of Inertia of Wall at its Base on Moment to be Resisted by the Wall.

improvement of formula is necessary to incorporate the effect of this factor. The effect of moment of inertia of wall would have been significant if the base of the wall have been prevented from rigid body movement. For realistic analyses this was not done.

### 6.2.2 Effect of Moment of Inertia of Wall Footing

To study the effect of moment of inertia of wall footing, thickness of wall footing was varied by keeping all other variables constant. Like the previous study this study was also carried out to investigate whether it is realistic to neglect the effect of stiffness of wall footing during the determination of lateral soil forces or not. To explore the effect of this parameter, wall footing having thickness 24 inch, 28 inch, 32 inch and 36 inches were selected; the resulting moment of inertia of area of the wall footing were  $0.67 \text{ ft}^4$ ,  $1.06 \text{ ft}^4$ ,  $1.58 \text{ ft}^4$  and  $2.25 \text{ ft}^4$ , i.e., the increment in moment of inertia of area of the wall footing with respect to the wall having footing thickness of 24 inch was 59%, 137% and 238% respectively. Results obtained from the finite element analyses are given in Table A.2. in Appendix A. The same results are graphically represented in Fig. 6.3 and Fig. 6.4.

From Table A.2 in Appendix A, it was observed that for walls of 9 ft height, increasing moment of inertia of wall footing by 59%, 137% and 238%, the change in lateral soil force was 4.5%, 1.4%, 2.0% and change in moment was 0.7, 2.8% and 3.0% respectively. For wall of 12 ft height, change in lateral soil force was 3.7%, 0.5%, 1.8% and changes in moment was 1.0%, 3.0% and 1.6% respectively. For wall of 15 ft height, change in lateral soil force was 5.5%, 1.6% and 2.1% respectively whereas the changes in moment was 2.4%, 3.7% and 5.3% respectively. For walls of 18 ft height changes in lateral soil force was 5.4%, 5.9%, 6.2% and the change in moment was 0.5%, 1.8% and 2.3% respectively.

From Fig. 6.3 and Fig. 6.4 it is clear that the percentage of variations would have been further smaller if they were calculated from the average line. Observing this fact and comparing the large percentage of increase in moment of inertia of wall footing with the small percentage of changes in lateral soil force and moments, it appears that the effect of moment of inertia of wall footing need not be considered during determining the values of lateral soil

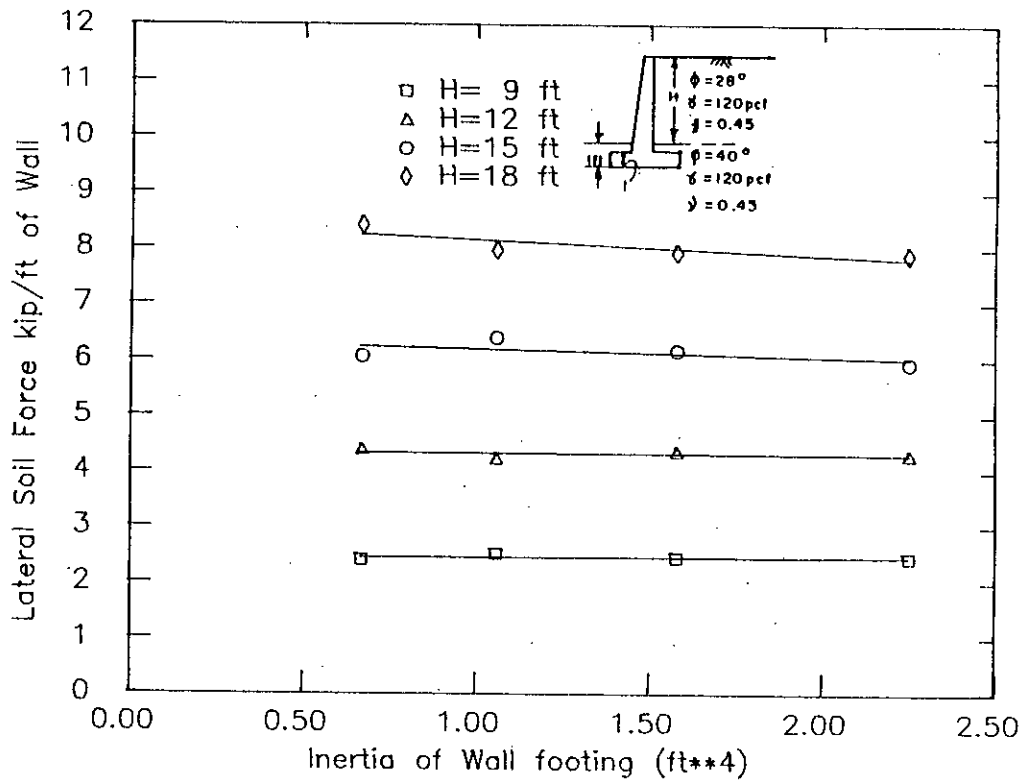


Fig.6.3 Effect of Inertia of Wall Footing on Lateral Soil Force

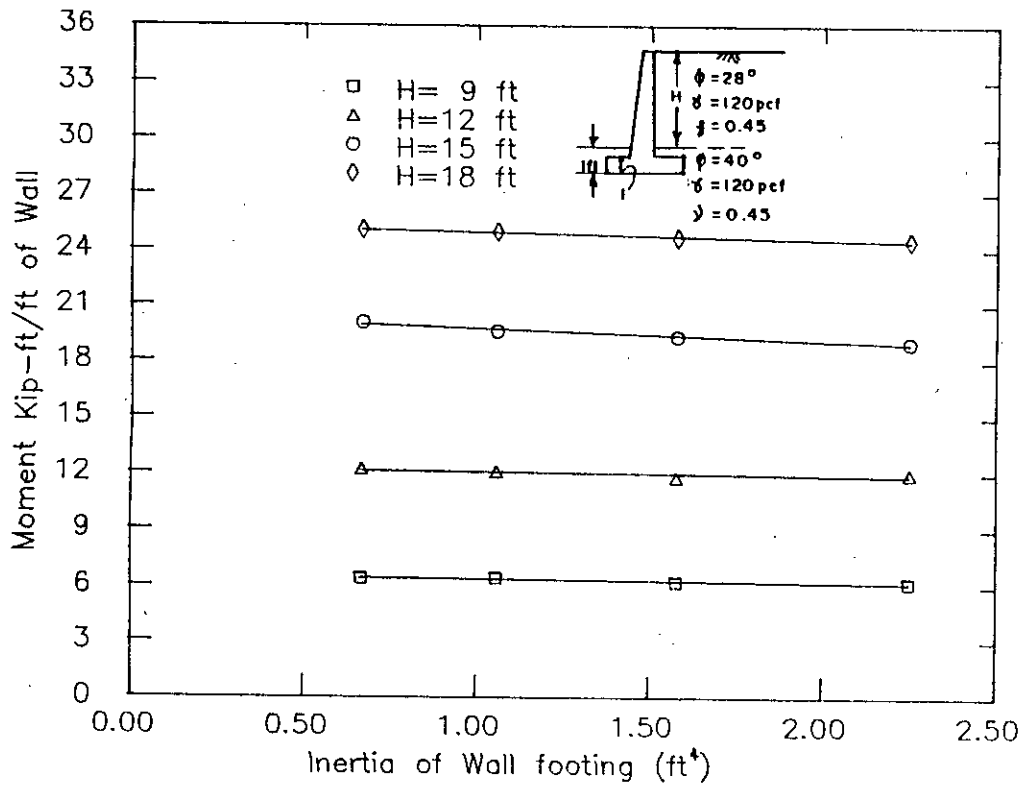


Fig.6.4 Effect of Inertia of Wall Footing on Moment to be Resisted by the Wall

force. So the traditional methods do not introduce any appreciable error by neglecting the effect of moment of inertia of wall footing.

### 6.2.3 Effect of Compressive Strength of Concrete

To study the role of compressive strength of concrete, concrete having strengths 2500, 2700, 3000 and 3500 psi were chosen for analyses purpose. Results obtained from the finite element analyses are presented in Table A.3 in Appendix A. They are graphically presented in Fig. 6.5 and Fig. 6.6. From Table A.3, for a wall of 9 ft height increasing  $f'_c$  by 8.0%, 20.0% and 40.0%, the lateral soil force is changed by 1.5%, 1.4% and 4.2%. At the same time, moments are changed by 1.0%, 0.7%, and 1.4%, respectively. For walls of height 12 ft, same increase in the  $f'_c$  value changes the lateral soil force by 3.5% ,5.5% and 1.0% whereas the moments are changed by 0.8%, 0.5% and 1.4%, respectively. For walls of height 15 ft, changes in lateral soil force are 1.9%, 2.9% and 1.8% and in moments are changed by 1.0%, 0.1%, 1.1%. For walls of 18 ft height, changes in lateral soil force are 5.5%, 0.7% and 0.3% and moments are changed by 0.2%, 0.5% and 0.7%.

Observing that the changes in lateral soil force and moments are small and considering that the band in which concrete strength is expected to vary is narrow, this parameter can also be neglected for a simplified analysis procedure.

### 6.2.4 Effect of Slope of Soil Surface

To study the effect of soil surface slope on the behaviour of retaining wall-soil system, back fill with surface slope of  $0^\circ, 5^\circ, 10^\circ, 15^\circ$  and  $20^\circ$  with the horizontal were considered. Table A.4 in Appendix A contains the results obtained from finite element analyses and Fig.6.7 and Fig.6.8 show the graphical representation of the obtained results.

From Table A.4, in Appendix A it can be seen that for walls of 9 ft height, changing the slope to  $5^\circ, 10^\circ, 15^\circ$  or  $20^\circ$  from  $0^\circ$  increases lateral soil force by 30%, 70%, 105% and 168% respectively, and changes in moment were 36%, 86%, 167% and 248%.

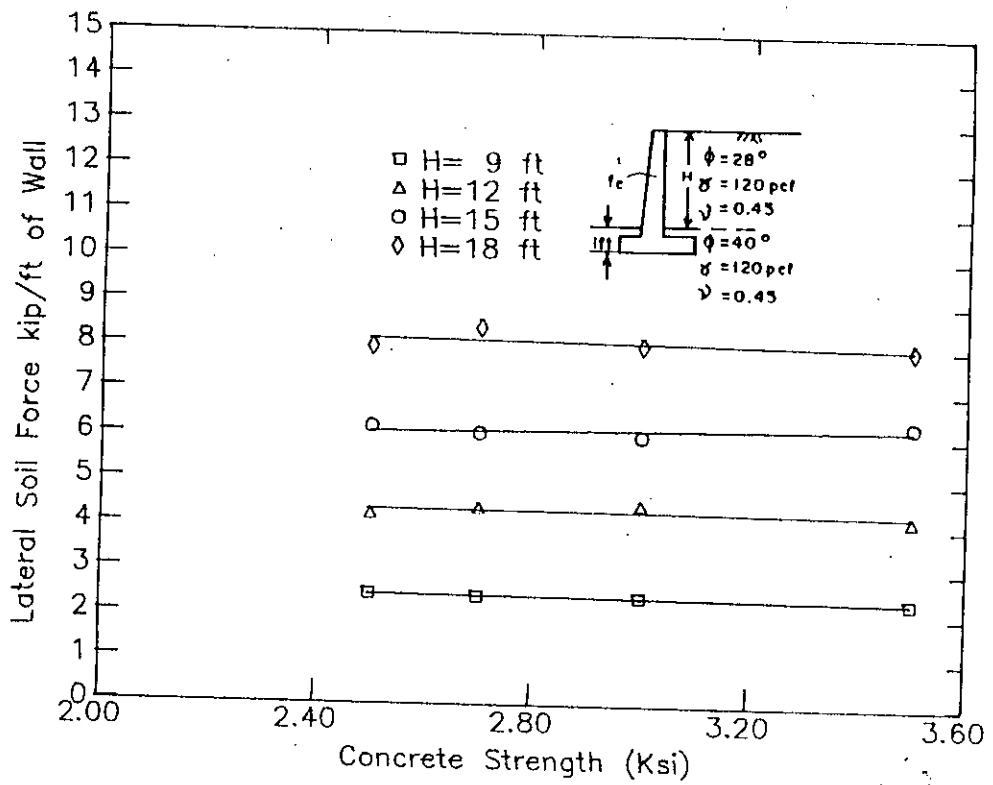


Fig.6.5 Effect of Concrete Strength on Lateral Soil Force

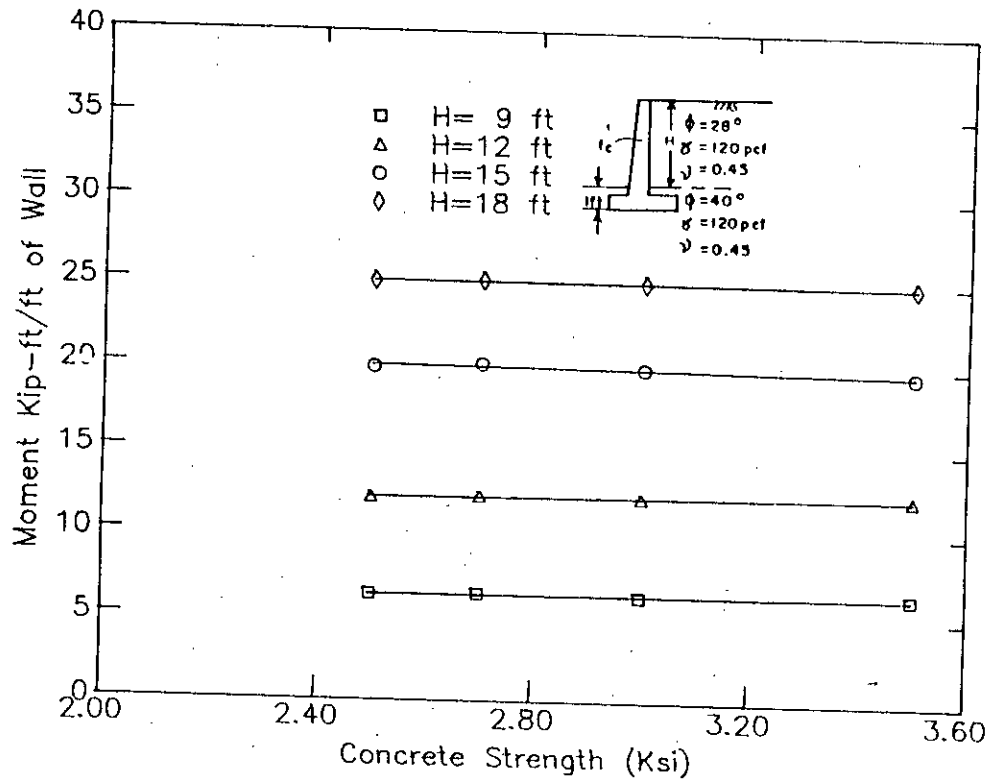


Fig.6.6 Effect of Concrete Strength on Moment to be Resisted by the Wall

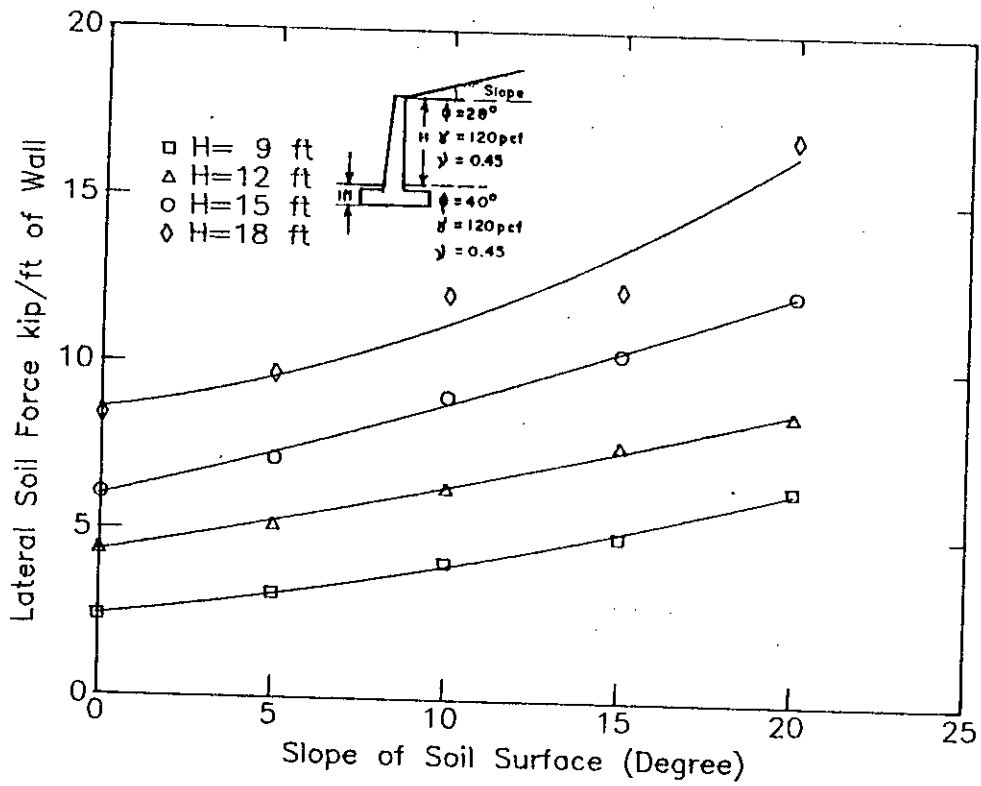


Fig.6.7 Effect of Slope of Soil Surface on Lateral Soil Force

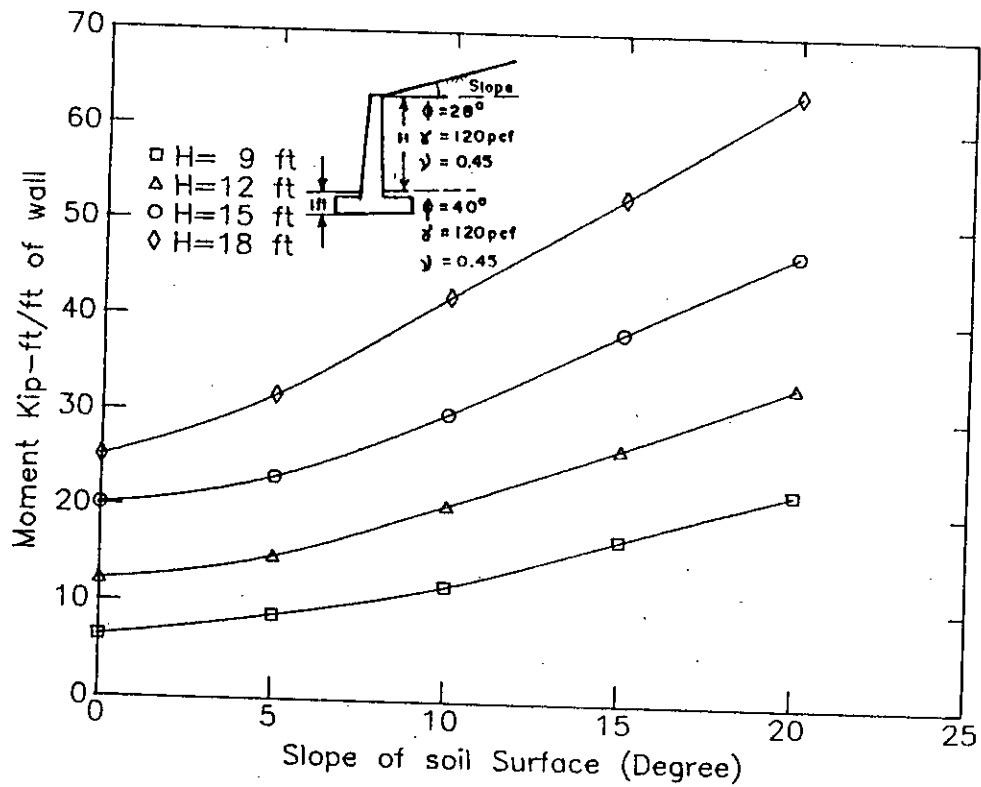


Fig.6.8 Effect of Slope of Soil Surface on Moment to be Resisted by the Wall



For walls with 12 ft height, changes in lateral soil force was 18%, 44.5%, 75%, 75% and 97% and for moments changes were 21%, 67%, 118% and 173%. For walls with 15 ft height, changes in lateral soil force was 18%, 49%, 71%, 102% and for moments changes were 15%, 49%, 92%, 134%. Similarly for wall of 18 ft height, changes in lateral soil force was 15%, 44%, 46% and 88% and for moments changes were 26%, 68%, 110% and 154%.

From the above, it is clear that for a small increase in the slope of soil surface with the horizontal there occurs an appreciable increase in the horizontal force and the moment that is to be resisted by the wall. This achievement is satisfactory since  $\beta$  equal to  $90^\circ$  would produce a wall with infinite height and hence the force and the moment.

It is interesting to note that for a given value of  $\beta$ , variation of percentage of change with respect to height is parabolic. It first decreases with height of wall and then again increases.

Variation of moment with respect to  $\beta$  can be approximated as

$$M_\beta = M_0 \left[ 1 + \left( 2 + \frac{\beta}{5} \right) \sin \beta \right]$$

where  $\beta$  is in degrees.

The above equation neglects the effect of height which is mentioned previously and is based on the average variation obtained from walls of different heights for any given value of  $\beta$ .

When the effect of height is taken into consideration,

$$M = M_0 \left[ 1 + \left\{ \left( 2 + \frac{\beta}{5} \right) \sin \beta \right\} (2.074 * 10^{-3} H^3 - 0.0669 H^2 + 0.587 H) \right]$$

Results (% of increase with respect to horizontal ) from finite element analysis and from proposed formulae is shown in Table A.5 in Appendix A.

Comparing the above tables it can be concluded that the proposed formulae is satisfactory.

### 6.2.5 Effect of Unit Weight of Backfill Material

Traditional methods, from their analytical formulation, show that lateral soil force is directly proportional to the unit weight of backfill material. To verify this proportionality, an attempt was made to analyse various retaining walls with backfill materials having unit weights of 100 pcf, 110 pcf, and 120 pcf. Results of the finite element analyses are given in Table A.6 in Appendix A. These results are also graphically presented in Figs. 6.9 and 6.10.

Figures 6.9 and 6.10 show that the lateral soil force and the moment varies linearly with unit weight of the backfill. Table A.7 in the Appendix A shows the variation of lateral soil force and the moment as a percentage of change with respect to unit weight of 100 pcf and 110 pcf. It is observed that the average variation for 10 pcf increment in 100 pcf unit weight is equal to 10% and for 20 pcf increment the variation is equal to 20%. Unit weight of backfill material is, indeed, a linear contributor to lateral soil force, as postulated in the traditional ways of thinking.

So it can be concluded that the traditional concept of  $M \propto \gamma$  and  $P_a \propto \gamma$  is satisfactory.

### 6.2.6 Effect of Poisson's Ratio of Backfill Material:

Traditional methods do not show any variation of lateral soil force or moment with Poisson's ratio  $\nu$ , but from the knowledge of elasticity it is expected that there must be some relationship of the lateral soil force and the moment with Poisson's ratio, since it establishes the relationship between the two orthogonal directions. To investigate the effect of Poisson's ratio, analyses were done for 9 ft, 12 ft, 15 ft and 18 ft walls using Poisson's ratio of 0.45, 0.46 and 0.47.

Table A.8 in Appendix A contains the results obtained from the finite element analyses and Figs 6.11 and 6.12 show the graphical representation of the results obtained from the analyses.

From Table A.8, it is observed that a small change in the Poisson's ratio causes an appreciable amount of change in the lateral soil force and moment

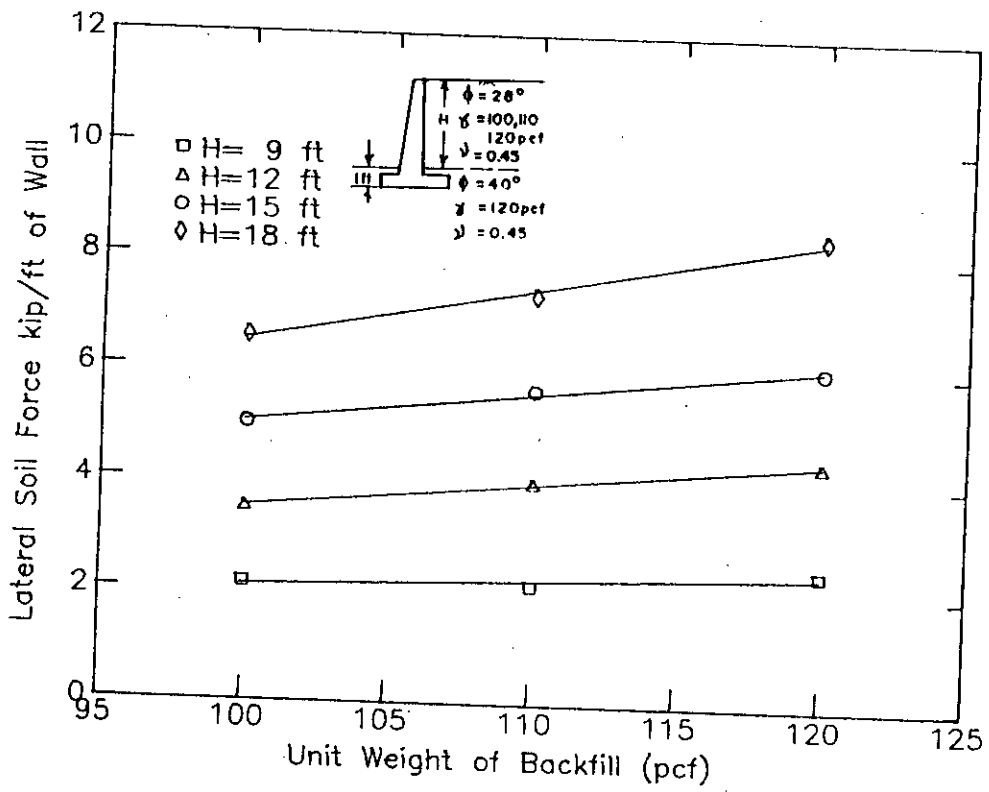


Fig.6.9 Effect of Unit Weight of Backfill on Lateral Soil Force

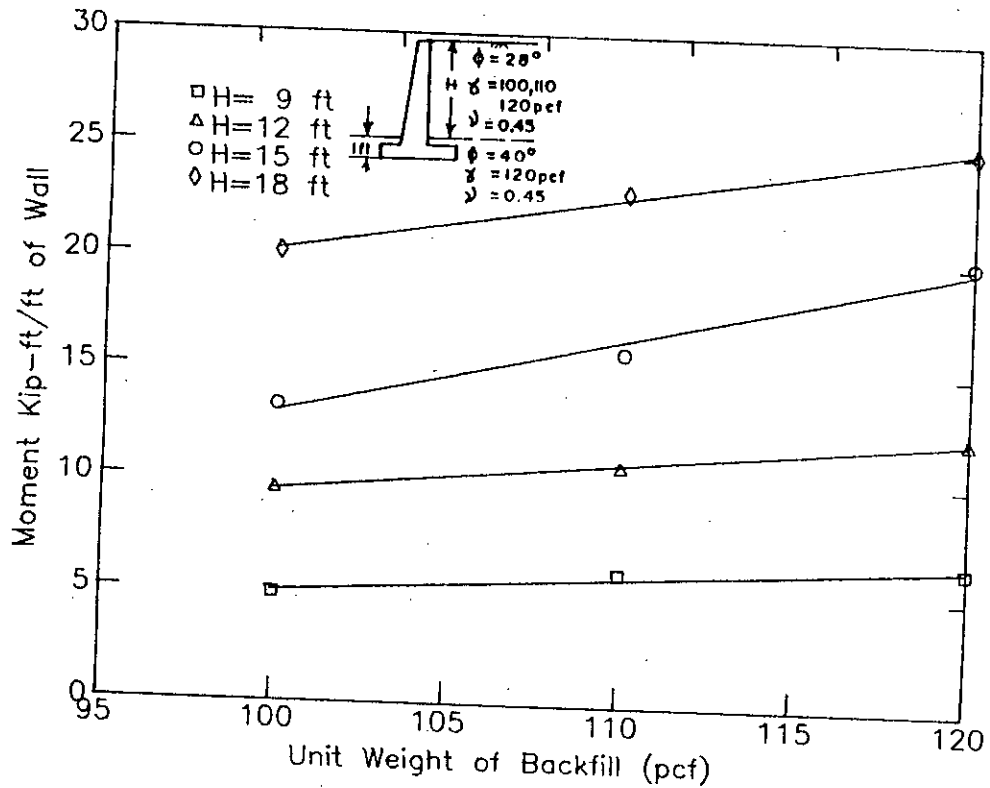


Fig.6.10 Effect of Unit Weight of Backfill on Moment to be Resisted by the Wall

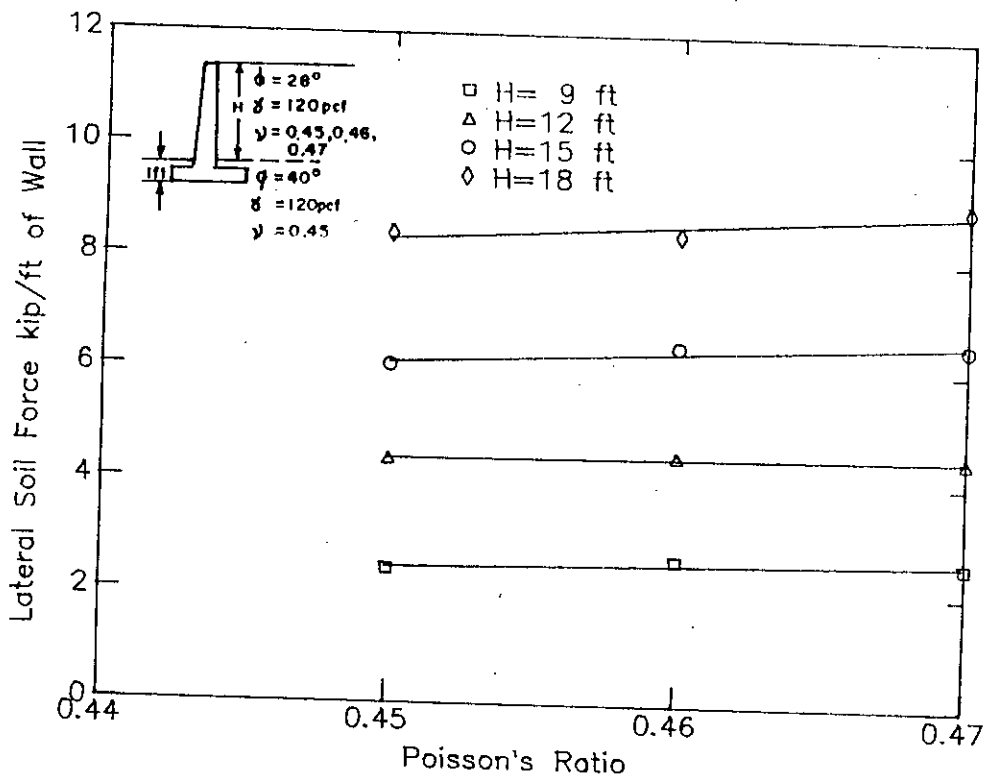


Fig.6.11 Effect of Poisson's Ratio on Lateral Soil Force

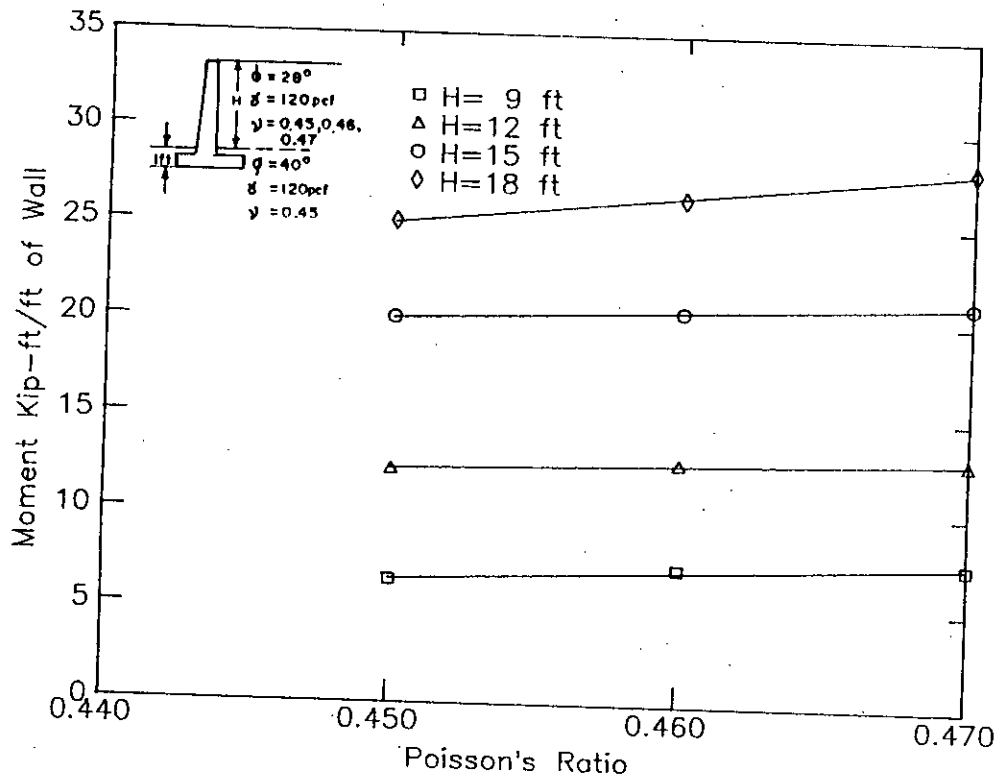


Fig.6.12 Effect of Poisson's Ratio on Moment to be Resisted by the Wall

which can not be neglected. From the table it has been noted that a change in the value of  $\nu$  from 0.45 to 0.46 i.e., an increment of 2.22% causes an average increase of lateral soil force of about 5%, a change in  $\nu$  from 0.46 to 0.47 i.e., an increment of 2.17% causes an average increase of 4.5% in the lateral soil force and moment. For the total change of  $\nu$  from 0.45 to 0.47, an increment of 4.44% is considered, a total increment of 7.75% in the average lateral soil force and moment is observed.

Now, it has been previously established that

$$M \propto \gamma$$

Assuming

$$M \propto \nu \gamma,$$

for walls with horizontal backfill taking  $M_o = \nu \gamma f(H)$   
using results presented in Table A.8

$$M_o = \nu \gamma [-0.0188767H^4 + 0.623182H^3 - 4.5024833H^2 + 17.6917H]$$

$$\text{and } M = M_o f(\beta, H)$$

### 6.2.7 Effect of Angle of Internal Friction of Backfill Material

In the absence of test results, octahedral shear stress and octahedral shear strain curves for different confining pressures for soil of angle of internal friction of  $28^\circ$  and  $40^\circ$  as reported by Seraj (1986) and Seraj and Rahman (1987) have been used. Table 6.9 in Appendix A shows the results of the finite element analyses.

From the results of finite element analyses, as presented in Table A.9, in Appendix A it is evident that as the value of  $\phi$  is changed from  $40^\circ$  to  $28^\circ$  i.e., when soil becomes loose, lateral pressure increases resulting an increase in lateral soil force and in moment. The variation in moment is simultaneously dependent on  $\phi$  and  $H$ . In the absence of adequate data, a thorough study for the effect of internal friction of soil was not possible. But studying that changing from loose soil ( $\phi = 28^\circ$ ) to stiff soil ( $\phi = 40^\circ$ ) the results are not appreciably changed; use of lower  $\phi$  values is, however, recommended to be on the safe side.

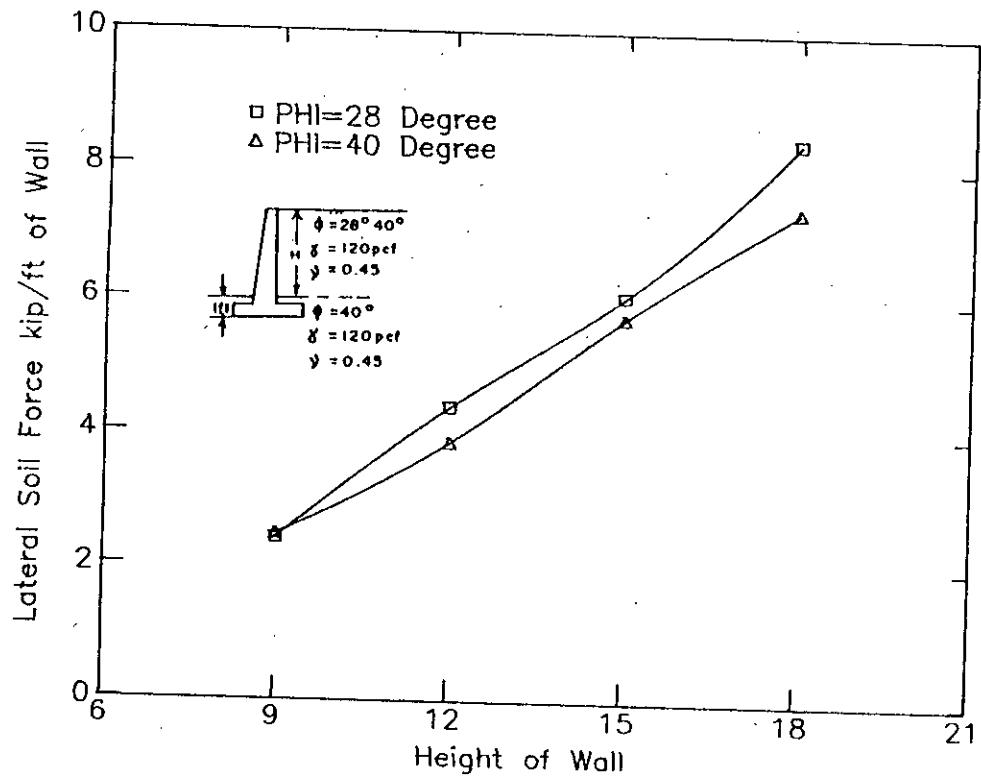


Fig.6.13 Effect of Angle of Internal Friction on Lateral Soil Force

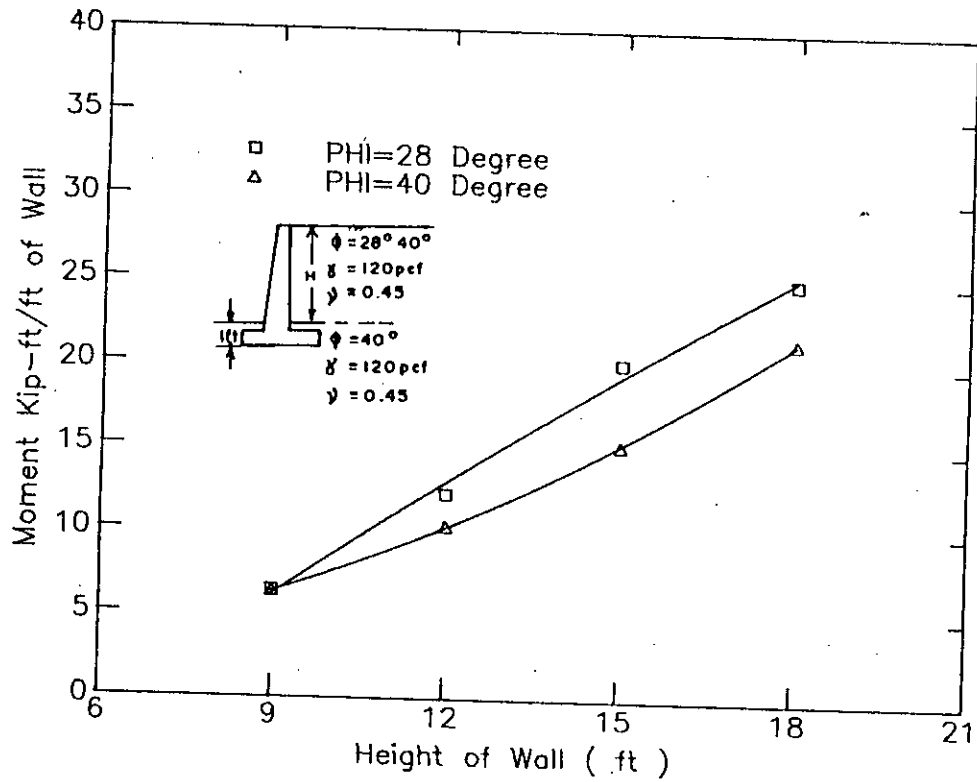


Fig.6.14 Effect of Angle of Internal Friction on Moment to be Resisted by the Wall

### 6.2.8 Effect of Embedment Depth of Wall into the Original Soil

Conventionally, retaining walls are designed for their total height by assuming a linear pressure distribution. These methods neglect any effect on pressure distribution, that may be caused by the depth of embedment, i.e., the depth of the wall into the soil. To investigate the effect, depth of embedment that were selected for analyses are 1 ft, 1.5 ft, 1.75 ft and 2 ft. Analyses were conducted for walls having 9 ft, 12 ft, 15 ft and 18 ft height. Results of finite element analyses are presented in Table A.10 in Appendix A and their graphical representation is given in Fig. 6.15. and 6.16.

Results of finite element analyses shows that for embedded depth of up to 1.75 ft, the magnitude of moment increases at a point for increasing the depth of embedment below that point. This is due to the fact that additional embedment results in additional restraint at the footing end of the wall. Consequently, the wall moment is increased. This finding is in line Ziegler (1987), as mentioned earlier.

For wall of 9 ft height, ratio of embedment to height were 0.11, 0.17, 0.19 and 0.22. Changing the embedment ratio from 0.11 to the others, the lateral soil force increases by 6.8%, 4.6%, 7.9% and in moment was 13.0%, 14.3%, 13.9% respectively. For wall of 12 ft height embedment ratio was 0.083, 0.125, 0.146, 0.167. Changing the embedment ratio from 0.083 to the others the changes in lateral soil force was 0.16%, 0.62% - 3.47% and changes in moments was 4.09%, 8.16%, 1.88%. for wall of 15 ft height embedment ratios were 0.067, 0.100, 0.167 and 0.133. Changing the embedment ratio from the first one to the others changes to the lateral soil force was 2.40%, 1.10%, 1.67%, and in moments was -0.06%, 2.18%, 0.47%. For wall of 18 ft height embedment ratios were 0.056, 0.083, 0.097 and 0.111. Changing the embedment ratio from 0.056 to the others the changes in lateral soil pressure forces was -2.04%, -3.15%, -3.27% and in Change moment was 3.76%, 3.95%, -0.46%. Inspection of the above percentage of changes lead to the conclusion that the effect of embedment on lateral soil pressure force and moment is not directly governed by the amount of embedment but is governed by the ratio of embedded depth and height of wall. For wall of smaller height, when the ratio was large, the changes were also large and for large walls where the ratio was small the effect was also small.

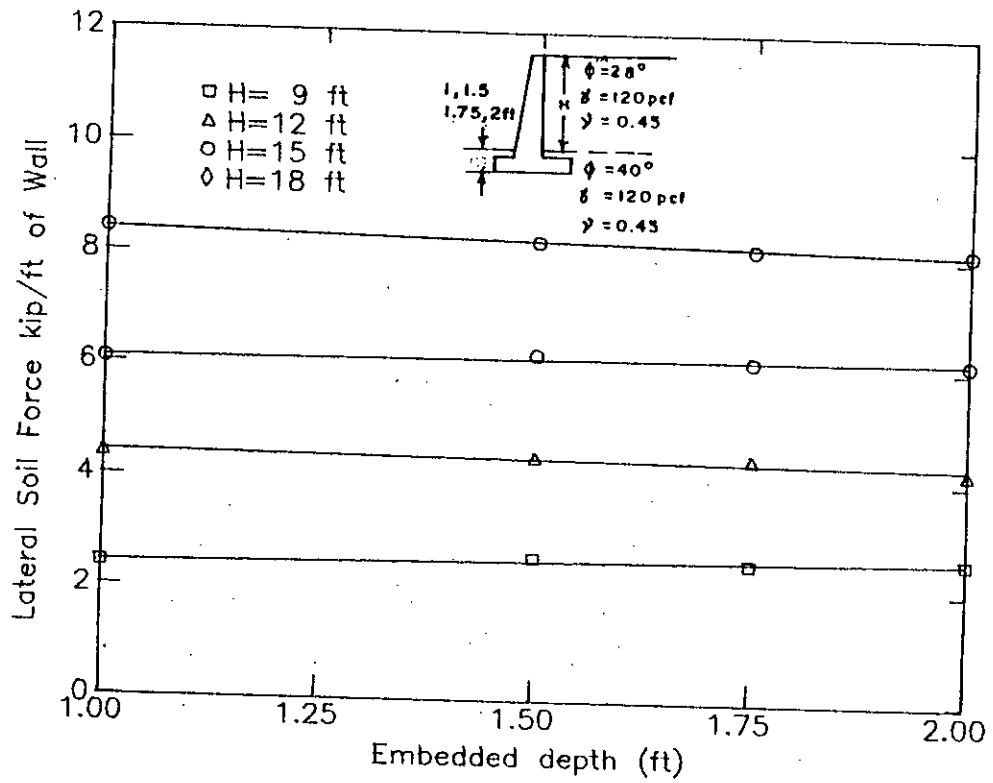


Fig. 6.15 Effect of Embedded Depth on Lateral Soil Force

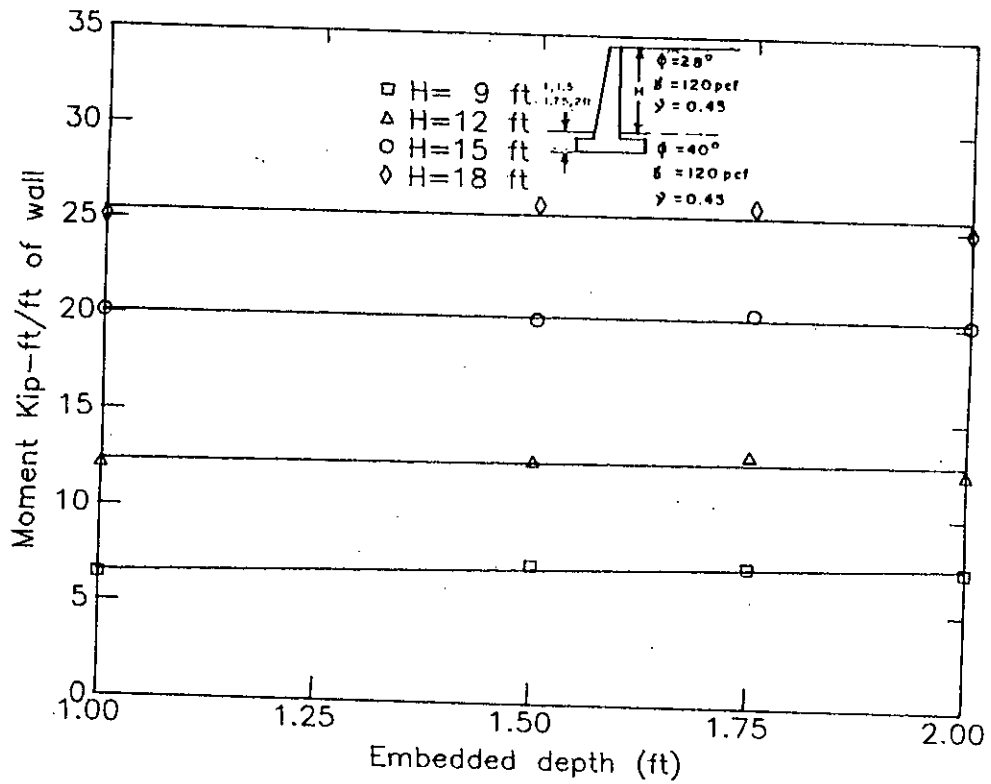


Fig. 6.16 Effect of Embedded Depth on Moment to be Resisted by the Wall



Another observation from the obtained results was that the pressure distribution changes with the change of embedment, by observing the values of moment and lateral soil force, since their ratio changes with amount of embedment, i.e., location of the resultant horizontal force changes. From the results of analyses and above discussion it appears that the lateral soil force and moment are influenced by the embedment ratio. For walls of small and moderate height, maximum increase was found to be 14.3%. For walls of larger height no significant variation was observed. For simplicity the values of lateral soil force and moment can be increased by 15% for any embedment ratio.  
i.e.,  $M = 1.15 M_0$

### 6.3 EFFECT OF LINE LOAD

To study the effect of line loading, line load of 1 kip/ft of width of wall with an increment of 1 kip/ft up to 10 kip/ft was applied. Results obtained from the analyses are presented in Tabular form in Table A.11 to A.14 in Appendix A. These results are obtained by deducting the effect of self weight from the combined effect of self weight and line load. The results are graphically presented in Figs. 6.17 to 6.24. The figures show the total effect of self weight and line loading. At any stage of loading, the effect of line load can be obtained by deducting the initial ordinate from the ordinate corresponding to that loading. For wall of 9 ft when load is applied at 4 ft away from the wall face, equation of moment for line loading becomes  $M_1$  equal to  $1.558P$  where  $M_1$  is the moment due to line load and  $P$  is the applied line load. And when the load is applied at 7.25 ft, 10.5 ft and 13.75 ft respectively equation of line load moment is given by  $M_1$  equal to  $1.231P$ ,  $M_1$  equal to  $0.884P$  and  $M_1$  equal to  $0.562P$ . For walls of height 12 ft, 15 ft and 18 ft load was applied at a distance of 4.00 ft, 8.92 ft, 13.83 ft and 18.75 ft. The equation of moment for these walls can be expressed as  $M_1 = K.P$ . The  $K$  values are given in Table.6.1

**Table 6.1 Values of K for equation  $M_1 = K.P$**

H ft	X = 4.00 ft	X = 8.92 ft	X = 13.83 ft	X = 18.75 ft
12	1.491	1.232	0.875	0.514
15	1.178	1.126	0.857	0.546
18	0.853	0.983	0.809	0.572

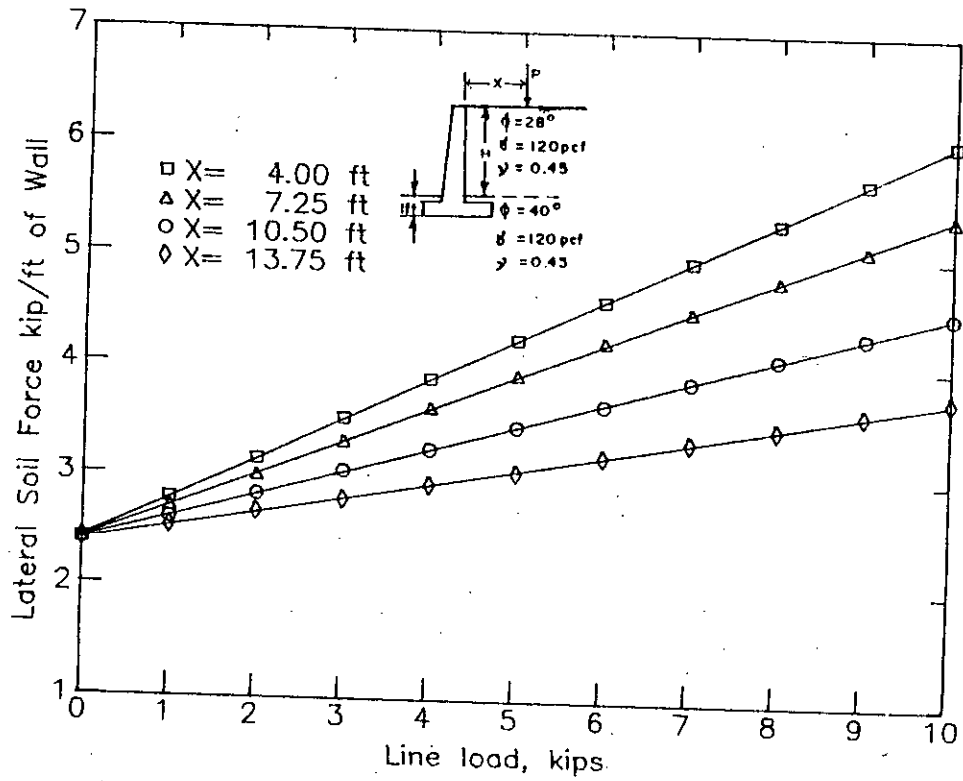


Fig. 6.17 Effect of Line load on Lateral Soil Force for a Wall of 9 ft Height

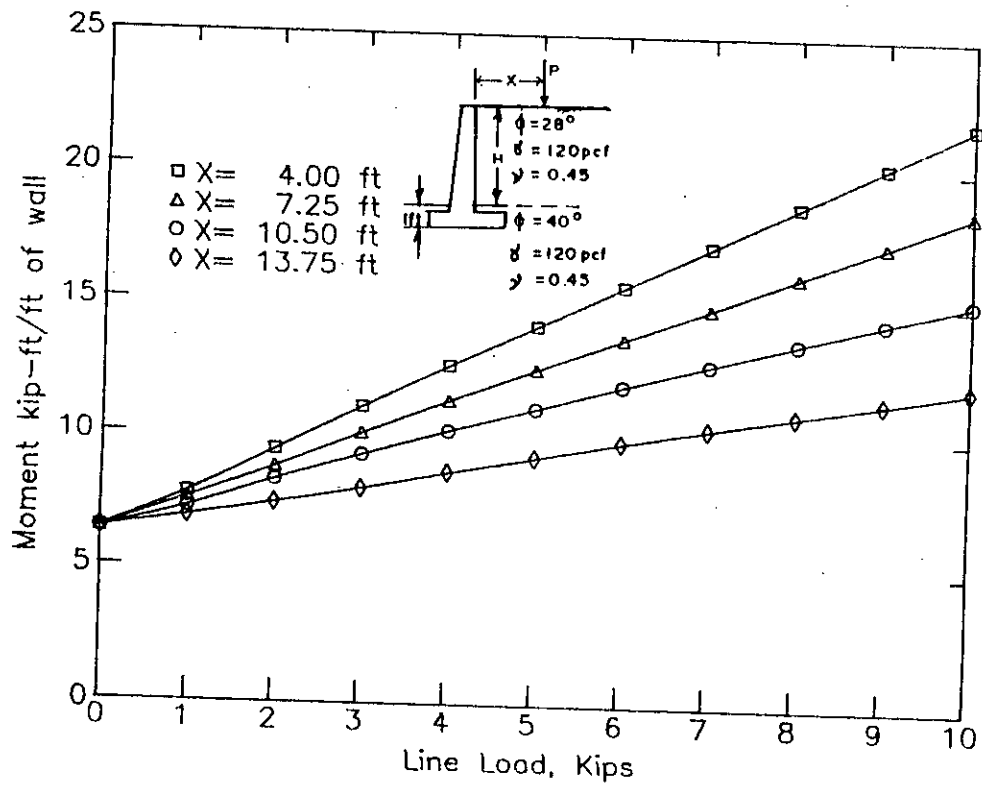


Fig. 6.18 Effect of Line load on Moment to be Resisted by a Wall of 9 ft Height

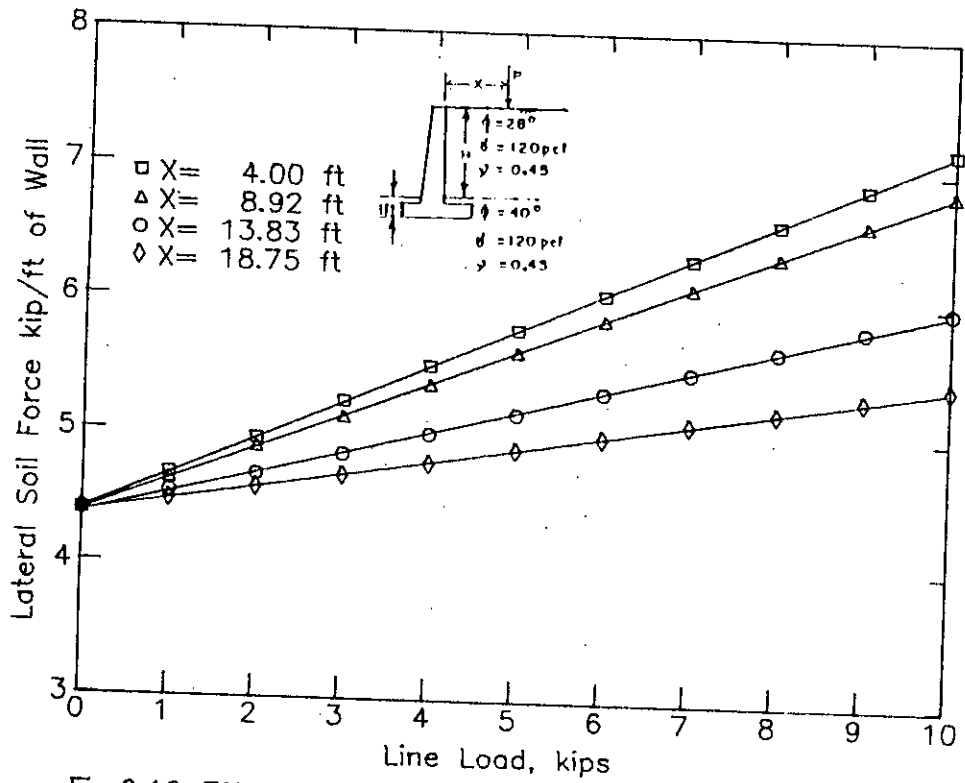


Fig. 6.19 Effect of Line Load on Lateral Soil Force for a Wall of 12 ft Height

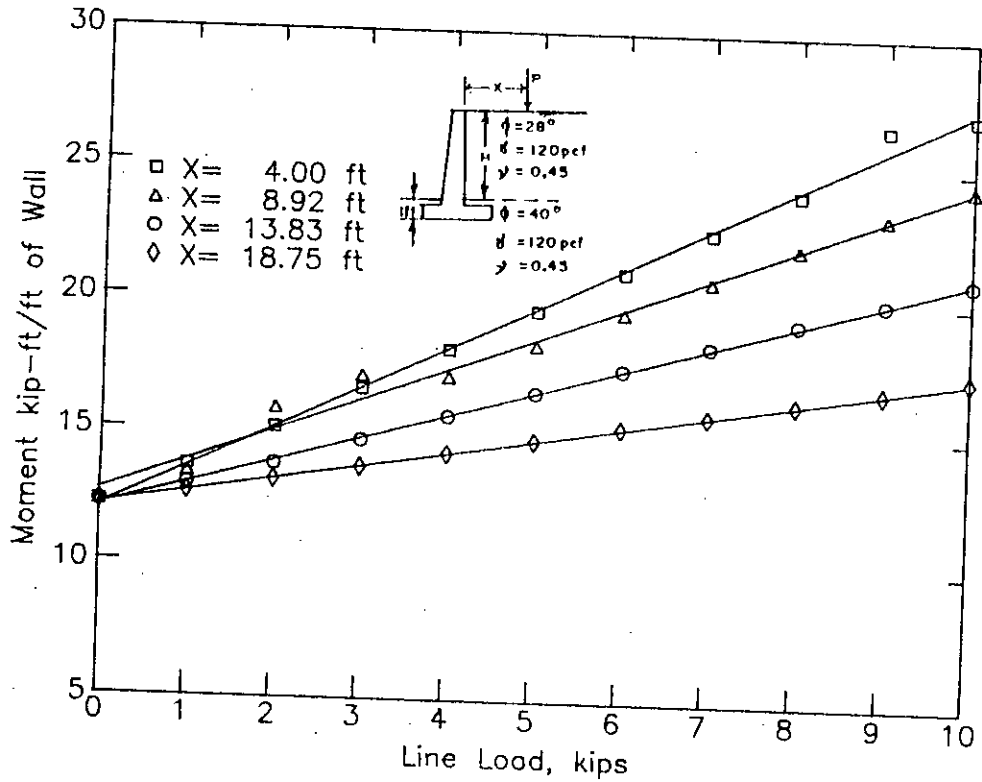


Fig. 6.20 Effect of Line Load on Moment to be Resisted by a wall of 12 ft Height

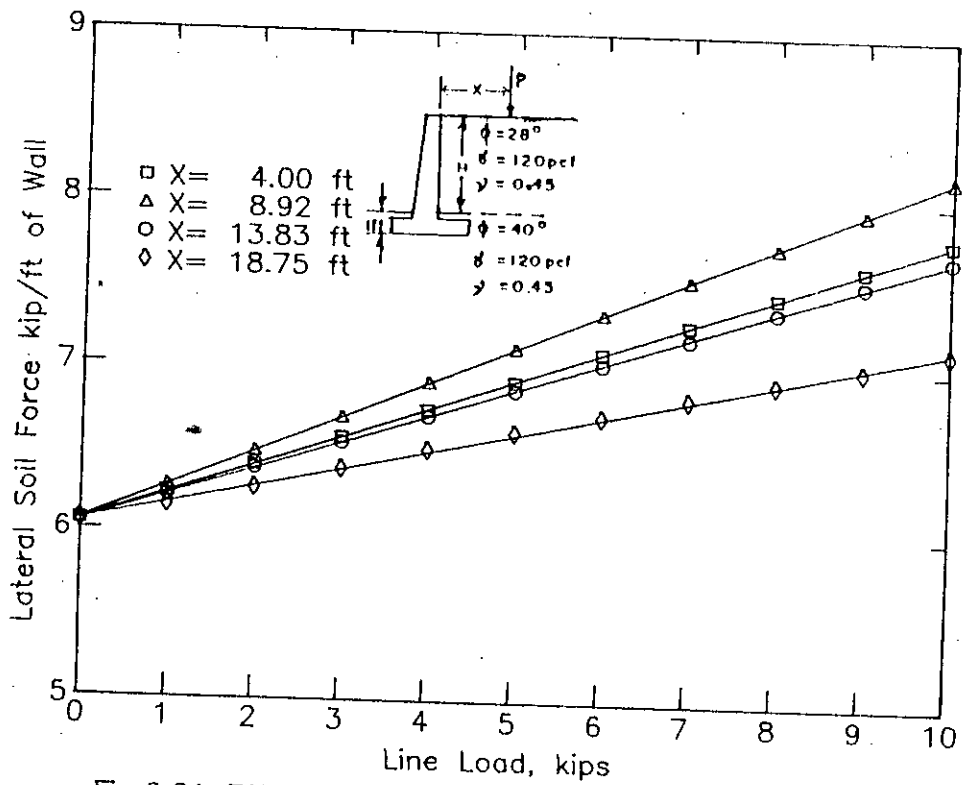


Fig. 6.21 Effect of Line Load on Lateral Soil Force for a Wall of 15 ft Height

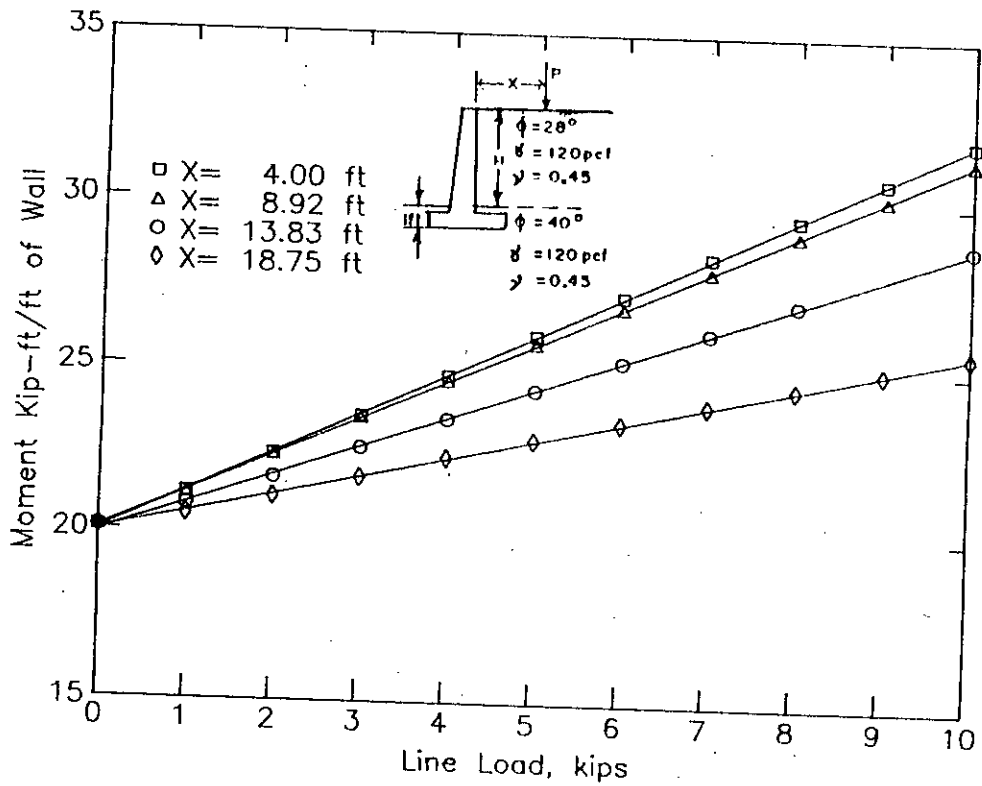


Fig. 6.22 Effect of Line Load on Moment to be Resisted by a Wall of 15 ft Height

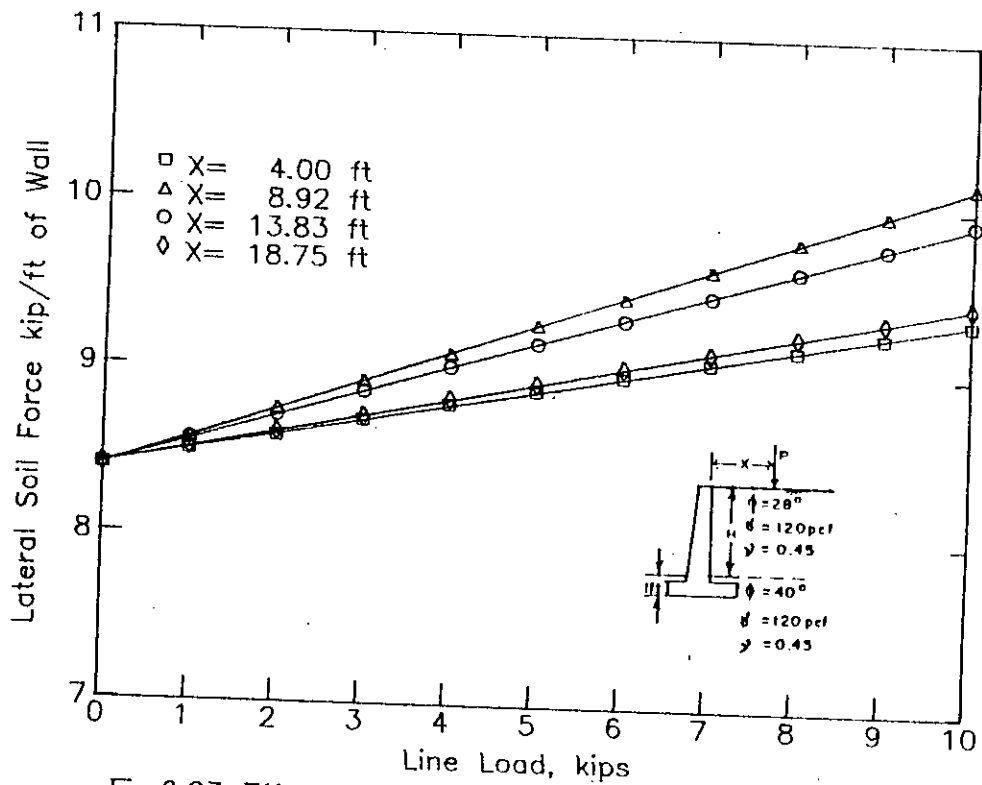


Fig. 6.23 Effect of Line Load on Lateral Soil Force for a Wall of 18 ft Height

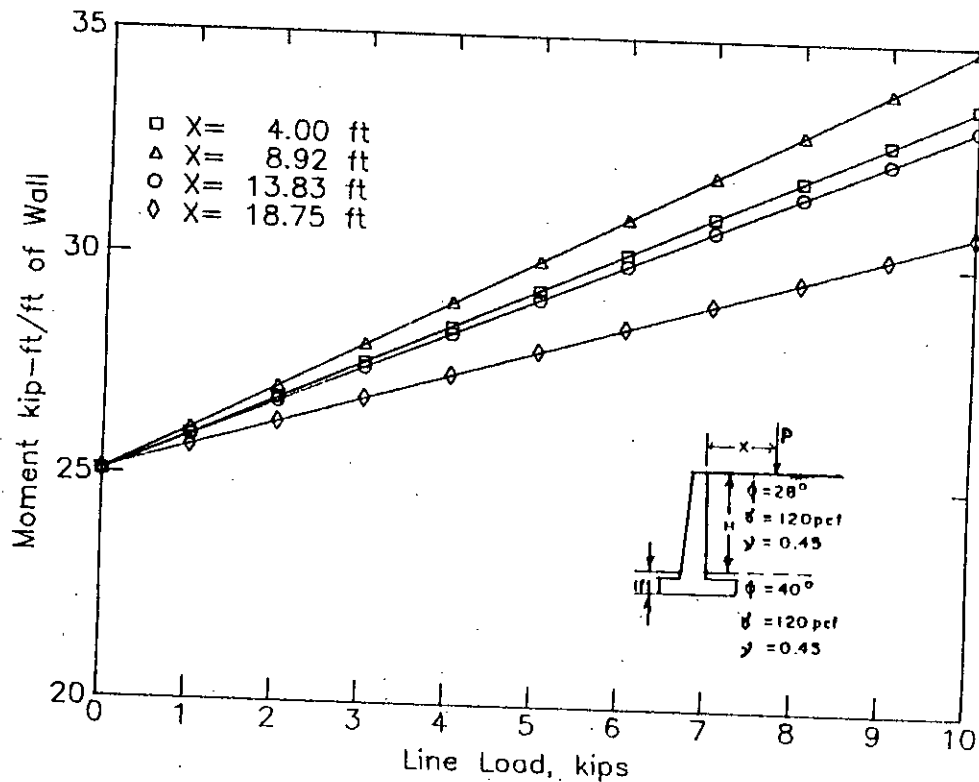


Fig. 6.24 Effect of Line Load on Moment to be Resisted by a Wall of 18 ft Height

The results of the analyses are plotted in Figs. 6.25 to 6.32 to observe the type of variation of shear and moment with respect to the position of applied load. From these figures, it has been observed that the variation of shear and moment can be approximated as exponentially decaying with respect to the position of applied load. From this observation, equation of line load moment was developed as

$$M_l = a' e^{-b'x} p$$

In the above equation  $x$  represents the distance of load from the wall face. Values of  $a'$  and  $b'$  for the walls analysed are given in Table 6.2

**Table 6.2 Values of  $a'$  and  $b'$  for the equation  $M_l = a' e^{-b'x} p$**

H, ft	$a'$	$b'$
9	2.4934	0.1043
12	2.1611	0.07195
15	1.6124	0.0525
18	1.6479	0.0551

Values presented in Table.6.2 were used to derive a single equation for all wall heights . The equation can be expressed as

$$M_l = a.e^{-bx} p$$

where,

$$a = 1.57 + \frac{1}{45}(H - 16.25)^2$$

$$b = 0.0511 + \frac{1}{880}(H - 16.25)^2$$

The above equation gives values which are higher than those obtained for 18 ft wall and  $x$  equal to 4 ft because this value was neglected during the regression analyses and in other cases slightly small or large values due to the large number of calculation and associated accumulated error to reach to the final equation.

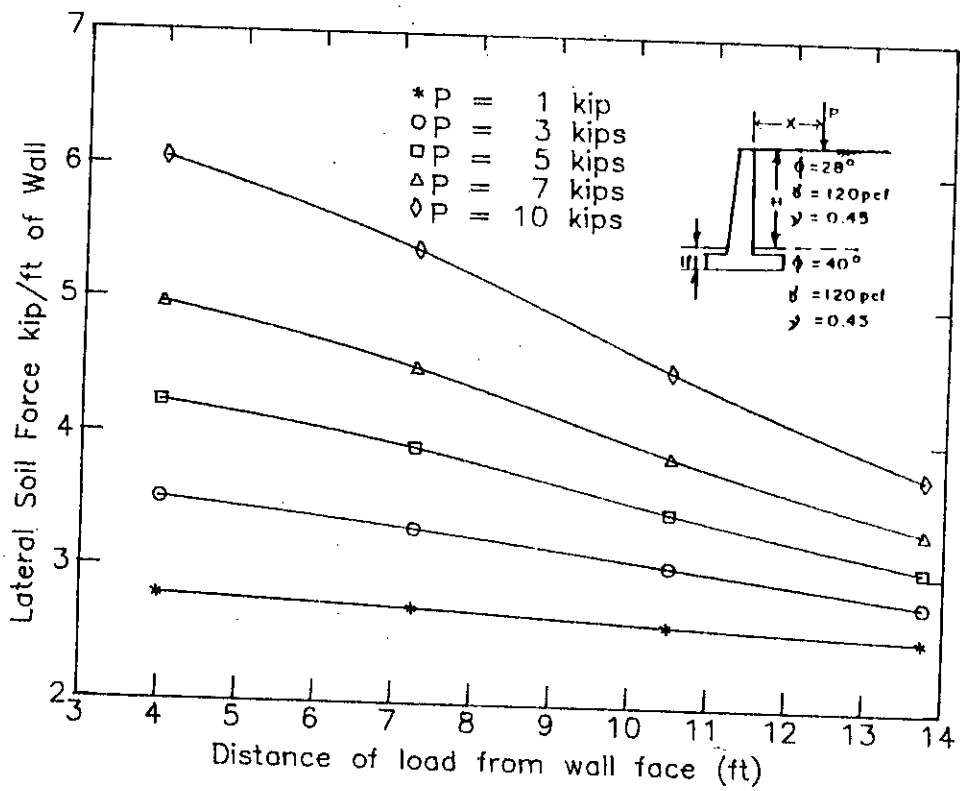


Fig.6.25 Effect of Distance of Load From Wall Face on Lateral Soil Force for a Wall of 9 ft Height

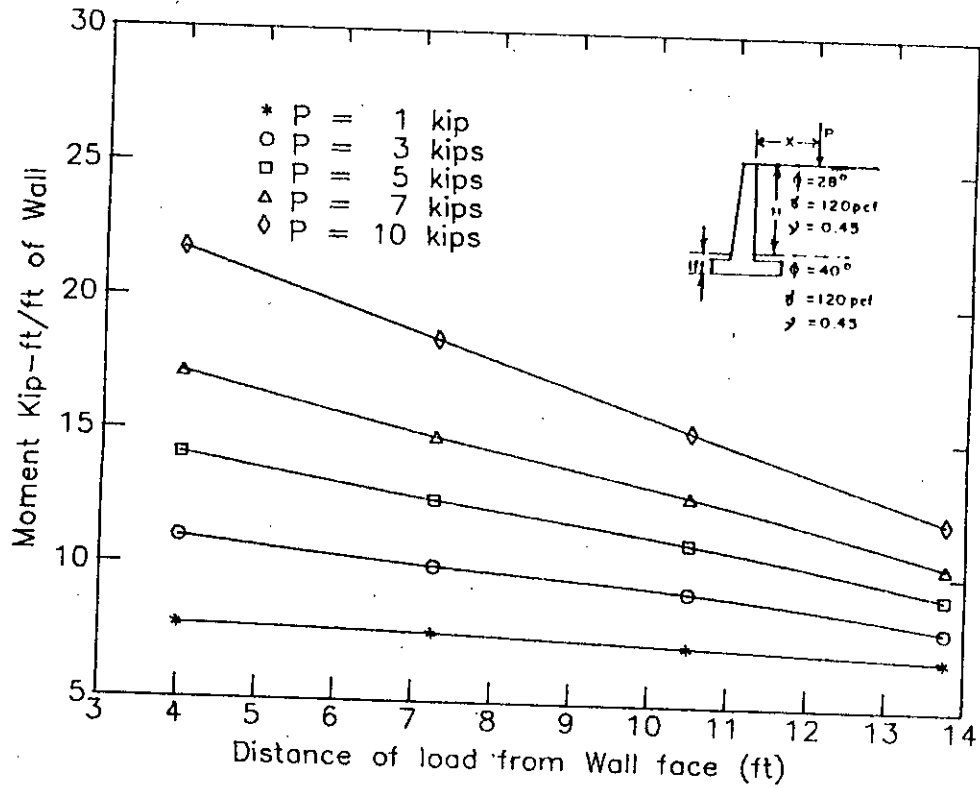


Fig.6.26 Effect of Distance of Load from Wall Face on Moment to be Resisted by a Wall of 9 ft Height

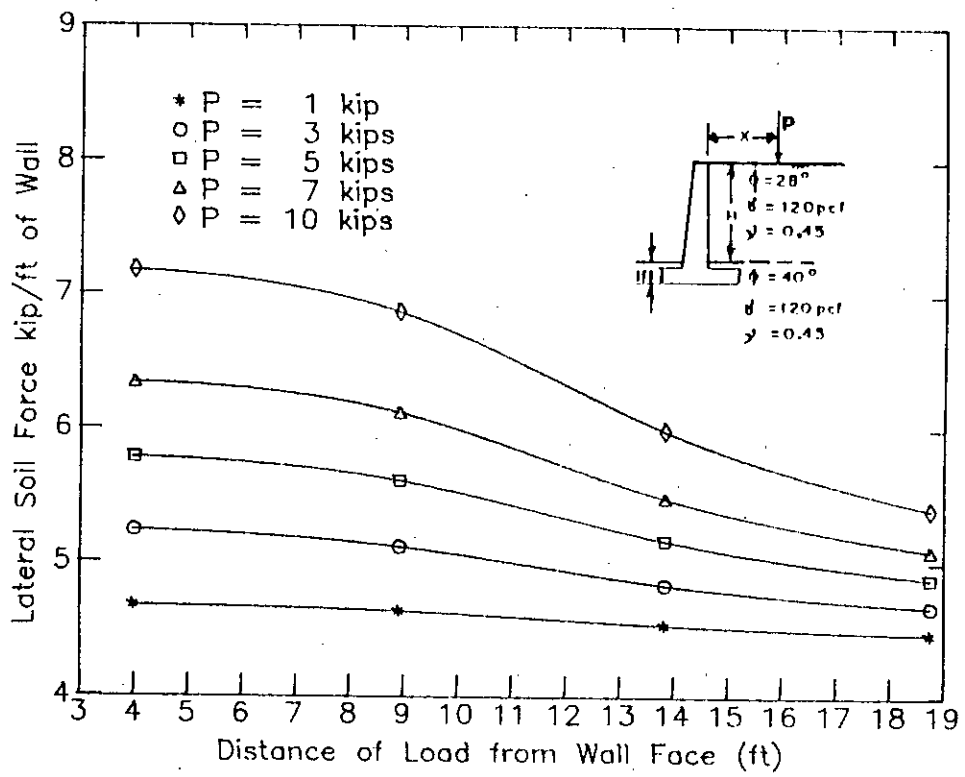


Fig.6.27 Effect of Distance of Load From Wall Face on Lateral Soil Force for a Wall of 12 ft Height

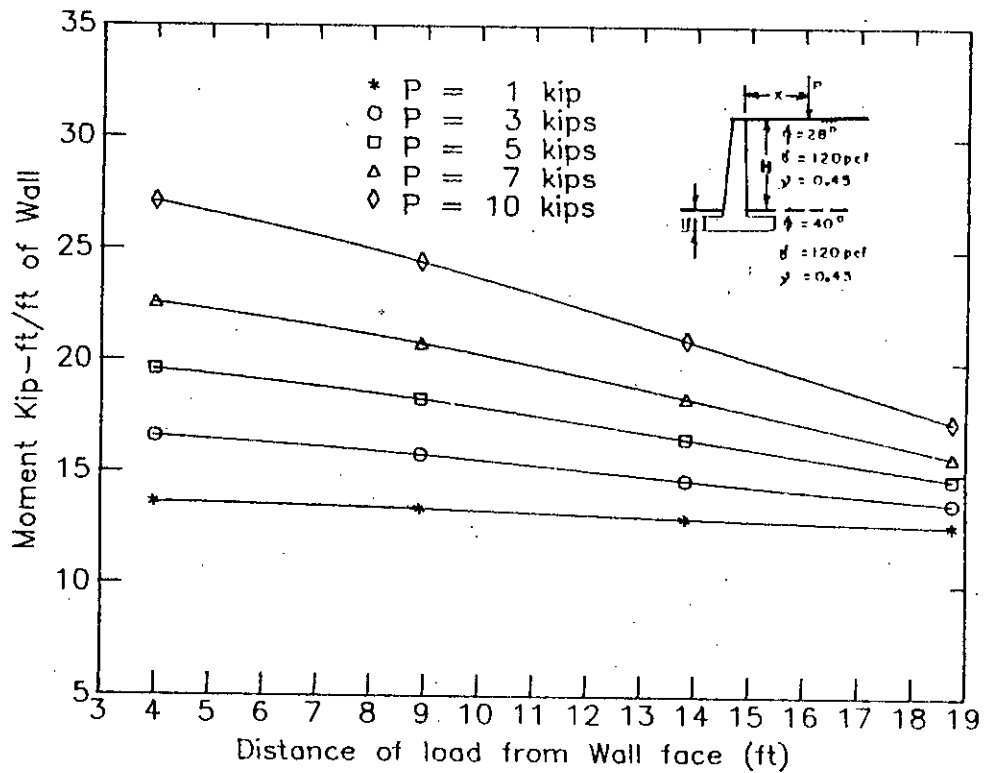


Fig.6.28 Effect of Distance of Load from Wall Face on Moment to be Resisted by a Wall of 12 ft Height



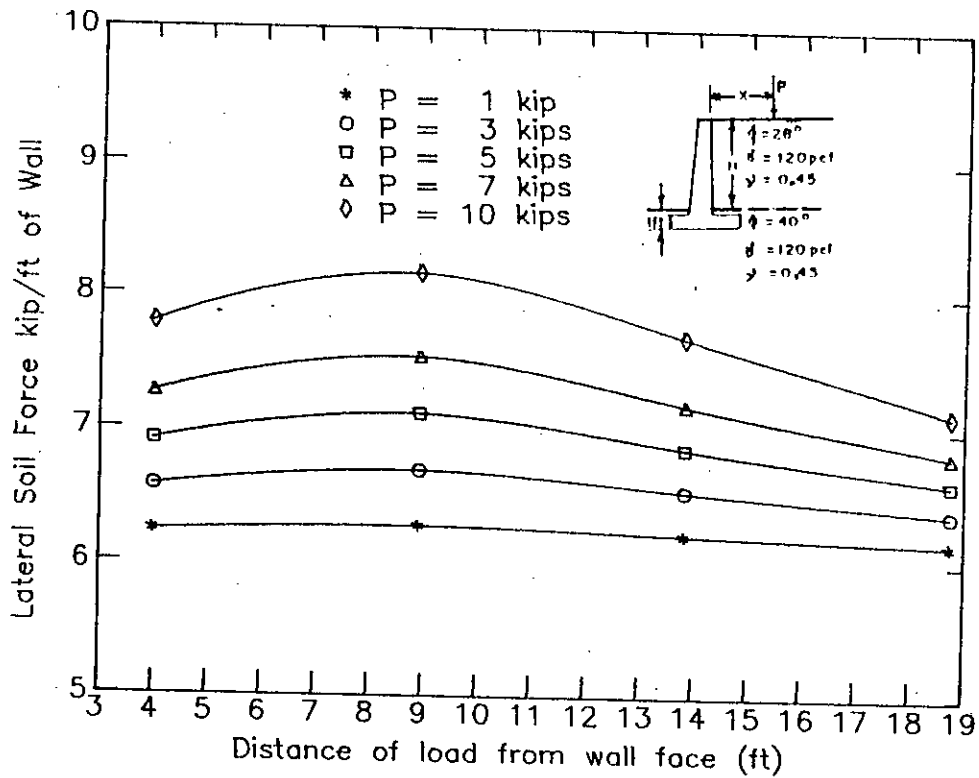


Fig. 6.29 Effect of Distance of Load from Wall face on Lateral Soil Force for a wall of 15 ft Height

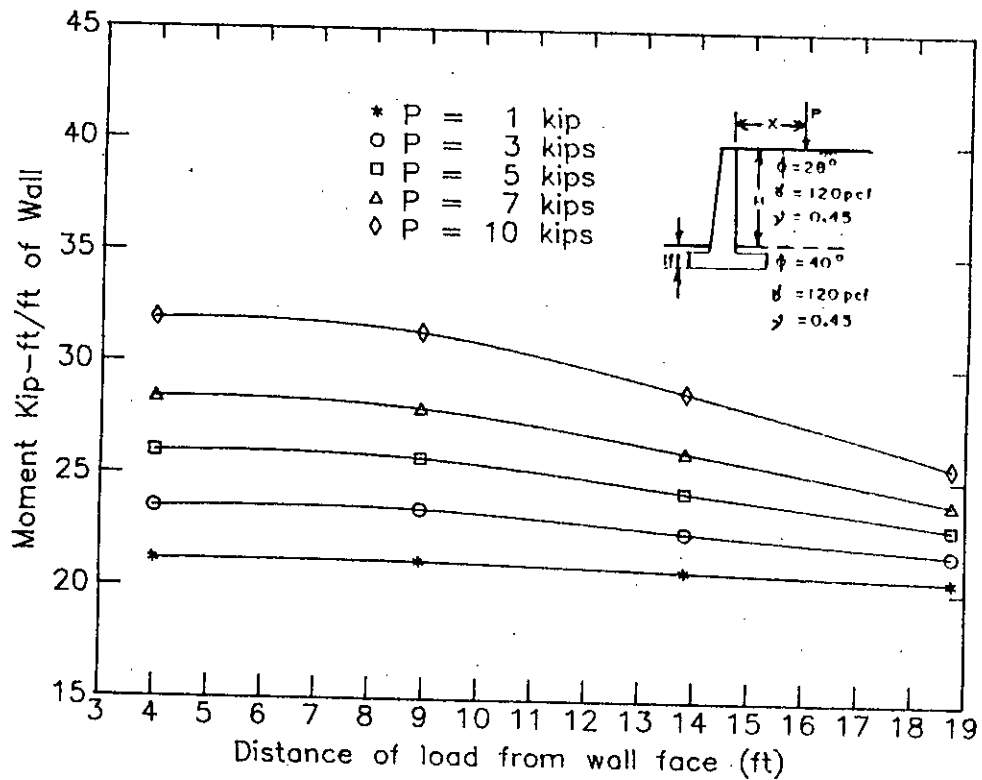


Fig. 6.30 Effect of Distance of Load From Wall Face on Moment to be Resisted by a Wall of 15 ft Height

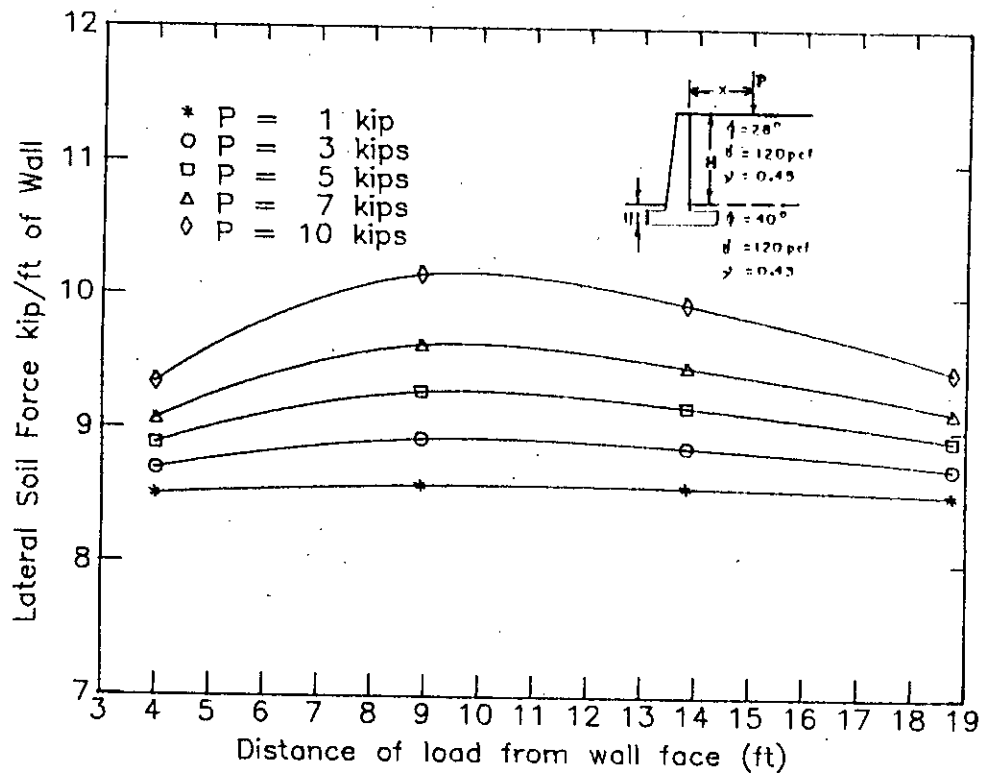


Fig. 6.31 Effect of Distance of Load From Wall Face on Lateral Soil Force for a Wall of 18 ft Height

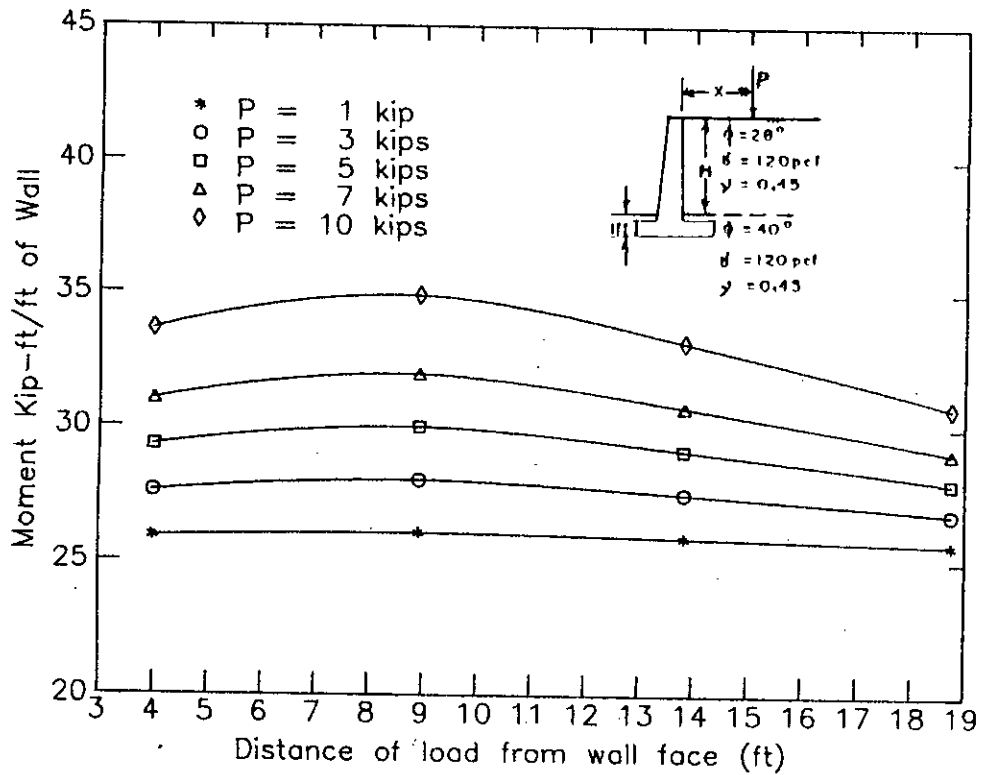


Fig. 6.32 Effect of Distance of Load from Wall Face on Moment to be Resisted by a Wall of 18 ft Height

## 6.4 EFFECT OF DISTRIBUTED LOAD

Distributed load of 1 kip/ft per ft width of wall with an increment of 1 kip/ft up to 10 kip/ft was applied to investigate the effect of uniformly distributed load on retaining walls. For wall of 9 ft height, loaded length was 9.75 ft whereas for wall of 12 ft, 15 ft and 18 ft height, the length of loading was kept constant at 14.75 ft. Results of finite element analyses are presented in Table A.15 in Appendix A, and graphically presented in Figs 6.33 and 6.34. Table A.15 gives the effect of uniformly distributed load only, whereas Fig. 6.33 and Fig 6.34 show the effect of self weight and uniformly distributed load. From the results and graphs it is observed that the variation of moment and shear with respect to load is linear. For 9 ft wall, the lateral soil force or stress shear is given by  $V_u$  equal to  $2.35 P_u$ ,  $M_u$  equal to  $9.62 P_u$ , where  $V_u$  is the lateral soil force due to the uniformly distributed load  $P_u$  only and  $M_u$  equal to moment due to  $P_u$  only. For a 12 ft wall these expressions are  $V_u=2.896 P_u$ ,  $M_u=14.195 P_u$ . For 15 ft wall  $V_u=2.551 P_u$  and  $M_u=14.01 P_u$ , similarly for 18 ft wall  $V_u=2.109 P_u$  and  $M_u=12.32 P_u$ . It is interesting to note that finite element analyses gives results which show that same load causes greater effect for walls of intermediate height.

## 6.5 DEFLECTED SHAPE AND STRESS-STRAIN IN SOIL

The basic assumption in the derivation of the traditional methods is that the wall moves horizontally, parallel to its original position, only that much which is required to develop the full shear resistance of the backfill soil, after this the top of the wall moves away from the backfill due to lateral soil force. In the finite element analyses the beam elements were allowed to move vertically, horizontally and to rotate in its own plane, i.e., no restriction was imposed on the movement along the vertical direction. To study the displacement behaviour, deflected shape of the wall of 9 ft height was plotted in Fig.6.35. To show the deflected shape clearly, displacements have been magnified ten times. It was observed that the movement of the wall occurs not only in horizontal direction but also in vertical direction. For the 9 ft wall, horizontal displacement at the top was 0.038 ft, and at the bottom of wall 0.0625 ft, the wall moved down wards by 0.0633 ft. The wall foundation moved horizontally by 0.0625 ft throughout its length, and vertically by 0.0526 ft at the outer side of toe and by 0.0737 ft at the outer side of heel. From the deflected shape it

was observed that the horizontal movement is greater at the base than that at the top, it appears to be more realistic since the load which acts vertically downward at the out side of heel of the wall foundation, and the horizontal force at the wall stem would cause the wall to rotate with respect to the top of the wall. Fig.6.36 shows the stress-strain diagram at two different depths, one at the base of wall footing another at a depth of 13 ft below the wall footing, but both on the same vertical line passing through the wall. It is observed that the soil elements in contact with the wall footing is highly strained in comparison to the soil at greater depth, but at same stress level.

#### **6.6 LIMITATIONS OF EQUATIONS DERIVED FROM INTERACTION ANALYSES**

Equations derived in this thesis do not consider the tensile separation of soil mass and the slip between the wall and soil. Thus these equations do not represent the field condition. So these equations are not recommended for any practical use, and should not be used any where without experimental verification and furthermore numerical analyses.

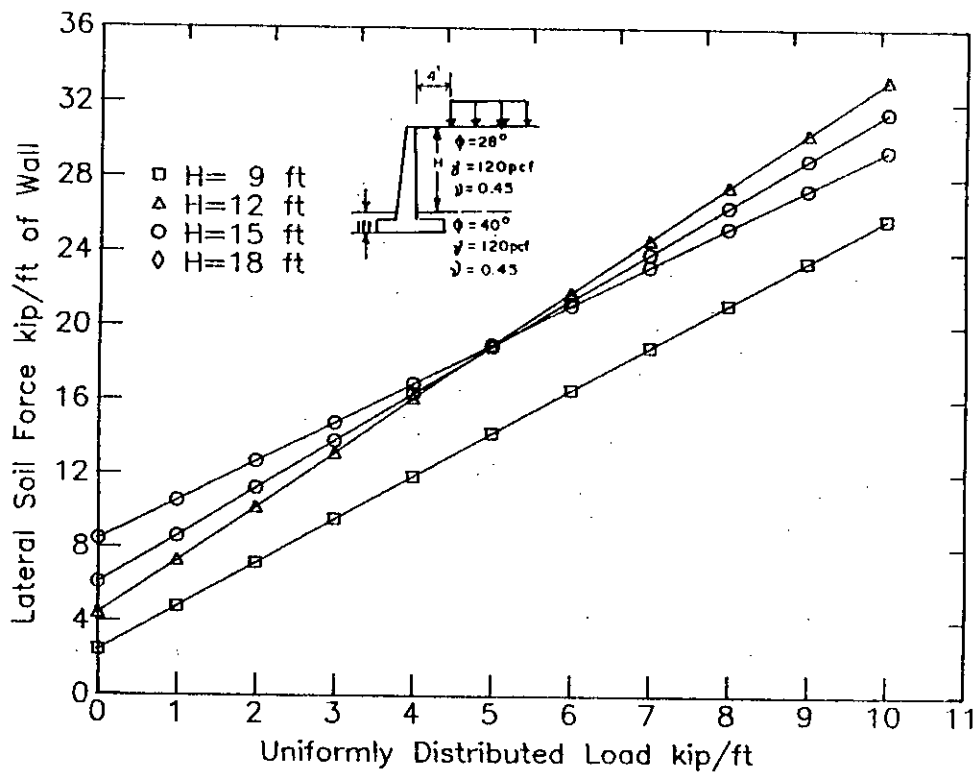


Fig.6.33 Effect of Distributed Load on Lateral Soil Force

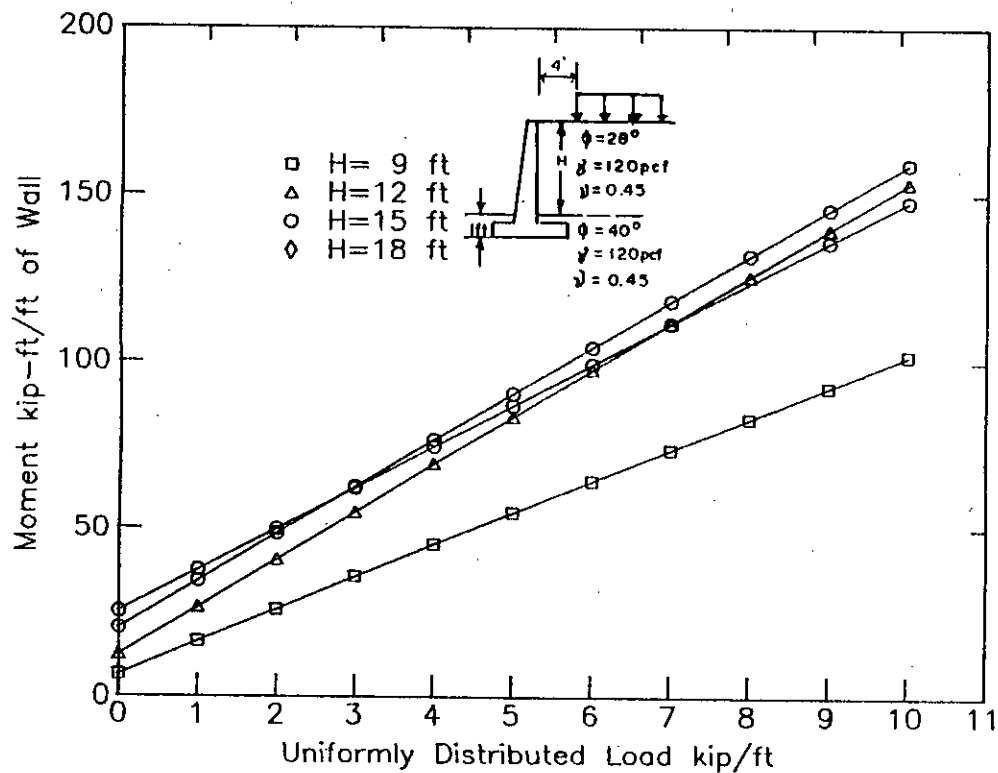


Fig.6.34 Effect of Uniformly Distributed Load on Moment to be Resisted by the Wall

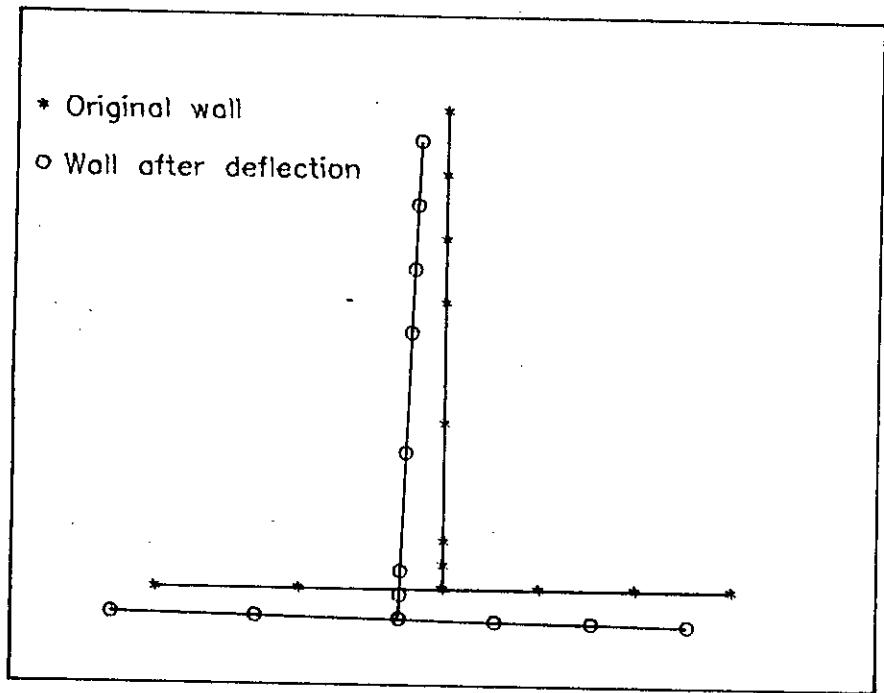


Fig.6.35 Deflected shape for the 9 ft high retaining wall

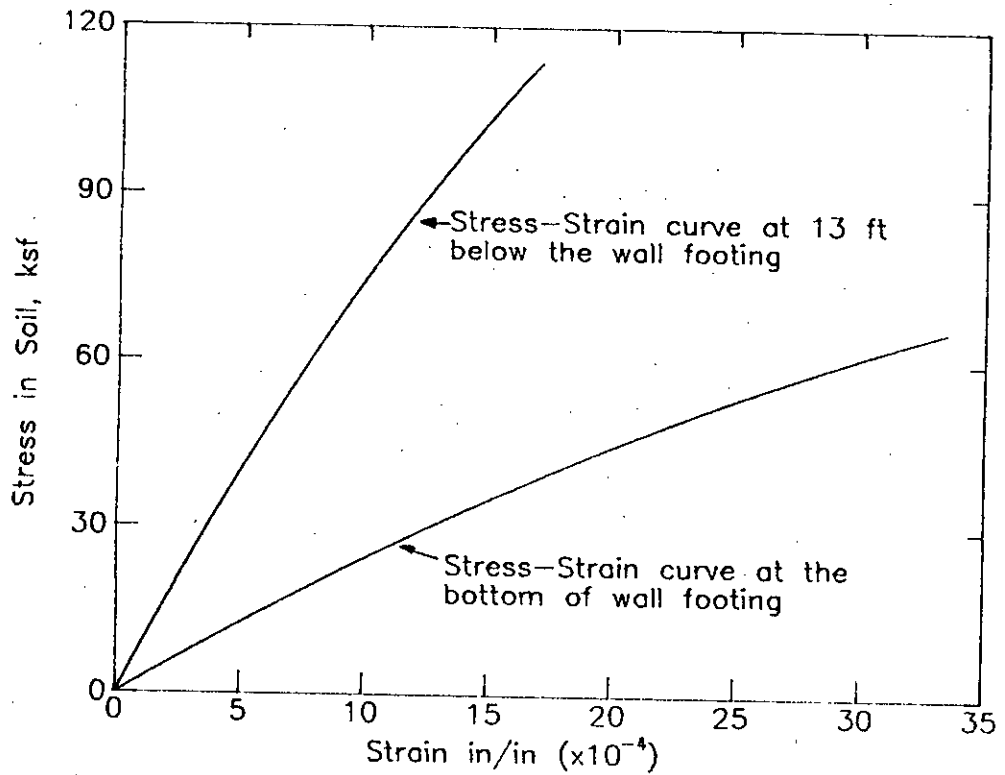


Fig.6.36 Stress-Strain diagram at two different locations in the soil below the wall footing ( wall height = 9 ft)

## CHAPTER 7

# COMPARISON OF FINITE ELEMENT ANALYSES RESULTS WITH RESULTS OF CONVENTIONAL METHODS

### 7.1 INTRODUCTION

The methods available for the analysis of a rigid retaining wall has been discussed in chapter 2. In chapters 3,4 and 5, finite element method for the analysis of the wall has been described and in chapter 6, the results obtained by the finite element method has been presented. This chapter compares the results of the finite element analyses with the results obtained from available methods.

### 7.2 COMPARISON OF RESULTS FOR SELF WEIGHT ONLY

As stated in Chapter 2, analyses for self weight can be done by Coulomb's method and Rankine's method for both lateral soil force and moment. In the Trial Wedge solution, one can determine the lateral soil force only. These methods do not include the effect of structural stiffness of the retaining wall or its footing, strength of concrete, Poisson's ratio of soil, effect of depth of embedment, effect of confining pressure, etc. To compare the results of the finite element analyses, walls with 9 ft, 12 ft, 15 ft and 18 ft height were studied. Unit weight of the retained earth was taken to be 120 pcf, angle of internal friction of soil was taken as  $28^\circ$  and the angle of soil surface with horizontal ( $\beta$ ) was varied from  $0^\circ$  to  $20^\circ$  with an increment of  $5^\circ$ .

Table A.16 in the Appendix A shows the results obtained from Coulomb's method, Rankine's method and finite element method. Due to over conservative results, Trial Wedge solution has been excluded from the results. Figures 7.1 to 7.8 show the graphical representation of obtained results. One of the assumptions that cause the difference in results between the available methods and the finite element method is that the traditional methods assume a linear variation of lateral pressure and that the resultant acts at a distance of one third the height of the wall, from the base of the wall. Finite element method does not use such kind of assumption. Instead it calculates the self weight of all the

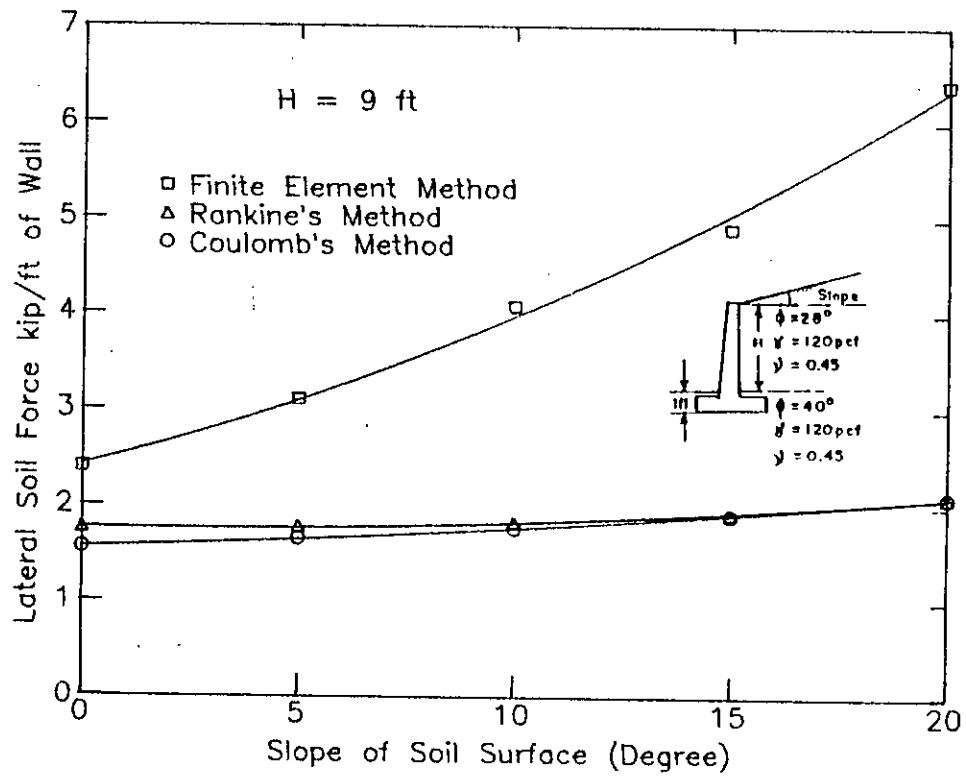


Fig.7.1 Comparison of Lateral Soil Force Varying Slope of Soil Surface .

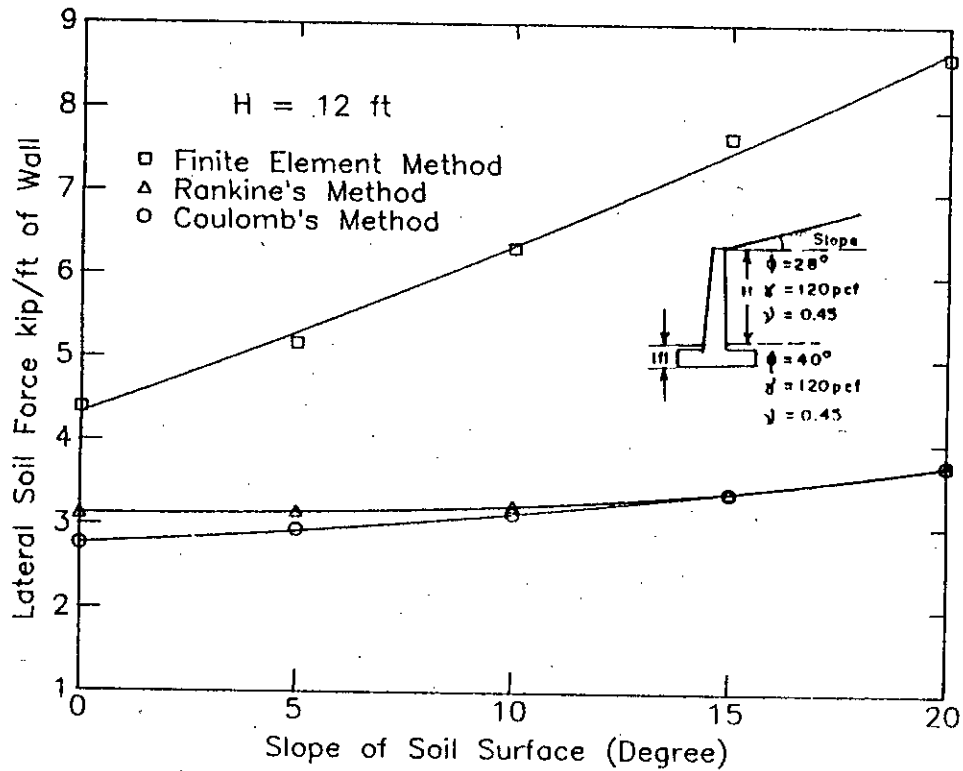


Fig.7.2 Comparison of Lateral Soil Force Varying Slope of Soil Surface .



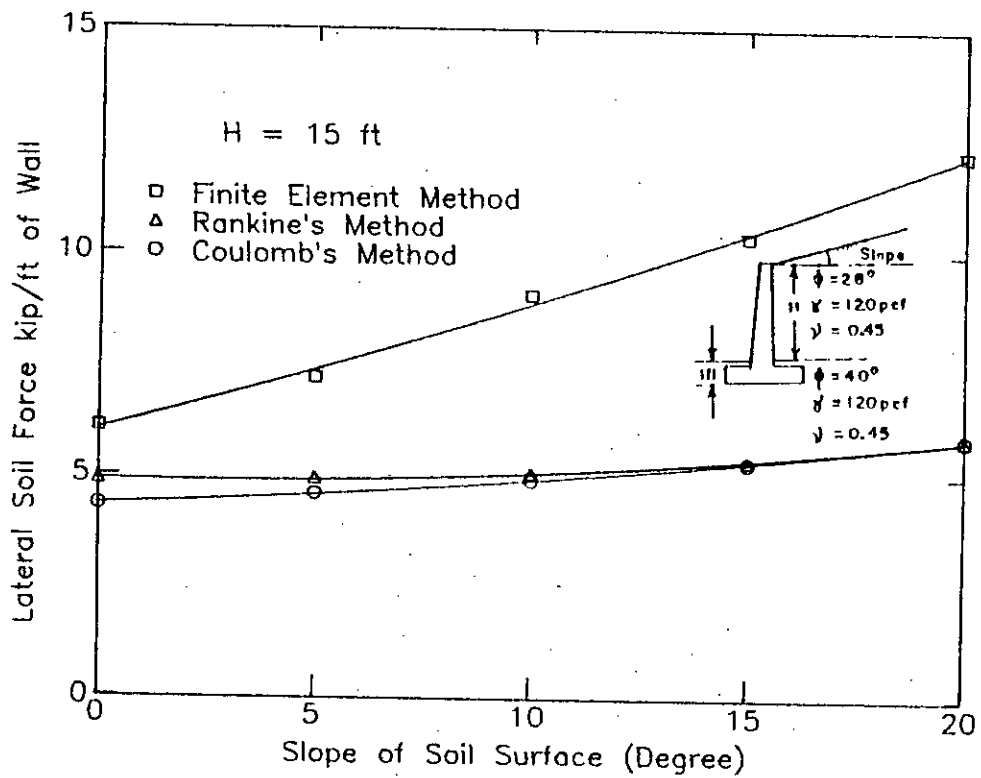


Fig.7.3 Comparison of Lateral Soil Force Varying Slope of Soil Surface .

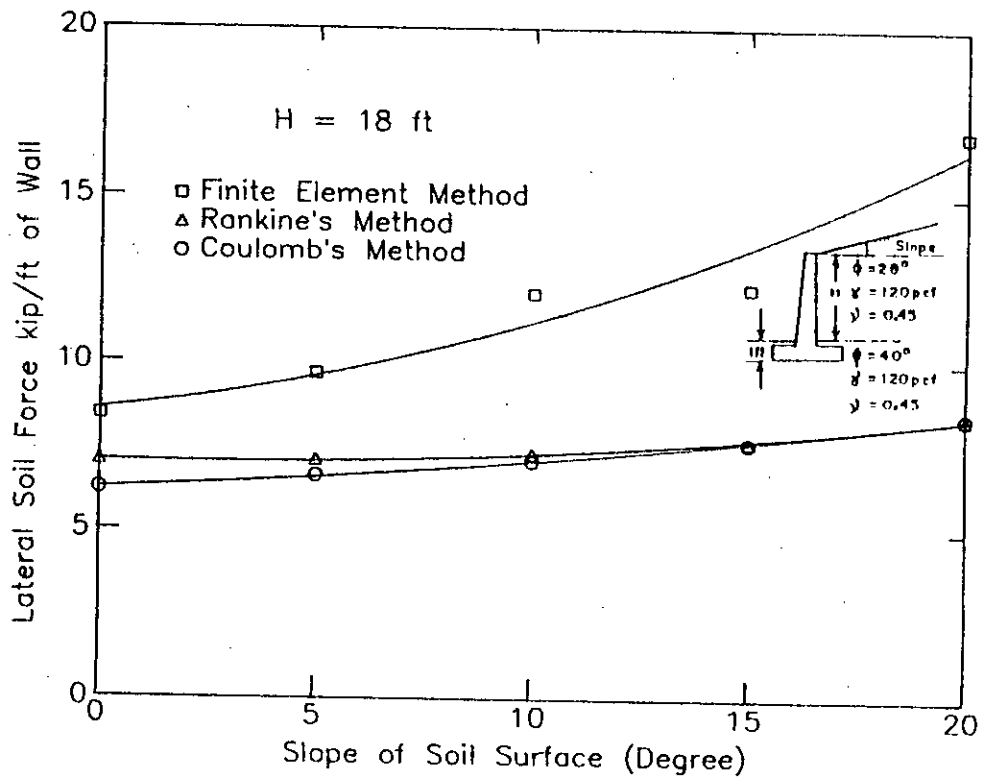


Fig.7.4 Comparison of Lateral Soil Pressure Force Varying Slope of Soil Surface .

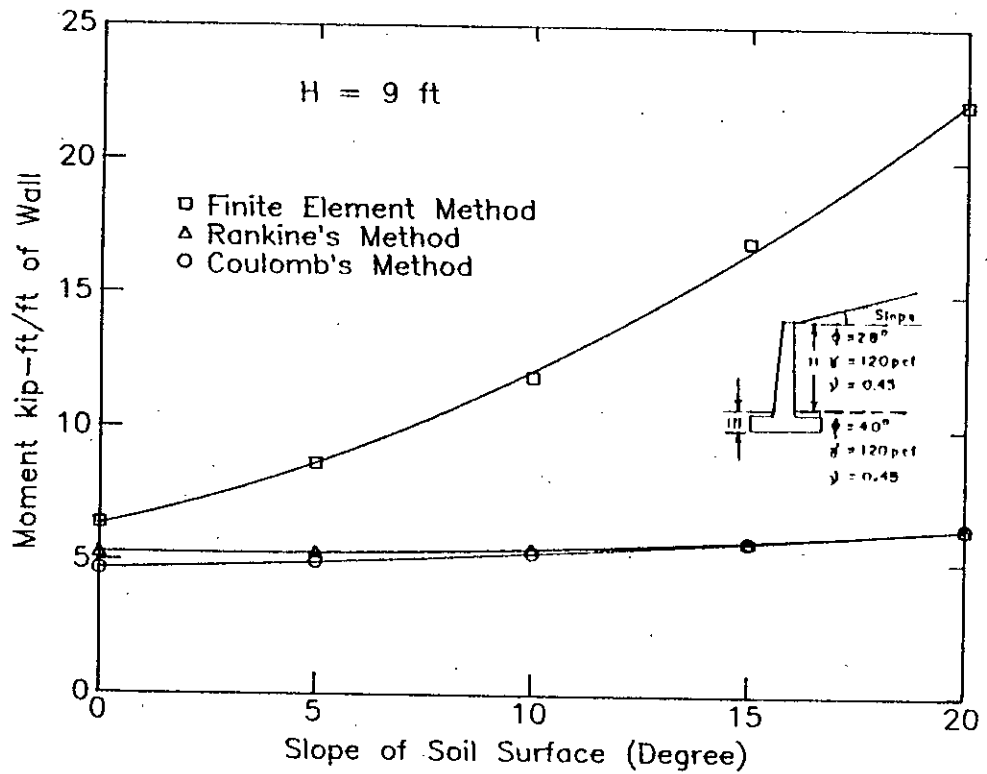


Fig.7.5 Comparison of Moment With Varying Slope of Soil Surface

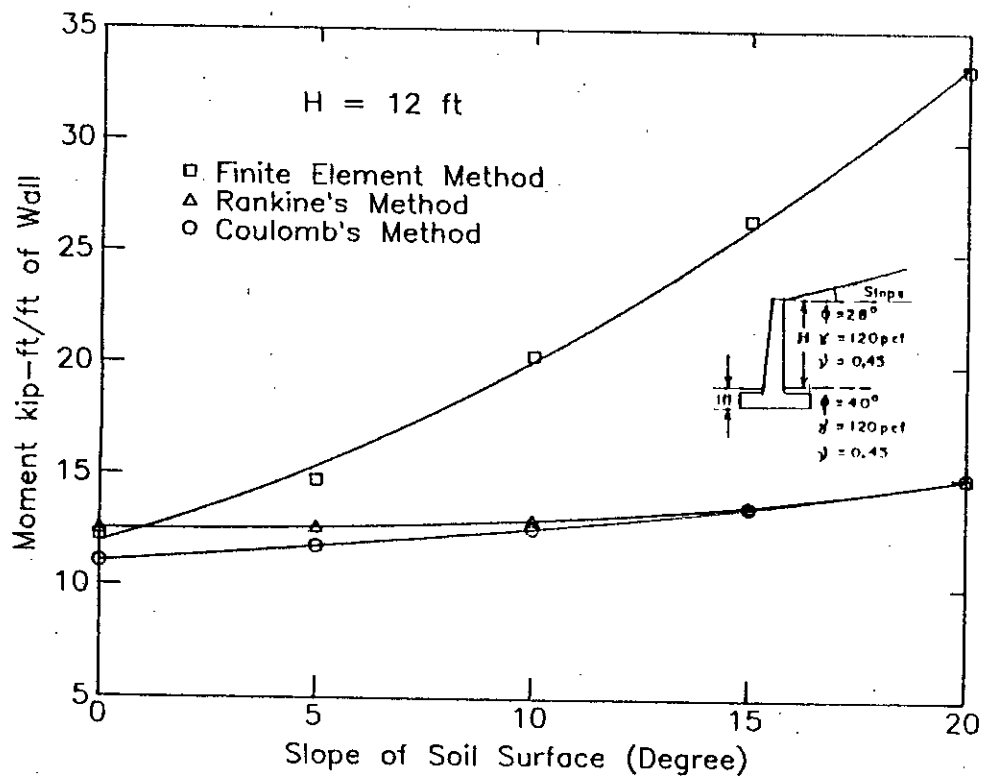


Fig.7.6 Comparison of Moment With Varying Slope of Soil Surface

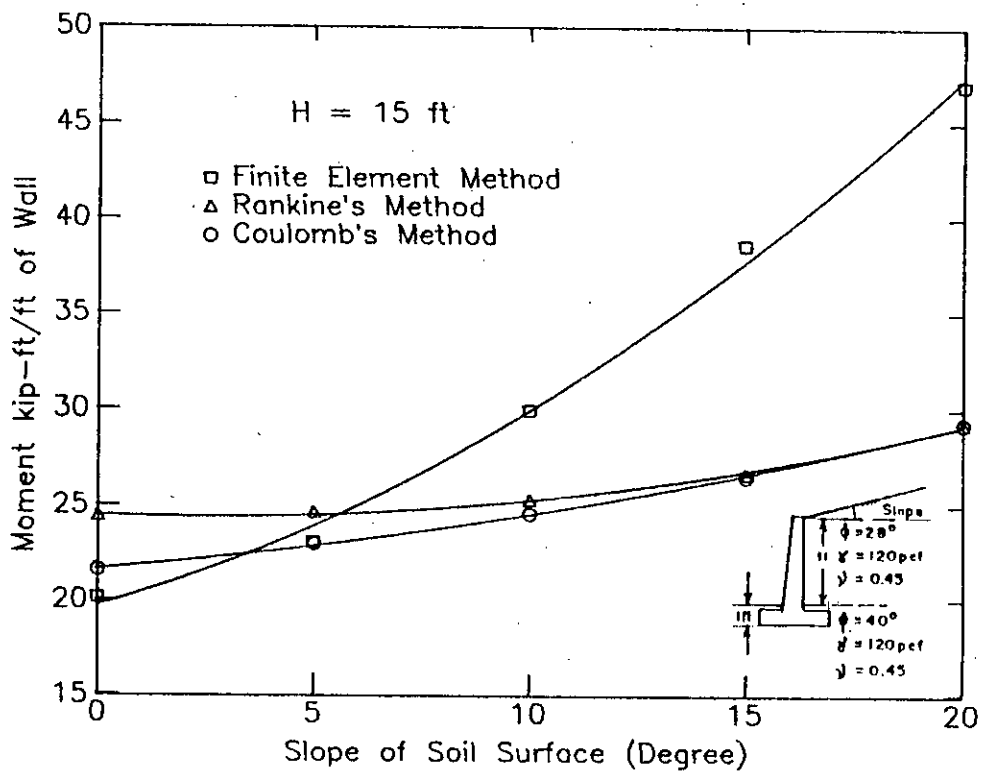


Fig.7.7 Comparison of Moment for Varying Slope of Soil Surface

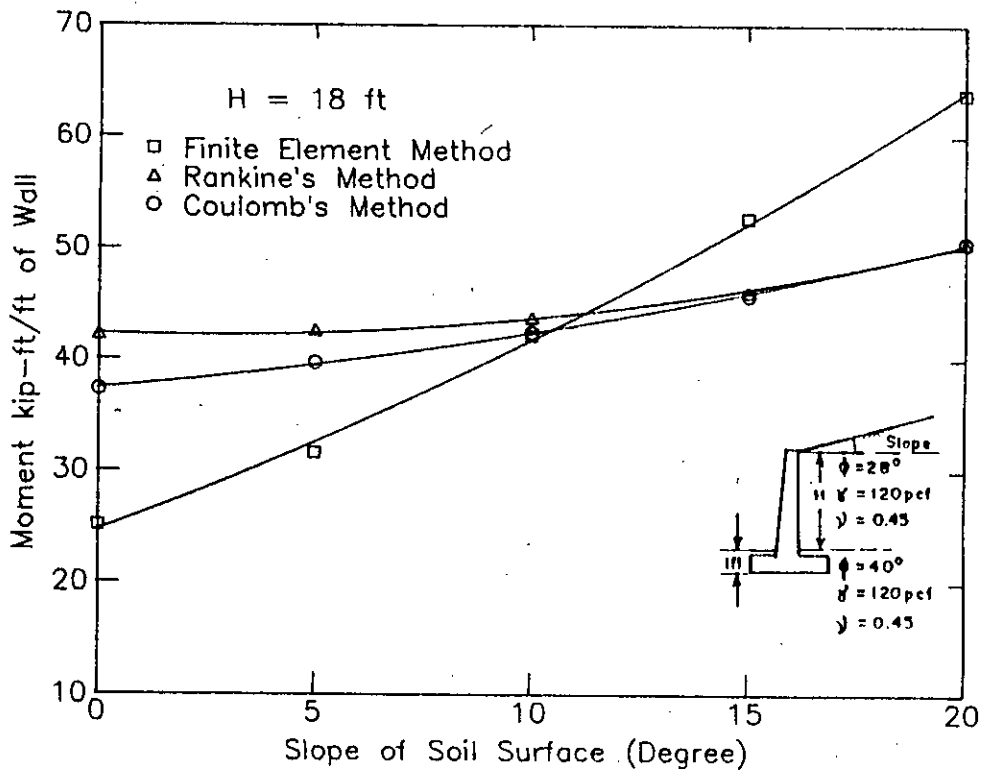


Fig.7.8 Comparison of Moment for Varying Slope of Soil Surface

isoparametric elements (representing the soil), beam elements (representing the wall and its base), stiffness of each type of elements, the load vector, the shear modulus, the octahedral strain and stress from the confining pressure using the soil data, solves hundreds of simultaneous linear equations to obtain the displacement matrix, and then arrive at the forces. For surcharge load, the finite element method reads the nodal load, then changes the load vector and does similar operations to reach at the final goal. It is expected that due to the absence of the assumption of a earth pressure coefficient and an assumed pressure variation, results of finite element analyses should be different. Results obtained from the finite element analyses were used to determine the location of the resultant force from the base of the wall and presented in terms of height of the wall in Table A.17. in Appendix A

Results of finite element analyses as presented in Table A.18 in Appendix A, confirms that the basic assumption used in the conventional methods is not accurate but approximate. It was observed that deviation from the assumption is increased with increasing wall height which indicate that the pressure distribution is not linear. Finite element analyses shows that the resultant horizontal force is located at  $h/2.60$  to  $h/6.04$  from the base of the wall.

It can be seen from Table A.17 that with increasing wall height, the relative location of resultant lateral soil force moves in the direction of wall footing. For wall of 9 ft height, the resultant is located at  $h/3.38$  distance from the base, for wall of 12 ft height it is  $h/4.31$ , for 15 ft wall the value is  $h/4.52$  and for 18 ft wall the location is at  $h/6.04$ . Values presented in Table A.17 indicate that the pressure distribution is almost linear when the confining pressure is relatively small but rapidly changes to polynomials of higher degrees with increasing confining pressure i.e., for walls of larger height. This statement can be used to support the expression of moment derived in article 6.2.6, which shows that the equation of moment is not a third degree parabola. From Table A.17, observing the location of lateral soil force for different angles of soil surface and for the same height of wall, it appears that the pressure distribution changes with the angle of soil surface. For wall of 9 ft height, the distance of resultant lateral soil force from the base is  $h/3.38$  ( $\beta = 0^\circ$ ),  $h/3.23$  ( $\beta = 5^\circ$ ),  $h/3.09$  ( $\beta = 10^\circ$ ),  $h/2.60$  ( $\beta = 15^\circ$ ),  $h/2.60$  ( $\beta = 20^\circ$ ), which show that the location rapidly change for the initial changes of surface slope but later on becomes more or less constant, which indicates that for a given height of wall,

increase in confining pressure leads to a more or less constant type of pressure diagram.

It appears from Table A.18 that finite element solution gives larger values of lateral soil force for walls of all heights. With the increase in the wall height, the difference between the finite element analysis results come closer to the results obtained from the traditional methods.

### **7.3 COMPARISON OF RESULTS FOR LINE LOAD**

To compare the results of finite element results with results given by Boussinesq equation or Trial Wedge method, line load of 10 kip per feet width of wall was selected. Wall heights of 9 ft, 12 ft, 15 ft and 18 ft were taken for analyses. For the 9 ft high wall, load was applied at a distance of 4 ft, 7.25 ft, 10.50 ft and 13.75 ft from the face of the wall. For 12 ft, 15 ft and 18 ft wall load was applied at a distance of 4 ft, 8.92 ft, 13.83 ft and 18.75 ft from the wall face. Results of the analyses are given in Table A.19 in Appendix A. Same results are graphically presented in Figs 7.9 to 7.16. Boussinesq equation or trial wedge method shows that the magnitude of forces acting on the wall decreases as the distance of the line load increase from the wall. But finite element method shows that, for walls of larger heights there is a critical location where the applied load shows maximum effect. For walls of height 15 ft and 18 ft the location is approximately  $0.6H$ . But walls with relatively smaller height, this critical location was not observed; rather these walls show that with increasing distance the magnitude of lateral soil force and moment decreases.

Magnitude of the lateral soil force obtained by finite element analysis seems to fall between that obtained by trial wedge method and the Boussinesq equation. Finite element method shows that for same line load, effects are greater for smaller wall but the other two methods show the reverse action.

Finite element method gives 3 to 11 times the value of lateral soil force given by Boussinesq method and 6 to 14 times the value of moment given by the same method. From the lateral soil force value and the magnitude of moment it was observed that Boussinesq equation gives a large variation of location of the resultant horizontal force when the position of the line load is changed but

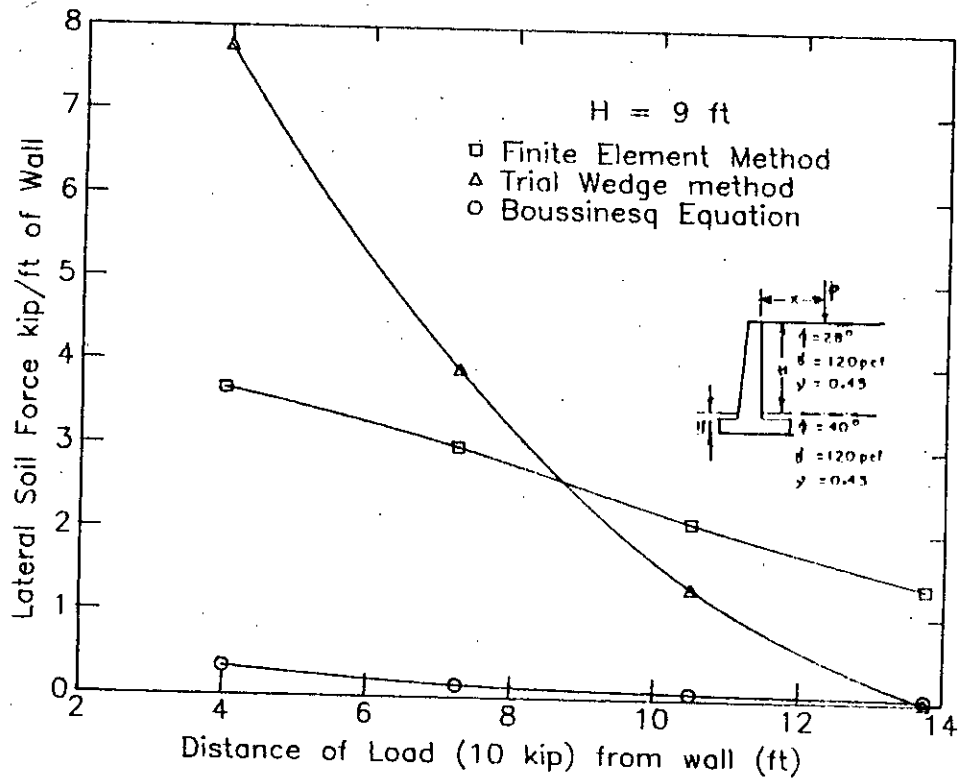


Fig.7.9 Comparison of Lateral Soil Force By Varying Position of Line load.

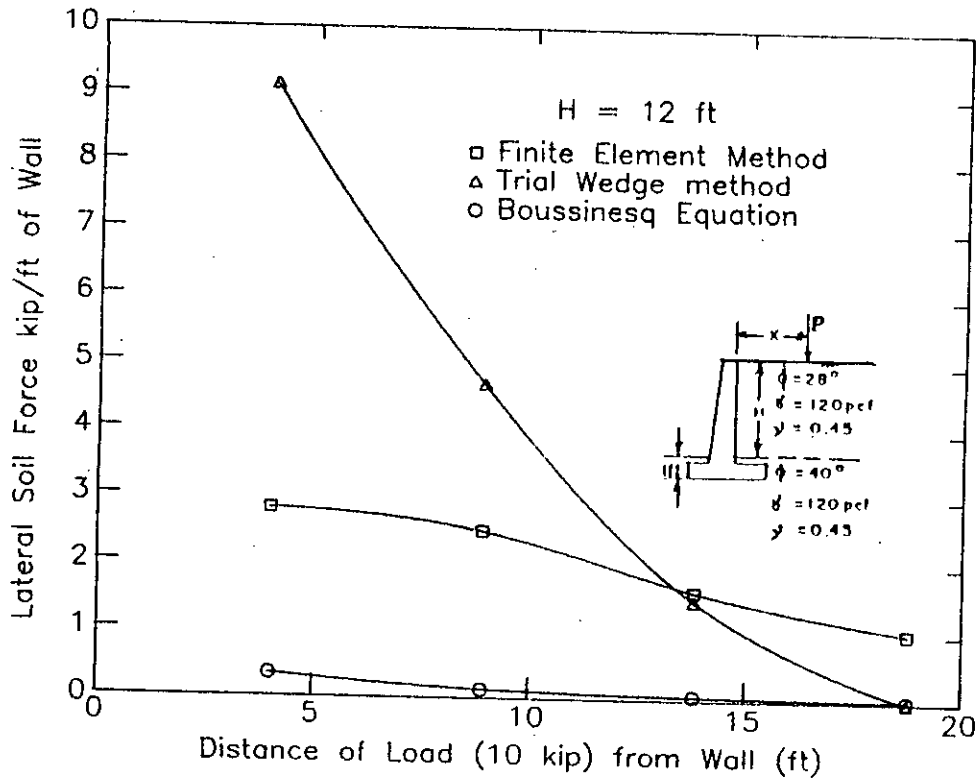


Fig.7.10 Comparison of Lateral Soil Force by Varying Position of Line load.

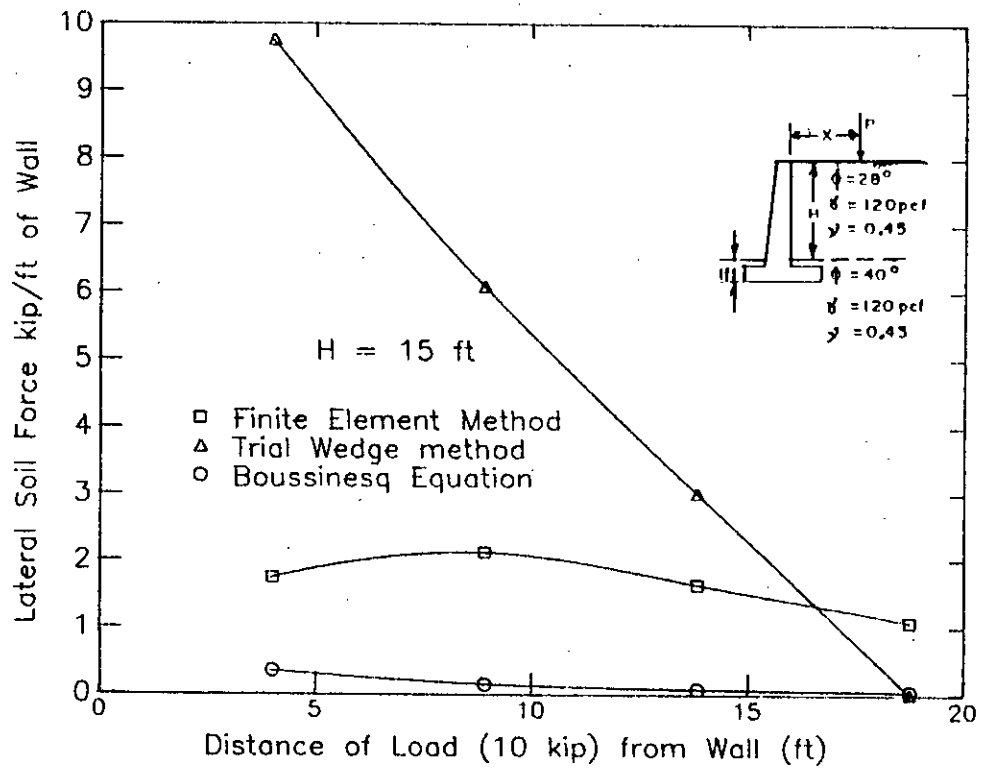


Fig.7.11 Comparison of Lateral Soil Force by Varying Position of Line load.

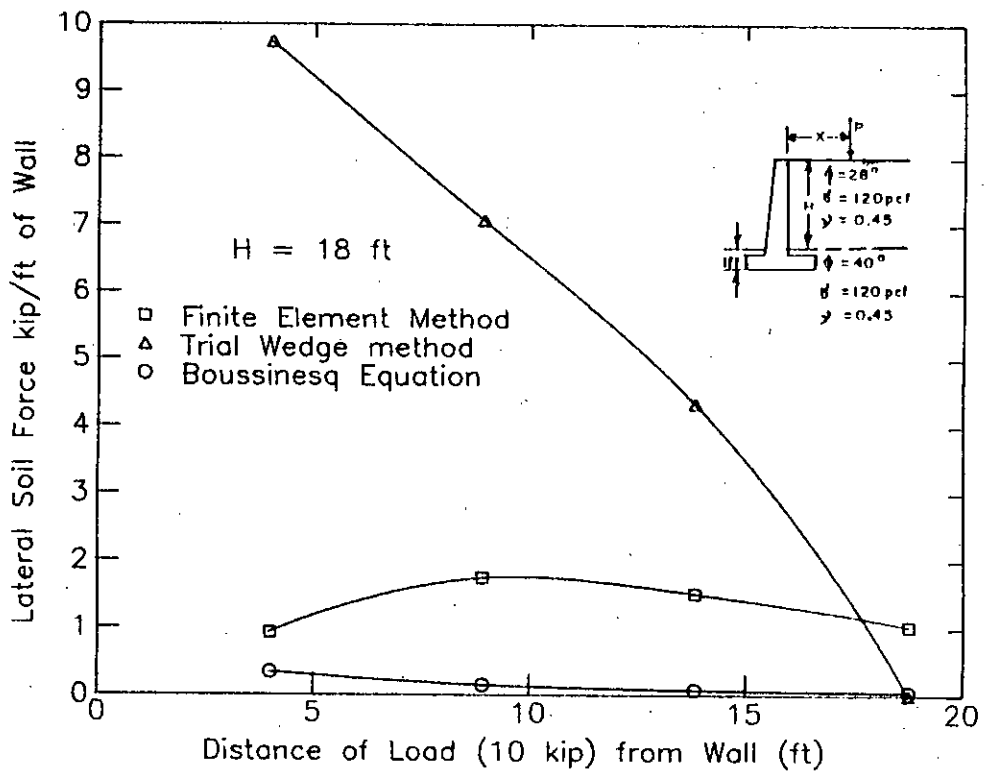


Fig.7.12 Comparison of Lateral Soil Force by Varying Position of Line load.

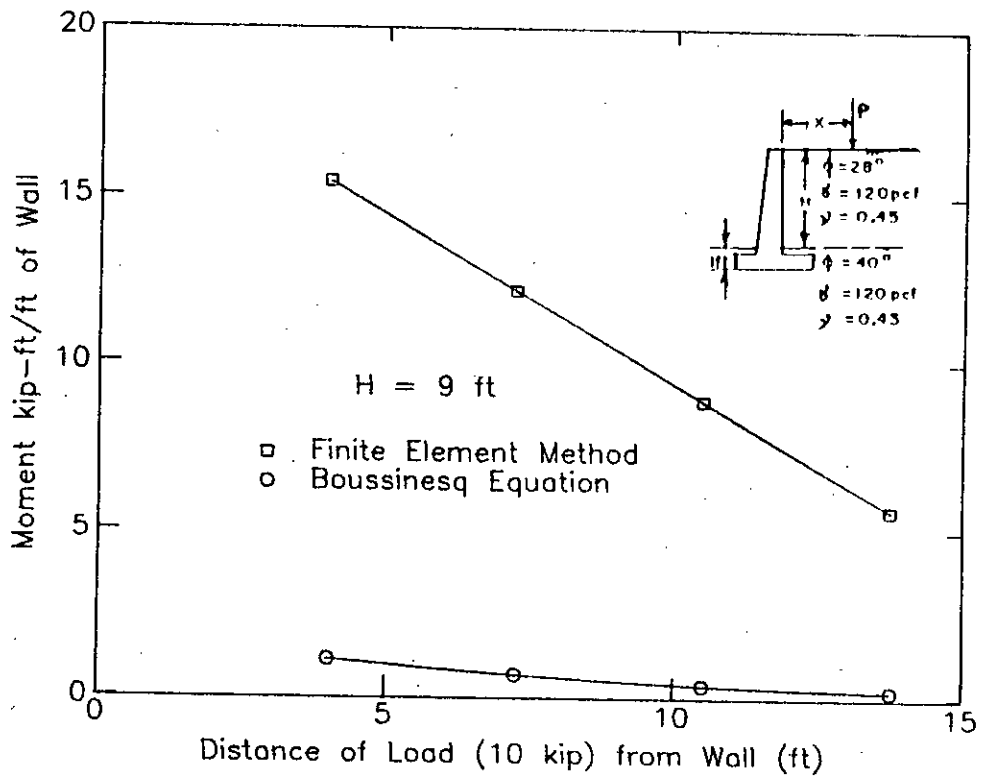


Fig.7.13 Comparison of Moment to be Resisted by Wall for Varying Position of Line load.

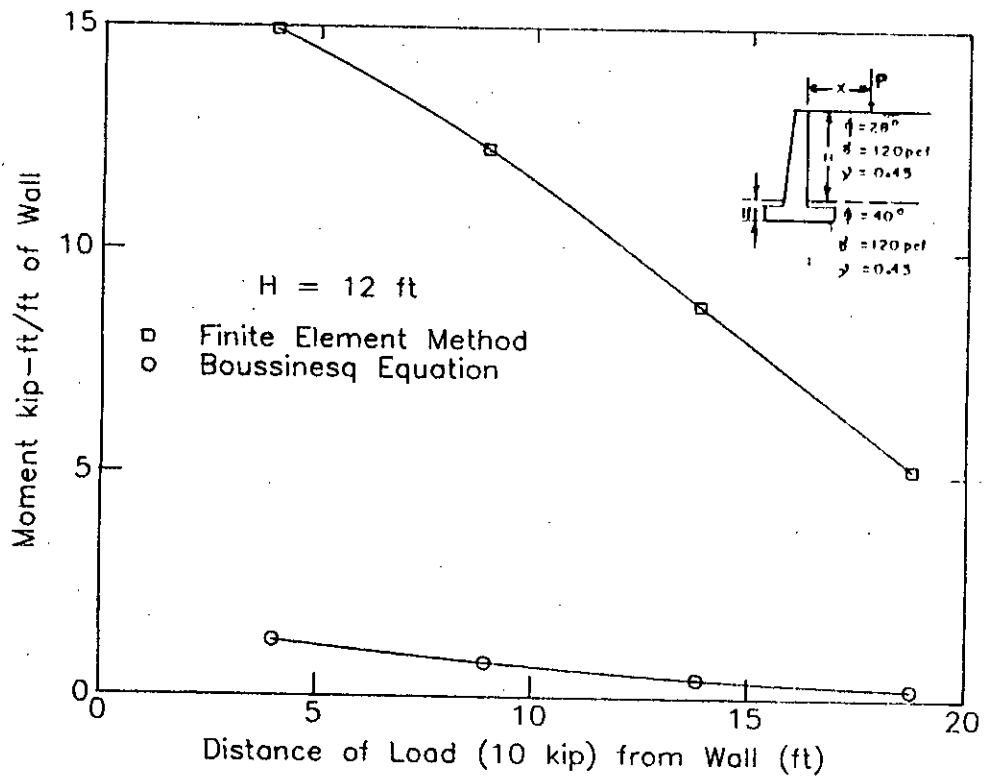


Fig.7.14 Comparison of Moment to be Resisted by Wall for Varying Position of Line load.



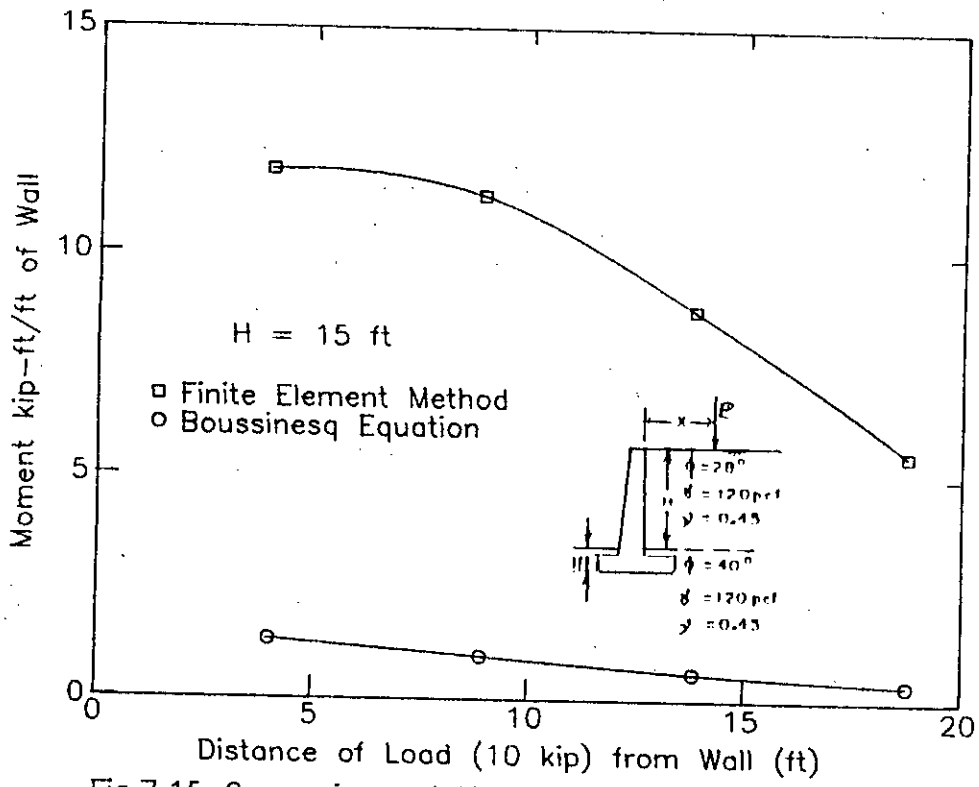


Fig.7.15 Comparison of Moment to be Resisted by Wall for Varying Position of Line load.

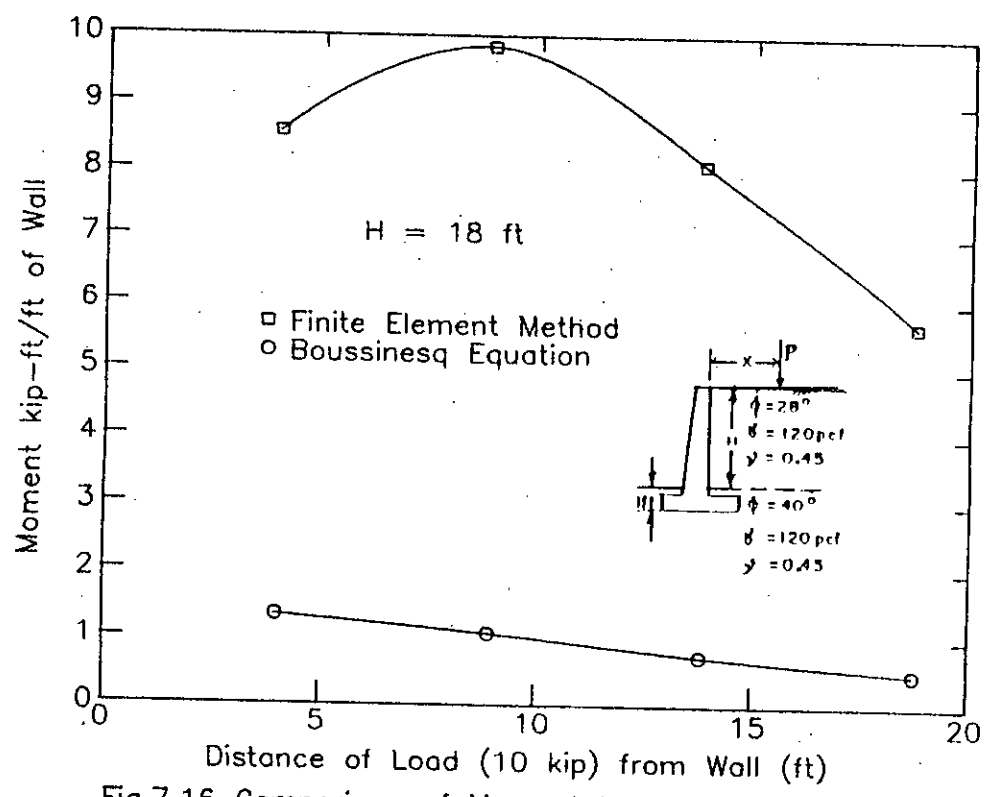


Fig.7.16 Comparison of Moment to be Resisted by Wall for Varying Position of Line load.

finite element method shows a very little change, the location is more or less constant for walls of small and moderate height, i.e., no appreciable change is observed for them. Average distance of the resultant force from the base for 9 ft, 12 ft, 15 ft and 18 ft wall can be written as  $h/2.17$ ,  $h/2.33$ ,  $h/2.72$  and  $h/2.83$ .

Trial wedge method gives very large value of the lateral soil force which is 2 to 10 times that given by finite element solution and appears to be unrealistic.

#### 7.4 COMPARISON OF RESULTS FOR UNIFORMLY DISTRIBUTED LOAD

The finite element results in this case was compared with Coulomb's method, Rankine's method and the method proposed by Ramon. For analyses by Ramon's method, load was applied in the Rankine zone so loaded length was different from finite element analysis for the available methods.

Table A.20 in Appendix A, shows the results obtained for different methods. These results are graphically presented in Figs 7.17 to 7.24. It has been observed that for walls with relatively smaller height, Ramon's method gives smaller values of lateral soil force than the Coulomb, Rankine or finite element method. But for relatively large walls, the finite element analysis gives smaller values of the above stated quantities. Finite element method shows a parabolic variation of lateral soil force and moment with wall height which is similar to the case of line load. But the other methods show that these quantities increase with wall height for same load. The similarity between all cases is that the magnitude of the lateral soil force and moment increase with the magnitude of the applied load and the variation is linear.

Rankine and Coulomb's method assumes a constant distribution of lateral pressure for the uniformly distributed load. So, the resultant lateral soil force is located at the mid height of the wall. Ramon gave a complicated expression for the location of the resultant force, which has already been described in article. 2.3.3. From the finite element analyses results the location of the force can be written as  $\bar{y} = \frac{h}{0.098h + 1.287}$ , which indicates that location of resultant force is independent of the magnitude of applied load.

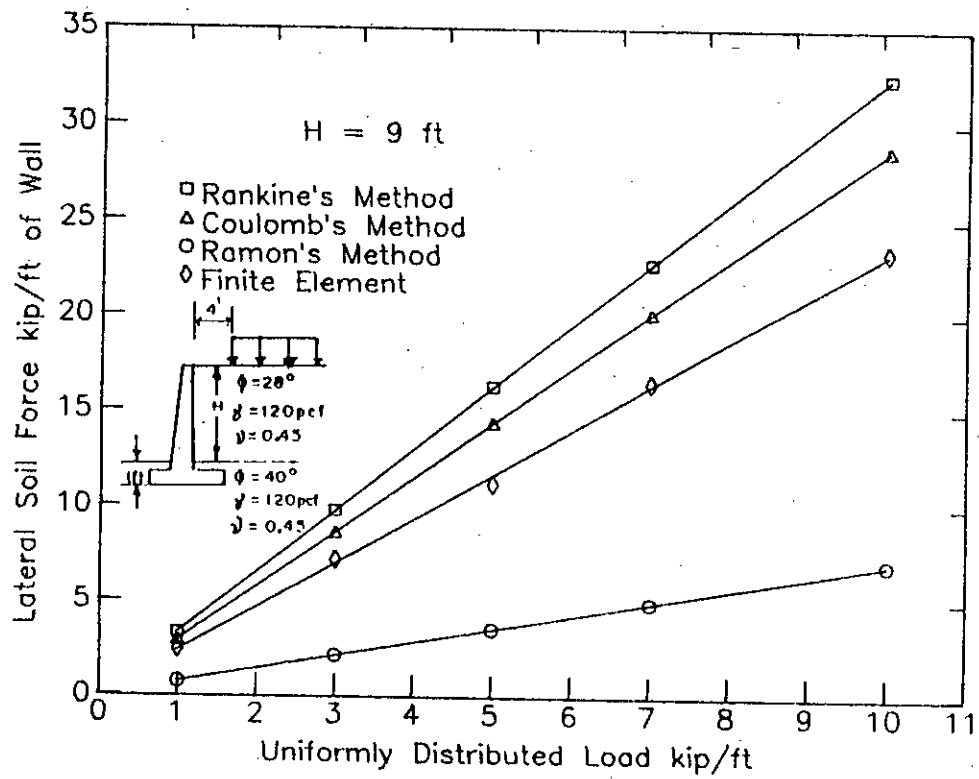


Fig. 7.17 Comparison of Lateral Soil Force for Uniformly Distributed Load.

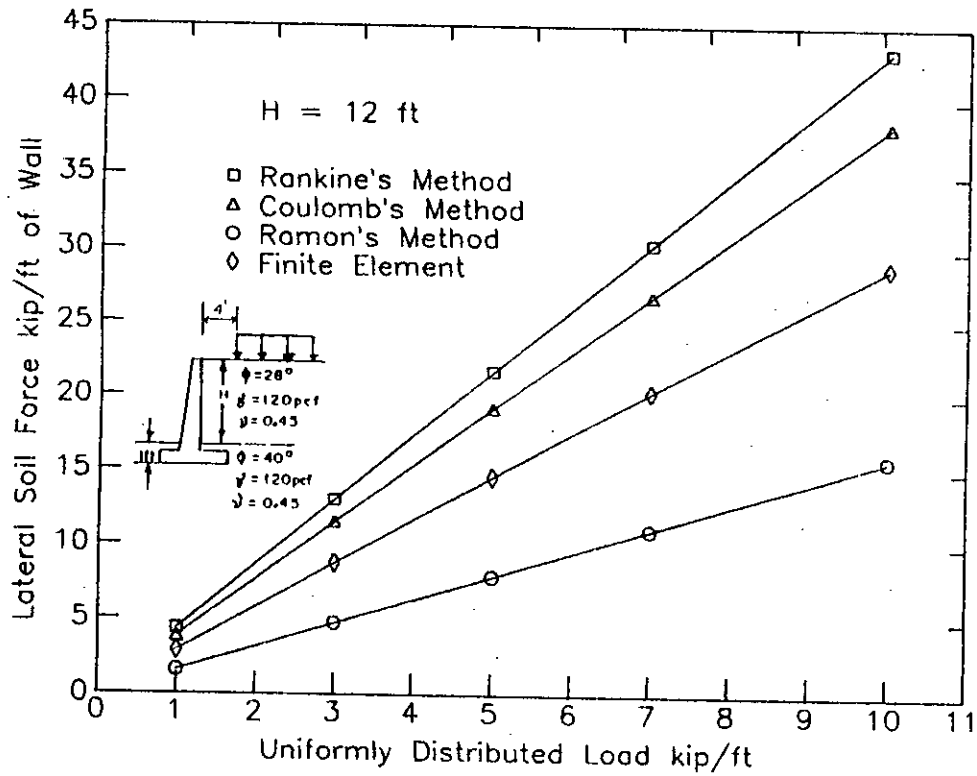


Fig. 7.18 Comparison of Lateral Soil Force for Uniformly Distributed Load.

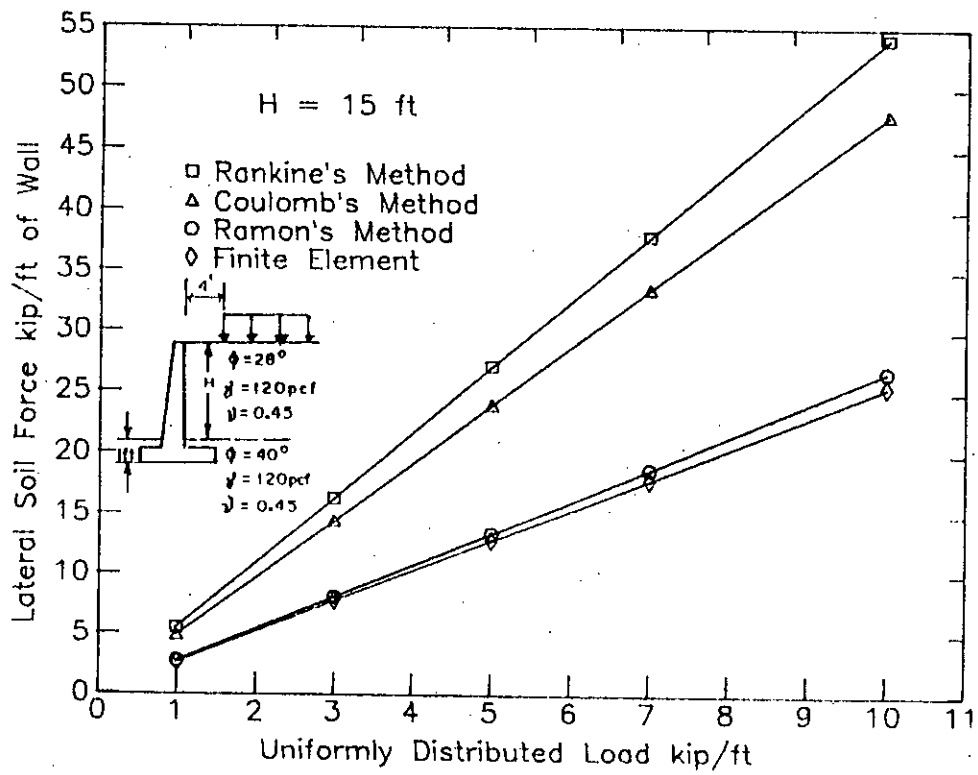


Fig.7.19 Comparison of Lateral Soil Force for Uniformly Distributed Load.

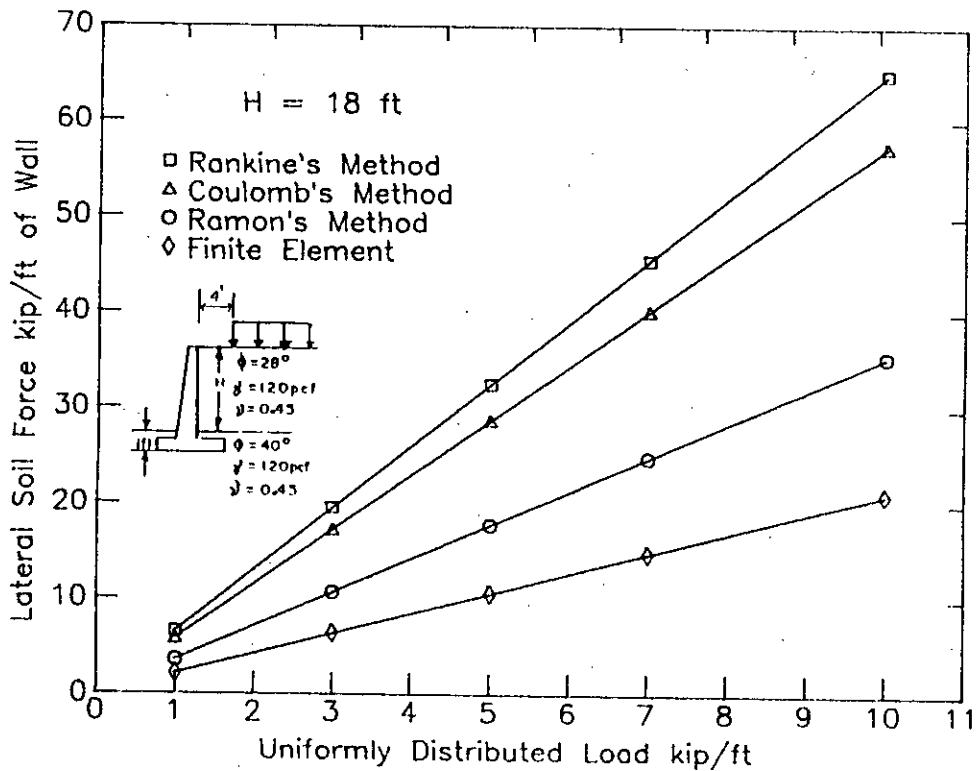


Fig.7.20 Comparison of Lateral Soil Force for Uniformly Distributed Load.

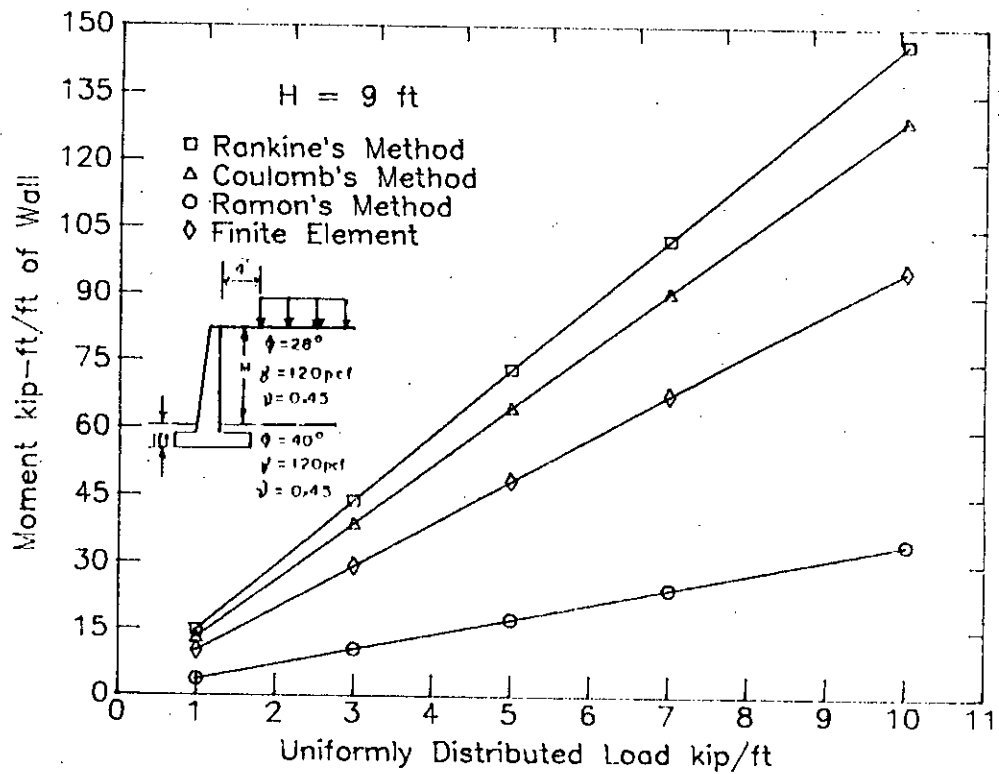


Fig.7.21 Comparison of Moment to be Resisted by Wall for Uniformly Distributed Load.

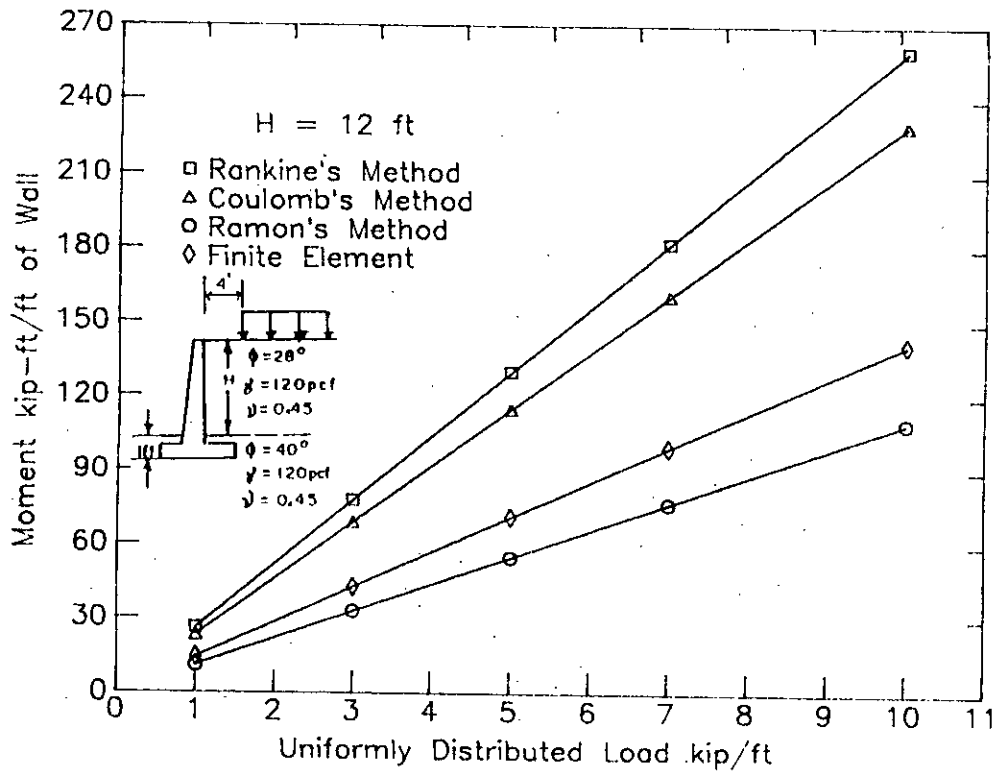


Fig.7.22 Comparison of Moment to be Resisted by Wall for Uniformly Distributed Load.

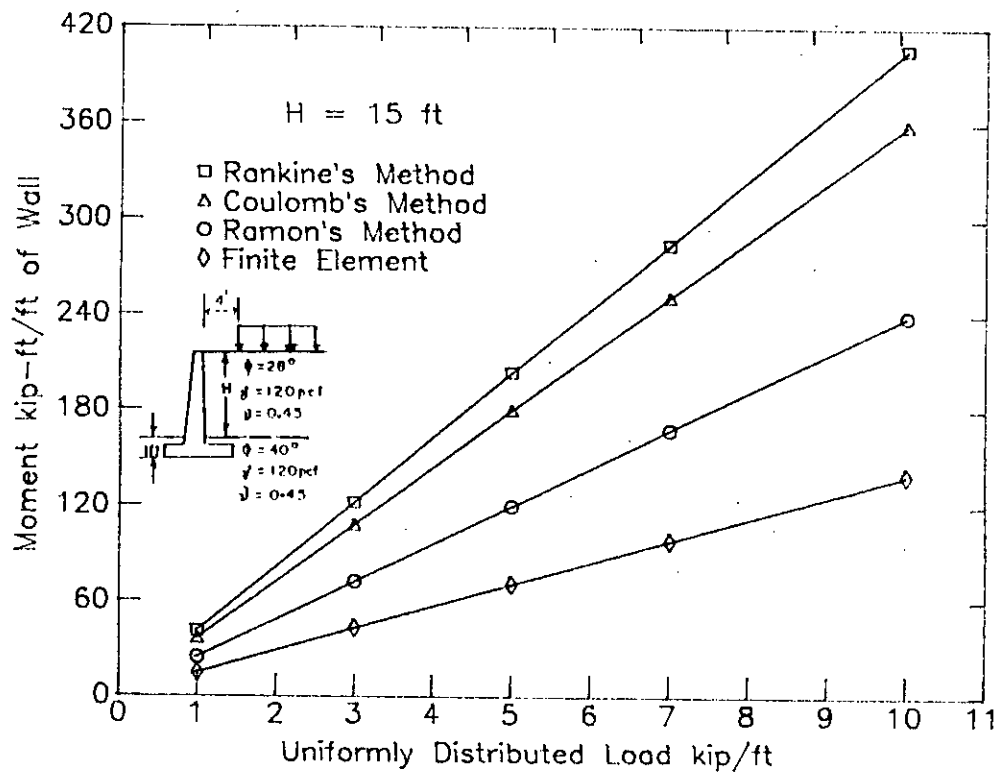


Fig. 7.23 Comparison of Moment to be Resisted by Wall for Uniformly Distributed Load.

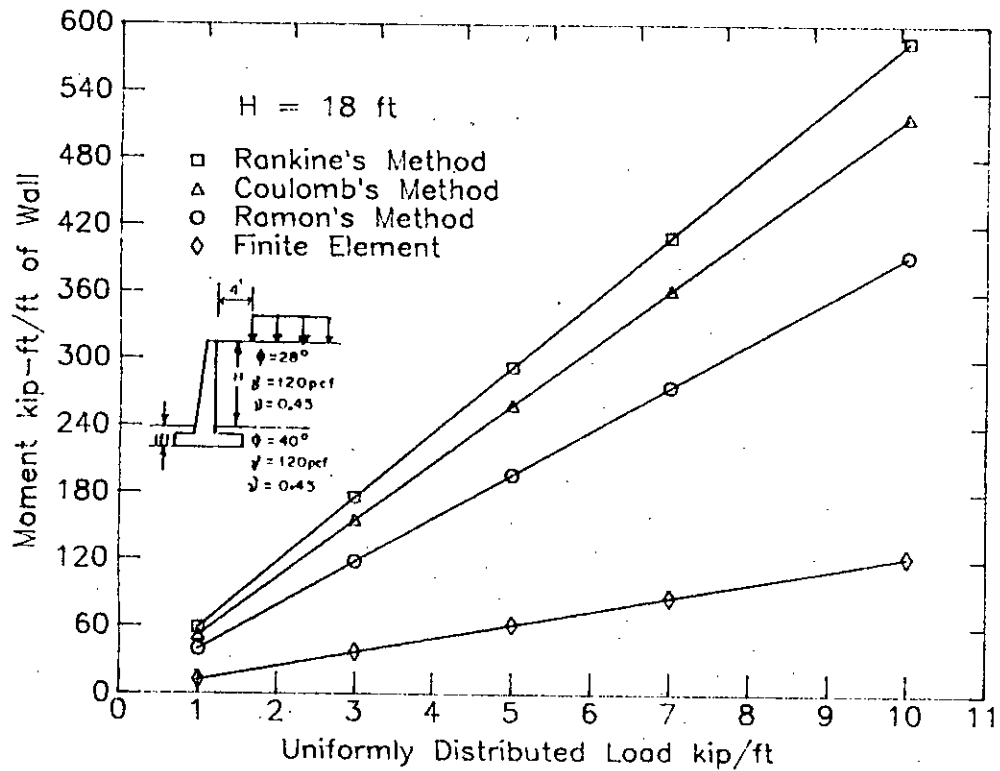


Fig. 7.24 Comparison of Moment to be Resisted by Wall for Uniformly Distributed Load.

## CHAPTER 8

# CONCLUSIONS AND RECOMMENDATIONS FOR FUTURE RESEARCH

### 8.1 CONCLUSIONS

The following are the conclusions that can be drawn from the preceding chapters:

- (1) The general finite element program used in this study for the non-linear two dimensional structure-soil interaction analysis appears to be an effective tool for investigating the phenomenon of interaction in rigid retaining walls.
- (2) The reliability of using finite element (FE) method in interaction analysis depends heavily upon the proper discretization of the structure-soil system. In case of retaining wall-soil system, apart from mesh size, extent of soil to be considered in the analysis is an important parameter. It has been observed that for the soil system, a horizontal extent of soil (extent of backfill) equal to about six times the wall height and vertical extent of soil equal to about three times the width of wall footing below the footing of the wall are adequate for fair analysis.
- (3) Traditional methods of neglecting the effect of stiffness of the wall, stiffness of the footing, and the strength of concrete seem to be justified as the parameters do not significantly influence the stress distribution either in the soil or in the wall components.
- (4) Finite element analysis shows that pressure distribution does not change linearly with depth and as a result the resultant horizontal force is not located at a distance of one third height of the wall, from the base of the wall.
- (5) Finite element analysis gives larger value of lateral soil force than Rankine's or Coulomb's method. The deviation is small when the backfill material is horizontal, but it sharply increases for sloping backfill.
- (6) Magnitude of moment to be resisted by the wall at its base as given by

finite element analysis is greater for wall of small height, compared to that given by Rankine's or Coulomb's method. However, Rankine's method and Coulomb's method give larger value of moment for intermediate to large walls, when the backfill material is horizontal, as compared to finite element analysis results. But finite element analysis shows that the magnitude of moment increases sharply with increasing slope compared to Rankine's or Coulomb's method.

- (7) Finite element analysis shows that the lateral soil force and moment is proportional to the unit weight of backfill material. This is similar to the solution of Rankine's and Coulomb's method.
- (8) Poisson's ratio affects the magnitude of lateral soil force and moment; although the traditional methods ignore the effect of Poisson's ratio completely.
- (9) Angle of internal friction of the backfill material has smaller effect on the lateral soil force and moment than those given by the Rankine's or Coulomb's method.
- (10) Ratio of depth of embedment of the wall into the original soil and height of wall affects the lateral soil force and moment.
- (11) Magnitude of moment to be resisted by the wall at its base for line loading has been found to be proportional to the magnitude of applied load, which is consistent with Boussinesq equation. The moment value was found to be exponentially decaying with the distance of load from the wall face. For larger walls, there is a critical location of load for which the effect of load is maximum. Finite element results fall between the Boussinesq and Trial wedge solution.
- (12) Rankine's, Coulomb's or Ramon's method show that for the same uniformly distributed load, greater lateral soil force and moment are obtained for larger walls. But finite element analysis shows that there is a critical wall height for a given load for which the effect of uniformly distributed load is maximum.



## 8.2 RECOMMENDATIONS

The following recommendations are made for future development of the present research work:

- (1) Tensile separation of soil element was not taken into consideration. The program can be improved to take care of tensile cracking.
- (2) Triangular elements instead of four node isoparametric elements, with crack propagation facility as stated in (1) would give a better picture of wall movement and failure plane. So program can be improved for this purpose.
- (3) Interface elements can be used in future studies to take care of wall friction that acts between the wall elements and soil elements. This will produce results that will represent the actual field behaviour more closely.
- (4) Walls with keys of different sizes and at different locations can be studied to analyse the performance of such walls.
- (5) The existing program may be used in future, after suitable modifications if needed, to analyse different tied retaining walls and sheet pile structures.

## REFERENCES

- BALADI G U (1979) : Lecture Series on Constitutive Equation, U.S. Army Engineer Waterways Experiment Station.
- BHATTACHARJEE S S (1989) : Transient Dynamic Analysis of Underground Structures, M.Sc. thesis, BUET.
- BOWLES J E (1988) : Foundation Analysis and Design, 4th edition, McGraw-Hill.
- CAQUOT A and J KERISEL (1948) : Tables for the Calculation of Passive Pressure, Active Pressure and Bearing Capacity of Foundations (translated by M.A. Bee, London), authier-Villars, Paris.
- CHOW Y K and TEH C I (1991) : Pile-Cap-Pile-Group Interaction in Non homogeneous Soil, Journal of Geotechnical Engineering, ASCE, Vol. 117, No.11, November 1991.
- COULOMB C A (1776) : Referred by Bowles J E (1988), Foundation Analysis and Design, 4th edition, McGraw-Hill.
- CUNNEL M D (1974) : The Application of Finite Elements to Problems of Soil Ph.D. thesis. University of Aston in Birmingham. Referred by Rahman (1978).
- DESAI C S and CHRISTIAN J T (1977) : Numerical Methods in Geotechnical Engineering, McGraw-Hill, New York.
- DESAI C S (1974) : Numerical Design Analyses for Piles in Sands. Journal of Geotechnical Engineering, ASCE, Vol. 100. No. GT6
- DESAI C S (1971) : Non-linear Analyses Using Spline Functions. J. Soil Mech. Found. Div. ASCE Vol.97 No. SM 10.
- DUCAN J M and CHANG C Y (1970) : Non-Linear Analyses of Stress and Strain in Soils. J. Soil Mech. Found. Div. ASCE Vol.96 No. SM5.
- GIRIJA VALLABHAN C V and JAIN R K (1972) : Octahedral Stress Approach to Analysis of Water Resources Structures. Proc. Symp. Application of Finite Element Method to Geotechnical Engg. Vicksburg, Mississippi.
- GUDEHUS G (1977) : Finite elements in geomechanics, John Wiley, London.

- HARRY G P (1988) : Modified Calculations of Pile-Group Settlement Interaction. *Journal of Geotechnical Engineering, ASCE*, Vol. 114, No.6, June 1988.
- HOOPER J A (1978) : Foundation Interaction Analysis, Ch.4 of *Developments in Soil Mechanics-1*, Ed. C.R. Scott, Applied Science, London.
- JANBU N (1957) : Earth Pressure and Bearing Capacity Calculations by Generalised Procedure of Slices, 4th ICSMFE, Vol. 2, pp. 207-212.
- JENNIGS A (1966) : A Compact Storage Scheme for the Solution of Symmetric Linear Simultaneous Equations, *Computer Journal* 9.
- JENNIGS A (1977) : *Matrix Computations for Engineers and Scientists*, John Wiley and Sons.
- JOHN S H (1993) : Beam-Column Analogy Model for Soil Structure Interaction Analysis, *Journal of Geotechnical Engineering, ASCE*, Vol. 119, No. 2, February, 1993.
- KARIM M R (1985) : An Investigation of The Behaviour of Soil-Steel Structures, M.Sc. Thesis, BUET.
- KONDNER RL (1963) :Hyperbolic Stress-strain Response: Cohesive Soils *J. Soil Mech. Found. Div. ASCE* Vol. 89, No. SM1.
- KATONA M G (1978) : On the Analyses of Long Span Culverts by Finite Element Method. Transportation Research Board.
- LEE L and SHEN C K (1969) : Horizontal Movement Related to Subsidence *J. Soil Mech. Foundation Div. ASCE*. Vol. 98 No. SM1.
- LEONARDS G A and ROY M B (1976) : Predicting Performance of Pipe Culverts Buried in Soil. Joint Highway Research Project. Report No. JHRP-76-15.
- MAURICIO O and MICHEL W O (1989) : Lateral Pile Interaction in Submerged Sand, *Journal of Geotechnical Engineering, ASCE*, Vol. 115, No.3, March 1989.
- MEYERHOF G G (1947) : The settlement analysis of building frames, *The structural engineer*, London.
- MEYERHOF G G (1979) : Soil-Structure Interaction and Foundations, S.O.A. Report 6thPan-Am. Conf. SMFE, Lima, Peru.

NAZNEEN S (1986) : Structure-Soil Interaction in Framed Buildings with Orthotropic Wall Infills, M.Sc. thesis, BUET.

NOBARI E S and DUNCAN J M (1972) : Effect of Reservoir Filling on Stresses and Movement in Earthand Rockfill Dams. Report No. TE-72-1, University of California Barkley.

POULOS H G (1981) : Soil-Structure interaction-General Report, Proc. of the 10th Int. Conf. on Soil Mech. and Foundation Engineering, Stockholm, 15-19 June, V.4.

RAHMAN M A (1978) : Interaction between foundations and structures, Ph.D. thesis, The University of Aston in Birmingham.

RAMON J (1981) : Total Lateral Surcharge Pressure Due to Strip Load. Journal of Geotechnical Engineering, ASCE, Vol.107, No. GT 10, October 1981.

RANKINE (1857) : Refereed by Bowles J E (1988), Foundation Analysis and Design, 4th edition, McGraw-Hill.

ROSENFARB J L and W F CHEN (1972) : Limit Analysis Solutions of Earth Pressure Problems, Fritz Eng. Laboratory report 355.14, Lehigh University, 53 pp.

RUSER J R and DAWKINS W P (1972) : 3D Finite Element Analysis of Soil-Structure Interaction. Proc. Symp. Application of Finite Element Method to Geotechnical Engg., Vicksburg, Mississippi, Ed. C.S. Desai, Vol. III.

SERAJ S M (1986) : Structure-Soil Interaction in Buried Rigid Culverts, M.Sc. thesis, BUET.

SERAJ S and RAHMAN A (1987) : Soil-Structure Interaction in Buried Rigid Culverts, Proceedings of the International Conference on Soil-Structure Interactions held in Paris, 5-7 May 1987, Ecole Nationale Des Ponts et Chaussesses (ENPC), ENPC Press, Paris, pp.453-460.

SERAJ S M (1993) : Application of the Compressive-Force Path Concept in the Limit State Design of Footings and Retaining Structures. Proceedings of the International Symposium on Limit State Design in the Geotechnical Engineering held in Copenhagen, 26-28 May, 1993, (edited by Danish Geotechnical Society (Dansk Geoteknisk Forening-dgf), 3vols., Denmark), Bulletin 10, Vol.2, pp.469-478.

SELVADURAI A P S (1979) : Elastic Analysis of Soil Foundation Interaction, Elsevier, Amsterdam.

SHIELDS D H and A Z TOLUNAY (1973) : Passive Pressure Coefficients by method of Slices, JSMFD, ASCE ,Vol. 99, SMIZ, Dec., pp: 1043-1053.

SOKOLOVSKI V V (1960) : Static's of Soil Media, 21e, Butterworth Scientific Publ., London, 237 pp.

TERZAGHI K (1943) : Theoretical Soil Mechanics, John Wiley & Sons, NY, 510 pp.

TIEN H Wu, RONALD M M, RONALD T E and PHILIP E B (1988) : Study of Soil-Root Interaction, Journal of Geotechnical Engineering, Vol.114. No.12. Dec 1988.

WONG K S and DUNCAN J M (1974) : Hyperbolic Stress-strain Parameters for Non-linear Finite Element Analyses and Movements in Soil Masses. Report No. TE 74-3 University of California, Berkeley.

ZIEGLER M (1987) : Displacement Dependent Earth Pressure on Retaining Walls in Sand. Proceedings of the International Conference on Soil-Structure Interaction held in Paris, 5-7 May 1987, Ecole Nationale Des Ponts et Chaussesses (ENPC), ENPC Press, Paris, pp701-708.

ZIENKIEWICZ O C, LEWIS R W and STAGG K G (1978) : Numerical Methods in Offshore Engineering, John Wiley.

APPENDIX A

**Table A.1 Effect of Moment of Inertia of Area of Wall at its Base on Lateral Soil Force ( $P_a$ ) and Moment (M)**

$I$ ft <sup>4</sup>	H = 9 ft		H=12 ft		H=15 ft		H=18 ft	
	$P_a$ Kip	M Kip-ft	$P_a$ Kip	M Kip-ft	$P_a$ Kip	M Kip-ft	$P_a$ Kip	M Kip-ft
.0833	2.608	6.518	4.170	11.603	6.222	18.785	7.873	23.526
.1323	2.539	6.544	4.311	11.861	4.422	19.401	7.891	24.718
.1975	2.392	6.361	4.375	12.165	6.052	22.066	8.401	25.053
.2813	2.580	6.642	4.439	12.123	6.302	19.729	8.424	24.877
.3858	2.671	6.251	4.319	12.531	6.097	19.992	7.894	25.759

**Table A.2 Effect of Moment of Inertia of Area of Wall Footing on Lateral Soil Force ( $P_a$ ) and Moment (M)**

$I$ ft <sup>4</sup>	H = 9 ft		H=12 ft		H=15 ft		H=18 ft	
	$P_a$ Kip	M Kip-ft	$P_a$ Kip	M Kip-ft	$P_a$ Kip	M Kip-ft	$P_a$ Kip	M Kip-ft
0.6667	2.392	6.361	4.375	12.165	6.052	20.066	8.401	25.053
1.5087	2.499	6.403	4.215	12.042	6.384	19.593	7.947	24.922
1.5803	2.426	6.186	4.354	11.757	6.148	19.316	7.905	24.596
2.2500	2.441	6.168	4.296	11.969	5.925	18.995	7.876	24.478

**Table A.3 Effect of Concrete Strength on Lateral Soil Force ( $P_a$ ) and Moment (M)**

$f'_c$ ksi	H = 9 ft		H=12 ft		H=15 ft		H=18 ft	
	$P_a$ Kip	M Kip-ft	$P_a$ Kip	M Kip-ft	$P_a$ Kip	M Kip-ft	$P_a$ Kip	M Kip-ft
2.5	2.428	6.300	4.229	12.074	6.179	19.858	7.964	25.099
2.7	2.392	6.361	4.375	12.165	6.052	20.066	8.401	25.053
3.0	2.394	6.257	4.461	12.138	5.996	19.849	8.023	24.971
3.5	2.325	6.391	4.118	12.244	6.293	19.631	7.989	24.930

**Table A.4 Effect of Slope of Soil Surface on Lateral Soil Force( $P_a$ ) and Moment (M)**

$\beta$ deg	H = 9 ft		H=12 ft		H=15 ft		H=18 ft	
	$P_a$ Kip	M Kip-ft	$P_a$ Kip	M Kip-ft	$P_a$ Kip	M Kip-ft	$P_a$ Kip	M Kip-ft
0	2.392	6.361	4.375	12.165	6.052	20.066	8.401	25.053
5	3.103	8.642	5.165	14.728	7.164	23.035	9.660	31.592
10	4.071	11.857	6.320	20.333	9.040	29.905	12.079	42.113
15	4.902	16.957	7.659	26.477	10.364	38.580	12.256	52.679
20	6.399	22.131	8.633	33.290	12.220	46.979	16.861	63.838

**Table A.5 Percentage of Increase in Moments with Respect to Horizontal Backfill, for Increase of Slope of Soil Surface by Finite Element Method and by Proposed Formulae**

$\beta$ deg	Finite element method				Proposed formulae			
	Height of wall				Height of wall			
	9 ft	12 ft	15 ft	18 ft	9 ft	12 ft	15 ft	18 ft
5	36	21	15	26	36	26	20	26
10	86	67	49	68	95	68	52	68
15	167	118	71	110	178	128	97	128
20	248	173	102	154	283	203	154	203

**Table A.6 Effect of Unit Weight of Backfill Material on Lateral Soil Force ( $P_a$ ) and Moment to be Resisted by the Wall (M)**

$\gamma$ pcf	H = 9 ft		H=12 ft		H=15 ft		H=18 ft	
	$P_a$ Kip	M Kip-ft	$P_a$ Kip	M Kip-ft	$P_a$ Kip	M Kip-ft	$P_a$ Kip	M Kip-ft
100	2.108	4.814	3.481	9.489	5.009	13.218	6.544	20.103
110	2.103	5.918	3.967	10.693	5.621	15.787	7.312	22.945
120	2.392	6.361	4.375	12.165	6.052	20.066	8.401	25.053



**Table A.7 Percentage of Change in Lateral Soil Force ( $P_a$ ) and Moment ( $M$ ) for Changing Unit Weight**

h (ft)	% of change in $P_a$			% of change in $M$		
	$\gamma=100$ to $\gamma=110$	$\gamma=110$ to $\gamma=110$	$\gamma=100$ to $\gamma=120$	$\gamma=100$ to $\gamma=110$	$\gamma=110$ to $\gamma=120$	$\gamma=100$ to $\gamma=120$
9	-	13.7	-	22.93	7.5	32.1
12	13.9	10.3	25.7	12.7	13.8	28.2
15	12.2	7.7	20.8	19.4	27.1	51.8
18	11.7	14.9	28.4	14.1	9.2	24.6

**Table A.8 Effect of Poisson's Ratio on Lateral Soil Force ( $P_a$ ) and the Moment ( $M$ )**

$\mu$	H = 9 ft		H = 12 ft		H = 15 ft		H = 18 ft	
	$P_a$ Kip	M Kip-ft	$P_a$ Kip	M Kip-ft	$P_a$ Kip	M Kip-ft	$P_a$ Kip	M Kip-ft
.45	2.392	6.361	4.375	12.165	6.052	20.066	8.401	25.053
.46	2.593	7.085	4.473	12.606	6.419	20.487	8.438	26.378
.47	2.549	7.410	4.470	12.877	6.482	21.066	8.959	28.063

**Table A.9 Effect of Angle of Internal Friction on Lateral Soil Force ( $P_a$ ) and Moment(M)**

h ft	$\phi = 28^\circ$		$\phi = 40^\circ$		% of change from $\phi=28^\circ$ to $\phi = 40^\circ$	
	$P_a$ kip	M kip-ft	$P_a$ kip	M kip-ft	$P_a$	M
9	2.392	6.361	2.446	6.301	-2.26	0.94
12	4.375	12.165	3.846	10.239	12.09	15.83
15	6.052	20.066	5.722	15.518	5.45	22.67
18	8.401	25.053	7.372	21.493	12.25	14.21

**Table A.10 Effect of Embedded depth on Lateral Soil Force ( $P_a$ ) and Moment (M)**

Embedded depth (ft)	H = 9 ft		H=12 ft		H=15 ft		H=18 ft	
	$P_a$ Kip	M Kip-ft	$P_a$ Kip	M Kip-ft	$P_a$ Kip	M Kip-ft	$P_a$ Kip	M Kip-ft
1.00	2.392	6.361	4.375	12.165	6.052	20.066	8.401	25.053
1.50	2.555	7.191	4.382	12.663	6.197	20.053	8.230	25.995
1.75	2.503	7.272	4.402	13.158	6.118	20.503	8.136	26.043
2.00	2.580	7.242	4.223	13.394	6.153	20.160	8.126	24.938

**Table A.11 Effect of Magnitude and Location of Line Load on Lateral Soil Force ( $P_a$ ) and Moment (M) for a Wall of 9 ft Height (Excluding Self Weight )**

P kip	X = 4 ft		X = 7.25 ft		X = 10.5 ft		X = 13.75 ft	
	$P_a$ kip	M kip-ft	$P_a$ kip	M kip-ft	$P_a$ kip	M kip-ft	$P_a$ kip	M kip-ft
1	0.39	1.397	0.309	1.18	.203	.834	.132	0.499
2	0.75	3.033	0.602	2.381	.431	1.909	.267	1.037
3	1.114	4.655	0.908	3.668	.643	2.867	.392	1.599
4	1.481	6.238	1.216	4.921	.852	3.795	.523	2.224
5	1.842	7.757	1.522	6.137	1.054	4.668	.650	2.830
6	2.204	9.277	1.823	7.312	1.262	5.563	.793	3.426
7	2.567	10.808	2.111	8.498	1.478	6.414	.935	3.985
8	2.929	12.334	2.406	9.725	1.693	7.245	1.072	4.528
9	3.294	14.069	2.696	10.926	1.906	8.065	1.208	5.063
10	3.660	15.412	2.986	12.139	2.109	8.844	1.348	5.617

**Table A.12 Effect of Magnitude and Location of Line Load on Lateral Soil Force ( $P_a$ ) and Moment (M) for a Wall of 12 ft Height ( Excluding Self Weight )**

P kip	X = 4 ft		X = 8.92 ft		X = 13.83 ft		X = 18.75 ft	
	$P_a$ kip	M kip-ft	$P_a$ kip	M kip-ft	$P_a$ kip	M kip-ft	$P_a$ kip	M kip-ft
1	0.295	1.440	0.255	1.173	0.155	0.754	0.090	0.452
2	0.569	2.908	0.501	2.332	0.296	1.548	0.191	0.946
3	0.850	4.411	0.738	3.609	0.454	2.479	0.293	1.467
4	1.128	5.915	0.982	4.876	0.612	3.418	0.399	2.016
5	1.405	7.417	1.230	6.111	0.776	4.355	0.504	2.548
6	1.680	8.883	1.481	7.362	0.942	5.269	0.608	3.062
7	1.955	10.390	1.734	8.609	1.107	6.182	0.711	3.562
8	2.235	11.905	1.985	9.871	1.276	7.104	0.818	4.083
9	2.516	13.438	2.240	11.100	1.442	7.936	0.925	4.597
10	2.796	14.916	2.483	12.252	1.606	8.754	1.023	5.135

**Table A.13 Effect of Magnitude and Location of Line Load on Lateral Soil Force ( $P_a$ ) and Moment (M) for a Wall of 15 ft Height ( Excluding Self Weight )**

P kip	X = 4 ft		X = 8.92 ft		X = 13.83 ft		X = 18.75 ft	
	$P_a$ kip	M kip-ft	$P_a$ kip	M kip-ft	$P_a$ kip	M kip-ft	$P_a$ kip	M kip-ft
1	0.182	1.083	0.214	1.041	0.162	0.723	0.099	0.421
2	0.352	2.264	0.424	2.233	0.327	1.566	0.212	0.985
3	0.520	3.439	0.635	3.381	0.486	2.472	0.327	1.592
4	0.688	4.679	0.845	4.526	0.648	3.371	0.443	2.195
5	0.858	5.913	1.057	5.667	0.809	4.273	0.556	2.760
6	1.033	7.124	1.266	6.776	0.970	5.168	0.660	3.316
7	1.208	8.32	1.476	7.886	1.132	6.068	0.764	3.869
8	1.383	9.475	1.687	9.012	1.296	6.952	0.864	4.420
9	1.557	10.649	1.898	10.141	1.459	7.845	0.962	4.953
10	1.727	11.836	2.111	11.279	1.627	8.716	1.065	5.506

**Table A.14 Effect of Magnitude and Location of Line Load on Lateral Soil Force ( $P_a$ ) and Moment (M) for a Wall of 18 ft Height ( Excluding Self Weight )**

P kip	X = 4 ft		X = 8.92 ft		X = 13.83 ft		X = 18.75 ft	
	$P_a$ kip	M kip-ft	$P_a$ kip	M kip-ft	$P_a$ kip	M kip-ft	$P_a$ kip	M kip-ft
1	0.096	0.855	0.173	0.987	0.154	0.824	0.106	0.593
2	0.193	1.708	0.346	1.965	0.305	1.637	0.210	1.166
3	0.290	2.547	0.519	2.952	0.456	2.440	0.311	1.739
4	0.386	3.381	0.693	3.937	0.607	3.241	0.415	2.310
5	0.476	4.248	0.866	4.920	0.760	4.048	0.518	2.872
6	0.567	5.109	1.042	5.901	0.911	4.852	0.622	3.434
7	0.657	5.969	1.218	6.883	1.063	5.658	0.724	3.996
8	0.748	6.829	1.396	7.866	1.215	6.463	0.828	4.549
9	0.839	7.692	1.573	8.848	1.371	7.266	0.931	5.113
10	0.930	8.556	1.750	9.83	1.524	8.075	1.031	5.669

**Table A.15 Effect of Uniformly Distributed Load on Lateral Soil Force ( $P_a$ ) and Moment (M) ( Excluding Self Weight )**

UDL kip/ft	h=9 ft		h=12 ft		h=15 ft		h=18 ft	
	$P_a$ kip	M kip-ft	$P_a$ kip	M kip-ft	$P_a$ kip	M kip-ft	$P_a$ kip	M kip-ft
1	2.37	9.86	2.87	14.18	2.53	14.11	2.11	12.39
2	4.73	19.47	5.78	28.42	5.14	28.39	4.24	24.74
3	7.12	29.16	8.72	42.66	7.71	42.45	6.32	36.97
4	9.447	38.89	11.69	57.14	10.26	56.47	8.44	49.37
5	11.80	48.42	14.57	71.25	12.79	70.32	10.55	61.68
6	14.14	57.86	17.42	85.37	15.33	84.17	12.68	74.07
7	16.44	67.24	20.29	99.38	17.83	98.03	14.78	86.35
8	18.75	76.66	23.14	113.46	20.36	111.76	16.88	98.55
9	21.07	86.05	25.99	127.44	22.91	125.54	18.96	110.72
10	23.40	95.50	28.84	141.41	25.44	139.26	21.06	122.91

**Table A.16 Lateral Soil Force ( $P_a$ ) and the Moment (M) for Dead Load only from Coulomb, Rankine and Finite Element Analyses ( $\phi=28^\circ$ )**

h ft	$\beta$ degree	Rankine's method		Coulomb's method $\delta = 22^\circ$		Finite element $\nu = 0.45$	
		$P_a$ kip	M kip-ft	$P_a$ kip	M kip-ft	$P_a$ kip	M kip-ft
9	0	1.75	5.26	1.55	4.65	2.39	6.36
	5	1.77	5.31	1.65	4.95	3.10	8.64
	10	1.82	5.46	1.76	5.30	4.07	11.86
	15	1.92	5.76	1.90	5.72	4.90	16.96
	20	2.10	6.31	2.10	6.31	6.40	22.13
12	0	3.12	12.48	2.76	11.02	4.38	12.17
	5	3.15	12.59	2.94	11.74	5.17	14.73
	10	3.23	12.94	3.14	12.56	6.32	20.33
	15	3.41	13.64	3.39	13.55	7.66	26.48
	20	3.74	14.95	3.74	14.97	8.63	33.29
15	0	4.87	24.37	4.31	21.53	6.05	20.07
	5	4.92	24.59	4.58	22.93	7.16	23.04
	10	5.05	25.27	4.90	24.53	9.04	29.91
	15	5.33	26.64	5.29	26.48	10.36	38.58
	20	5.84	29.21	5.84	29.24	12.22	46.98
18	0	7.02	42.11	6.20	37.21	8.4	25.05
	5	7.08	42.48	6.61	39.62	9.66	31.59
	10	7.28	43.68	7.06	42.39	12.08	42.11
	15	7.67	46.04	7.62	45.75	12.26	52.68
	20	8.41	50.47	8.42	50.53	16.86	63.84

**Table A.17 Ratio of Wall Height and Distance of Resultant Horizontal Lateral Soil Force From the Base of Wall obtained from Finite Element Analyses**

$\beta$ degree	H=9 ft	H=12 ft	H=15 ft	H=18 ft
0	3.38	4.31	4.52	6.04
5	3.23	4.21	4.66	5.51
10	3.09	3.73	4.53	5.16
15	2.60	3.47	4.03	4.18
20	2.60	3.11	3.91	4.75

**Table A.18 Percentage of Difference in Lateral Soil Force ( $P_a$ ) and Moment (M) in Rankine and Coulomb's method with Respect to Finite Element Method**

h ft	$\beta$ degree	Rankine's method		Coulomb's method	
		$P_a$	M	$P_a$	M
9	0	26.8	17.3	35.1	26.9
	5	42.9	38.5	46.8	42.7
	10	55.3	53.9	56.8	55.3
	15	60.8	66.0	61.2	66.3
	20	67.2	71.5	67.2	71.5
12	0	28.8	-2.5	37.0	9.4
	5	39.1	14.5	36.0	20.3
	10	48.9	36.4	50.3	38.2
	15	55.5	48.5	55.7	48.8
	20	56.7	55.1	56.7	55.0
15	0	19.5	-21.4	28.8	-7.3
	5	31.3	-6.7	36.0	0.5
	10	44.1	15.5	45.8	17.9
	15	48.6	30.9	48.9	31.4
	20	52.2	37.8	52.2	37.8
18	0	16.4	-68.1	26.2	-48.5
	5	26.7	-34.5	31.6	-25.4
	10	39.7	-3.7	41.6	-0.7
	15	37.4	12.6	37.8	13.2
	20	50.1	20.9	50.1	20.8

**Table A.19 Lateral Soil Force and Moment for Line Load of 10 kip, by Boussinesq, Trial wedge & Finite Element Method ( Excluding Self wt)**

height of wall, ft	Distance of Line load, ft	Boussinesq Equation $\nu = 0.45$		Trial wedge $\phi = 28^\circ$	Finite Element $\nu = 0.45, \phi = 28^\circ$	
		$P_a$ kip	M kip-ft		$P_a$ kip	M kip-ft
9	4.00	.333	1.11	7.76	3.66	15.41
	7.25	.140	0.66	3.91	2.99	12.14
	10.50	.068	0.36	1.32	2.11	8.84
	13.75	.036	0.20	-	1.35	5.62
12	4.00	.342	1.23	9.13	2.80	14.92
	8.92	.128	0.763	4.67	2.48	12.25
	13.83	.059	0.412	1.47	1.61	8.75
	18.75	.030	0.22	-	1.02	5.14
15	4.00	.343	1.30	9.75	1.73	11.84
	8.92	.141	0.938	6.07	2.11	11.28
	13.83	.072	0.586	3.00	1.63	8.72
	18.75	.040	0.357	-	1.07	5.51
18	4	.340	1.33	9.73	0.93	8.56
	8.92	.148	1.06	7.06	1.75	9.83
	13.83	.081	0.735	4.33	1.52	8.08
	18.75	.048	0.488	-	1.03	5.67



**Table A.20 Lateral Soil Force and Moment for Uniformly Distributed Load by Coulomb, Rankine, Ramon and Finite Element Method. ( $\phi = 28^\circ$ )**

h ft	UDL kip/ft	Rankine's method $\phi = 28^\circ$		Coulomb's method $\delta = 22^\circ, \phi = 28^\circ$		Ramon's method $\phi = 28^\circ$		Finite element method $v = 0.45, \phi = 28^\circ$	
		$P_a$ kip	M kip-ft	$P_a$ kip	M kip-ft	$P_a$ kip	M kip-ft	$P_a$ kip	M kip-ft
9	1	3.25	14.62	2.87	12.92	0.7	3.45	2.37	9.86
	3	9.75	43.86	8.61	38.76	2.1	10.34	7.16	29.16
	5	16.25	73.10	14.36	64.6	3.5	17.24	11.8	48.42
	7	22.74	102.34	20.10	90.44	4.9	24.14	16.44	67.4
	10	32.45	146.2	28.71	129.2	7.0	34.48	23.40	95.5
12	1	4.33	26.0	3.83	22.97	1.58	10.96	2.87	14.18
	3	13.00	78.0	11.49	68.91	4.73	32.89	8.72	42.66
	5	21.66	130.0	19.15	114.9	7.88	54.81	14.57	71.25
	7	30.32	182.0	26.81	160.8	11.03	76.73	20.29	99.38
	10	43.32	260.0	38.3	229.7	15.76	109.6	28.84	141.41
15	1	5.42	40.61	4.79	35.89	2.67	23.91	2.53	14.11
	3	16.25	121.8	14.36	107.7	8.02	71.73	7.71	42.45
	5	27.08	203.1	23.93	179.5	13.36	119.6	12.79	70.32
	7	37.91	284.3	33.5	251.2	18.70	167.4	17.83	98.03
	10	54.15	406.1	47.85	358.9	26.72	239.1	25.44	139.26
18	1	6.5	58.5	5.74	51.68	3.55	39.28	2.11	12.39
	3	19.5	175.5	17.23	155.0	10.64	117.8	6.32	36.97
	5	32.5	292.5	28.71	258.4	17.73	196.4	10.55	61.68
	7	45.5	409.5	40.19	361.8	24.82	274.9	14.78	86.35
	10	65.0	585.0	57.42	516.8	35.46	392.7	21.06	122.91

